

21093

NATIONAL LIBRARY  
OTTAWA



BIBLIOTHÈQUE NATIONALE  
OTTAWA

NAME OF AUTHOR.....ROY EARL REID.....

TITLE OF THESIS.....A FRACTURE TOUGHNESS  
.....STUDY OF GAS TRANSMISSION  
.....LINE PIPE.....

UNIVERSITY.....OF ALBERTA, EDMONTON, ALTA.....

DEGREE FOR WHICH THESIS WAS PRESENTED.....MASTER OF SCIENCE.....

YEAR THIS DEGREE GRANTED.....SPRING 1974.....

Permission is hereby granted to THE NATIONAL LIBRARY  
OF CANADA to microfilm this thesis and to lend or sell copies  
of the film.

The author reserves other publication rights, and  
neither the thesis nor extensive extracts from it may be  
printed or otherwise reproduced without the author's  
written permission.

(Signed).....*Ray Earl Reid*.....


PERMANENT ADDRESS:  
.....P.O. BOX 88 SUB 1069  
.....CALGARY, ALTA.....

DATED.....MAY 22.....1974.....

THE UNIVERSITY OF ALBERTA

A FRACTURE TOUGHNESS STUDY OF GAS  
TRANSMISSION LINE PIPE

BY:

 ROY E. REID

A THESIS

SUBMITTED TO THE FACULTY OF GRADUATE STUDIES AND RESEARCH  
IN PARTIAL FULFILMENT OF THE REQUIREMENTS FOR THE DEGREE  
MASTER OF SCIENCE

DEPARTMENT OF MECHANICAL ENGINEERING

EDMONTON, ALBERTA

SPRING, 1974

UNIVERSITY OF ALBERTA  
FACULTY OF GRADUATE STUDIES AND RESEARCH

The undersigned certify that they have read, and recommend to the Faculty of Graduate Studies and Research, for acceptance, a thesis entitled "A FRACTURE TOUGHNESS STUDY OF GAS TRANSMISSION LINE PIPE", submitted by ROY E. REID in partial fulfilment of the requirements for the degree of Master of Science.

*[Signature]*  
.....  
G. FORD

*[Signature]*  
.....  
*[Signature]*  
.....

Date January 18, 1974

## ABSTRACT

Pipeline failures, some of catastrophic proportions, have occurred in transmission line systems throughout the world. Detailed investigations indicate that a knowledge of fracture behavior may permit designers to control or prevent similar pipeline failures.

Currently, research efforts are being directed toward the application of the theory of linear elastic fracture mechanics to medium strength steels. One such medium strength pipeline steel, API-X65, is being utilized extensively throughout North American Pipeline systems. Therefore the fracture behavior of this steel using the methods of linear elastic fracture mechanics was chosen for this investigation.

The research program consisted of Tension, Three Point Notch Bend; Two-Thirds Charpy V-Notch and the recently developed Double-Cantilever Beam tests. Plane strain fracture toughness ( $K_{IC}$ ) values were determined from the test results at temperatures ranging from ambient to -193 degrees centigrade. Laboratory scale tests to study the effects of material damage were undertaken using precompressed Three Point Notch Bend Specimens. Results indicated that precompression significantly decreases fracture toughness and raises the transition temperature. Double-Cantilever Beam (DCB) test specimens yielded both initiation and arrest fracture toughness values. A close correlation was also found when DCB and Three Point Notch Bend tests results were compared.

A design concept for the X65 pipe steel was projected from a detailed analysis of all physical test results.

Three Point Notch Bend tests were conducted on an old service failure sawtooth shaped fracture segment from a 6 inch pipe line. Test results indicate that the material was likely well below design specification.

## ACKNOWLEDGMENTS

Sincere appreciation is extended to the many persons involved in the work which has led to the completion of this thesis.

In particular, the author wishes to thank Dr. G. Ford, Dean of Engineering, for his valued supervision and guidance; Mr. Helmut Schroeder and Mr. Tom Simpson, who prepared the physical test specimens; fellow graduate students for their assistance with the laboratory tests; and also Miss Helen Wozniuk for typing the thesis.

Gratitude is also expressed to the National Research Council of Canada and the Alberta and Southern Gas Company Limited who assisted financially in the research program, and to Canadian Phoenix Pipe and Steel Limited who donated the X65 pipe materials.

## TABLE OF CONTENTS

	<u>Page</u>	
<b>CHAPTER I</b>	<b>INTRODUCTION</b>	
1.1	Introduction	1
1.2	Research Methods and Objectives	4
<b>CHAPTER II</b>	<b>THEORY OF FRACTURE</b>	
2.1	Introduction	6
2.2	Analytical Basis	7
2.3	Plastic Zone Influence	13
2.4	Onset and Arrest of Fast Fractures	15
2.5	Experimental Test Methods	15
2.5.1	Charpy Impact Test	16
2.5.2	Three Point Notch Bend Test	17
2.5.3	Double-Cantilever Beam Test	20
2.6	Material Damage	25
<b>CHAPTER III</b>	<b>EXPERIMENTAL TEST SPECIFICATIONS</b>	
3.1	Introduction	26
3.2	Test Material	26
3.3	Test Material Allocation	30
3.4	Specimen Precracking	31
3.5	Experimental Methods - Three Point Notch Bend	32
3.5.1	Bend Specimen Design	32
3.5.2	Specimen Removal	34

TABLE OF CONTENTS (continued)

	<u>Page</u>
CHAPTER III continued	
3.5.3 Notch Bend Test Facilities	35
3.5.4 Notch Bend Specimen Testing Procedures	37
3.5.5 Material Damage - Precompression	39
3.6 Tensile Tests	40
3.7 Two-Thirds Charpy V-Notch Tests	41
3.7.1 Charpy Specimen Design	41
3.7.2 Charpy Test Facilities and Loading Procedure	42
3.8 Double-Cantilever Beam Test	43
3.8.1 Specimen Design	43
3.8.2 DCB Test Facilities	46
3.8.3 DCB Loading and Instrumentation	49
3.9 Metallurgical Photomicrographs	52
3.10 Sources of Error	53
CHAPTER IV TEST RESULTS AND DISCUSSION	
4.1 Introduction	54
4.2 Tensile Tests	54
4.3 Metallurgical Photomicrographs	61
4.4 Two-Thirds Charpy V-Notch Test	63
4.5 Three Point Notch Bend Test	71
4.5.1 X65 Pipe Steel	71
4.5.2 Sawtooth Fracture Segment	79



TABLE OF CONTENTS (continued)

	<u>Page</u>
CHAPTER IV continued	
4.6 Double-Cantilever Beam Tests	82
4.7 Correlation Between Test Methods	90
4.8 Specimen Orientation	95
4.9 Specimen Precracking	95
4.10 Effects of Material Damage	96
4.11 X65 Material Design Concept	97
CHAPTER V CONCLUSIONS AND RECOMMENDATIONS	
5.1 Summary	99
5.2 Areas of Further Study	100
BIBLIOGRAPHY	102
APPENDIX A	105

LIST OF TABLES

<u>Table</u>		<u>Page</u>
3.1	Nominal Chemical Composition - X65 Pipe Steel	29
3.2	Mechanical Properties - X65 Steel	29
3.3	Sawtooth Fracture Segment Three Point Notch Bend - Nominal Specimen Dimensions	35
4.1	Experimental Mechanical Properties - X65 Steel	55
4.2	Notch Bend Fracture Toughness - X65 Steel	80
4.3	Summary - Comparative Test Results for X65 Steel	94

## LIST OF FIGURES

<u>Figure</u>		<u>Page</u>
1	Irwin Crack Model	10
2	Modes of Fracture	11
3	Notch Bend Loading Schematic	19
4	DCB Test Configuration	21
5	Typical DCB Fracture Behaviour	23
6	Finished X65 Pipe Cylinder	27
7	Unformed X65 Skelp Plate	27
8	Sawtooth Fracture Segment	28
9	Profile Sawtooth Fracture Segment	28
10	Three Point Notch Bend Specimen Configuration	33
11	Gilmore With Low Temperature Bath	36
12	Specimen Positioned for Notch Precompression	36
13	Tensile Specimen Design	40
14	Two-thirds Charpy Test Specimen	42
15	DCB Plate Test Specimen	44
16	DCB Pipe Test Specimen	44
17	DCB Test Facilities	47
18	DCB Specimen at Zero Load	47
19	DCB Mounting Schematic	48
20	X65 Plate, Tensile Stress vs Strain	56
21	X65 Plate, Poissons Ratio	57

LIST OF FIGURES (continued)

<u>Figure</u>		<u>Page</u>
22	X65 Plate, Tensile Stress vs Strain	58
23	X65 Plate, Poissons Ratio	59
24	X65 Pipe, Tensile Stress vs Strain	60
25	X65 Plate, Impact Energy vs Temperature	64
26	X65 Pipe, Impact Energy vs Temperature	65
27	Percentage of Room Temperature Impact Energy vs Temperature	66
28	Percentage Crystallinity vs Temperature	67
29	X65 Pipe, Charpy Transverse Crack Fracture Surfaces	69
30	X65 Plate, Charpy Transverse Crack Fracture Surfaces	69
31	X65 Pipe, Charpy Longitudinal Crack Fracture Surfaces	70
32	X65 Plate, Charpy Longitudinal Crack Fracture Surfaces	70
33	Average $K_{IC}$ vs Temperature for Static Notch Bend Tests	72
34	$K_{IC}$ vs Temperature for Precompressed Static Notch Bend Specimens	73
35	X65 Plate, Transverse $K_{IC}$ vs Temperature	74
36	X65 Pipe, Transverse $K_{IC}$ vs Temperature	75
37	X65 Plate, Longitudinal $K_{IC}$ vs Temperature	76
38	Typical Three Point Notch Bend Fracture Surfaces	77
39	Sawtooth Fracture Segment, Transverse $K_{IC}$ vs Temperature	81
40	$K_{IC}$ vs Temperature for X65 DCB Specimens at First Initiation Point	84

LIST OF FIGURES (continued)

<u>Figure</u>		<u>Page</u>
41	X65 Plate, Average Longitudinal $K_{IC}$ vs Temperature	85
42	X65 Pipe, Average Longitudinal $K_{IC}$ vs Temperature	86
43	X65 Plate, Average Transverse $K_{IC}$ vs Temperature	87
44	X65 Pipe, Load vs Displacement at 100 Degrees Centigrade	89
45	X65 Pipe, DCB Fracture Surface Sequence	91
46	X65 Plate, DCB Fracture Surface Sequence	91
47	X65 Plate, DCB Load vs Displacement at -193 Degrees Centigrade	92
48	Enlargement X65 DCB Fracture Surface at -193 Degrees Centigrade	93
A1	X65 Plate Section I	106
A2	X65 Plate Section II	107
A3	X65 Plate Section III	108
A4	X65 Pipe Section I	109
A5	X65 Pipe Section II	110
A6	X65 Pipe Section III	111
A7	Sawtooth Fracture Segment, Notch Bend Specimen Locations	112

## LIST OF SYMBOLS

a	crack length
$a_0$	notch depth
c	crack length; subscript to indicate critical values
f	applied force
n	DCB compliance constant
p	plastic work term
r, $\theta$	polar co-ordinates
r <sub>y</sub>	radius of plastic zone
v	crack opening displacement
w	DCB specimen width
y	deflection
x, y, z	Cartesian co-ordinates
A	fracture area; DCB compliance constant
B	specimen thickness
C <sub>1</sub>	constant
E	Youngs' Modulus
F	tensile force, load
G	strain energy release rate
G <sub>c</sub>	strain energy release rate at onset of rapid fracture propagation
I	moment of inertia
K	stress intensity factor, fracture toughness
K <sub>a</sub>	crack arrest stress intensity factor

LIST OF SYMBOLS (continued)

$K_C$	critical stress intensity factor
$K_I$	stress intensity factor for Mode I fracture
$K_{Ia}$	Mode I crack arrest stress intensity factor
$K_{Ic}$	critical Mode I stress intensity factor
$L$	specimen length
$P$	load
$\dot{P}$	time rate of change of load - lb/min.
$\dot{S}$	time rate of change of stress - p.s.i./min.
$W$	work done
$G$	strain energy release rate
$B$	non-dimensional plastic zone parameter
$\gamma$	surface energy
$\delta$	displacement
$\dot{\delta}$	cross head velocity, rate of change of displacement
$\epsilon$	strain
$K$	Kies stress intensity factor
$\lambda$	shear stress
$\mu$	micro inches per inch = $10^{-6}$ in./in.
$\nu$	Poisson's ratio
$\pi$	numerical constant 3.14159
$\sigma$	tensile stress
$\sigma_y$	stress at material yield point
long.	longitudinal crack direction
transv.	transverse crack direction
API	American Petroleum Institute
ASTM	American Society for Testing Materials

## CHAPTER I

### INTRODUCTION

#### 1.1 Introduction

Pipeline system designs of the 1970's will undoubtedly be profoundly influenced by ecological considerations of pending Government legislation. Prevention of environmental damage will be equal in importance with economics to pipeline designs. The planned North American High-Arctic cold service pipeline systems will tax existing research abilities, technological skills and manufacturing facilities to the limit on the basis of economics alone.

It is acknowledged that some pipelines will fail. In the past, a number of quite spectacular line failures have occurred. Investigations into these failures have resulted in attempts to apply all or a portion of the theory of Linear Elastic Fracture Mechanics (LEFM) to pipeline design. Specifically, research efforts have been directed towards achieving a thorough understanding of the phenomena of "brittle fracture" and its application to pipeline materials.

Prior to announcements in the late 1960's that Arctic pipelines may be required in service by as early as 1975, brittle fracture of gas and oil transmission lines had not been thoroughly researched. Historically, brittle fracture of many engineering materials has been investigated in considerable detail over the past century. Early attempts were directed at determining a material "transition temperature"



based on data from notched bar impact tests. These led to more specific theoretical research by A.A. Griffith (1) in 1921, in which he considered the effects of a flaw in an infinite plate. Subsequently, Griffith proposed a "Rupture Criterion" which related a maximum permissible flaw size to a given stress level. Theoretical and applied fracture research continued during the ensuing years through the advent of World War II. Little real advancement of the subject was achieved during this period. Subsequently, the Liberty Ship failures of the early war years, resulted in a resumption and redirection of research efforts of the study of brittle fracture as related to practical engineering designs and materials. This intensive research program resulted in the determination of a correlation between service failure material conditions and the Charpy V-notch impact test energy value. However, it was subsequently determined that the Charpy 15 ft. lb. energy value criterion could not be universally applied disregarding stress level, material type, etc. Nonetheless, the Charpy energy correlation did serve as a basis of study from which acceptable theories were later formulated by Irwin (2), Orowan (3) and others, all of which were extensions of the earlier Griffith rupture criterion.

Detailed investigations of the early 1950's Comet aircraft in-flight failures and a number of early transmission line ruptures, led to the establishment of the fracture mechanics analysis approach to the problem of brittle fracture. Present day refinements of the basic theory have evolved through related advances in studies involving the application of high strength steels to aerospace and nuclear re-

actor designs. LEFM is the accepted method for evaluating the material resistance to crack propagation of high strength steels to determine their likely fracture behavior.

Extension of LEFM theory to medium and lower strength steels has not been successfully achieved. Small scale laboratory test specimens rarely produce fractures at stress levels below gross yield strength, which is where the majority of field fractures are most likely to occur. Research efforts are continuing based on the application of a portion of the high strength LEFM theory. Limited success has been obtained by Turner (4), Ford (5) and others, using mild steel specimens and relating strain rate, crack propagation impact energy and crack notch root radius at varying temperatures and specimen sizes. Results indicate these factors are related to the critical stress field intensity,  $K_{Ic}$  for the failure mode under consideration.

Current purchaser pipeline specifications require pipe manufacturers to meet minimum fracture toughness values. This specification measures the capacity of a material to withstand localized strain without fracture, specifically, the resistance of a material to crack propagation at a given temperature. Fracture toughness values are determined from consideration of temperature, strain rate and mode of failure. Materials of high fracture toughness exhibit characteristic shear fracture surfaces and are typically ductile high energy type failures, with a distorted surface appearance. Low fracture toughness materials produce cleavage or brittle fractures, and are low energy failures which usually occur with less than expected ductility. Brittle

fractures commonly originate at material discontinuities such as flaws, and are influenced by lower temperatures and/or higher strain rates. Typically, brittle fractures are faceted in appearance and exhibit characteristic "chevron markings" - a herringbone type pattern pointing back toward the fracture origin.

## 1.2 Research Methods and Objectives

In this investigation three uncorrelated fracture toughness test methods -- Charpy V-Notch, Three Point Notch Bend and Double-Cantilever Beam, are used to evaluate the fracture mechanics behavior of a medium strength pipe steel. The steel used is the Canadian Phoenix 36 inch submerged arc welded API LX-65, of 65,000 psi minimum yield strength. Identical fracture tests are conducted on the unrolled X65 skelp material and the finished (form rolled and cold expanded) pipe. Tensile tests and photomicrographs of both material conditions are also conducted. Additionally Three Point Notch Bend Tests on an early sawtooth shaped service failure segment are also undertaken.

The objectives of the research are:

- (A) 1. To verify the manufacturer's mechanical specifications.
2. To comment on the effects of orientation of test specimens on the material properties.
3. To determine the fracture toughness and transition temperatures for the X65 pipe materials.
4. To determine the applicability and effectiveness of the three fracture toughness test methods to an API pipe steel.

5. To determine the influence of form rolling and cold expansion sizing.

6. To determine the effects of incidental material field damage -- precompression.

7. To determine the effects of specimen precracking at the notch root.

8. To propose a pipeline material design concept.

(B) Sawtooth fracture segment:

1. To determine the Notch Bend Toughness value for the service failure.

2. To comment on material condition at failure.

CHAPTER II  
THEORY OF FRACTURE

2.1 Introduction

Fracture is separation of a material by the progressive extension of a crack. The fracture process consists of three inter-related steps: crack initiation, crack growth and crack propagation. Crack initiation starts at a localized flaw in the material microstructure; and the development of a crack at a defect is defined as initiation (6). Generally, defects or other crack initiators act as stress raisers. During proof test, handling, or operation, defect stresses may be multiplied many times. The material if stressed beyond its elastic capacity near the defect, may yield or rupture locally and produce a growing crack. When yielding predominates, high stresses at the defect undergo relaxation and crack growth of this type is termed self-limiting. The crack is stable and will not continue to grow unless the nominal stress is increased. Crack growth is a time dependent process and the rate mechanism is effected by both static and dynamic effects.

Crack propagation occurs when the stable self-limiting growth phase is disrupted or unattainable. This may occur in the presence of a large initial defect under high loading rate, such that instability occurs. The crack being unstable, undergoes rapid crack extension without further increase in stress. The point of initial imbalance is referred to as the onset of crack propagation.

## 2.2 Analytical Basis

Progressive crack extension may be analyzed using the methods of Linear Elastic Fracture Mechanics developed by Irwin (2), (7) and Orowan (3), based on the Griffith Rupture Criterion of 1921 (1). Griffith postulated that the strength of a material could be calculated using a critical instability relationship between the solid state surface energy and the crack size. He concluded that instability would occur when the strain energy release rate during crack extension exceeded the rate of increase in surface energy. He postulated the Griffith Energy Equation which states that:

$$\frac{d}{da} \left( \frac{-\sigma^2 \pi a^2}{E} + 4a\gamma \right) = 0 \quad (1)$$

or more specifically,

$$\sigma^2 = \frac{2\gamma E}{\pi a} \quad (2)$$

Accordingly the energy release rate  $G$  and the surface tension may be related by the expressions;

$$\sigma^2 = \frac{GE}{\pi a} \quad (3)$$

where

$$G = 2\gamma$$

Modifications and extensions to the basic Griffith energy

relationships were derived by Irwin (2) and extended by Orowan (3). In 1947, Irwin postulated that a complete understanding of the analysis of crack propagation could be achieved if one considered the imbalance between the Griffith theory strain energy release rate, and the plastic work required for crack extension. From results on slow bend tests of low carbon steels Irwin proposed a mechanism for fast fracture based on the general instability relation,

$$\frac{de}{dA} = \frac{dW}{dA} \quad (5)$$

where  $dA$  = incremental fracture area  
 $dW$  = work done  
 $de$  = release of strain energy

Irwin concluded that when the slope  $dW/dA$  changes abruptly fast fracture occurs. Irwin and Kies (8) published a theory of fracture dynamics in 1952 relating the instability criterion to pressure vessel design.

During this same period, Orowan (3) introduced the concept of plastic work - "p" to account for plastic distortion at the fracture surface. He concluded that the brittle fracture of steels could be analysed by adopting a modified Griffith Relation:

$$\sigma^2 = \frac{2pE}{\pi a} \quad (6)$$

In 1954, Irwin and Kies<sup>(9)</sup> obtained expressions relating the strain energy release rate to specimen compliance changes due to crack growth. In a paper released in 1957, Irwin (7) related the Griffith strain energy release rate to the stress and strain at the leading edge of a tensile (Mode I) crack opening. It is this crack stress field analysis by Irwin, based on the Griffith energy balance, which forms the basis for the Linear Elastic Fracture Mechanics method of analysis.

For purposes of linear stress analysis, a crack is regarded as a flat separation bounded within the material by a leading edge that is approximated as a simple curve. The Irwin crack model is shown in Figure 1, and the analysis is based on a plane strain stress system. A tensile (Mode I) crack stress system is assumed, although Modes II and III may be used (Figure 2).

The crack stress field analysis is derived using a mathematical model relating linear elasticity to the stress intensity factor "K". It is based on the earlier semi-inverse method of Westergaard (10), who derived a two dimensional stress solution for a Mode I crack in an infinite plate using complex variables and an Airy stress function.

Irwin applied this analysis to the portion of the elastic stress field which enclosed the advancing edge of the crack (Figure 1). He noted that the Mode I tensile force results in elevated tension adjacent to the perimeter of the leading crack edge, which is somewhat relaxed by local plastic strains confined to the plastic zone (dotted



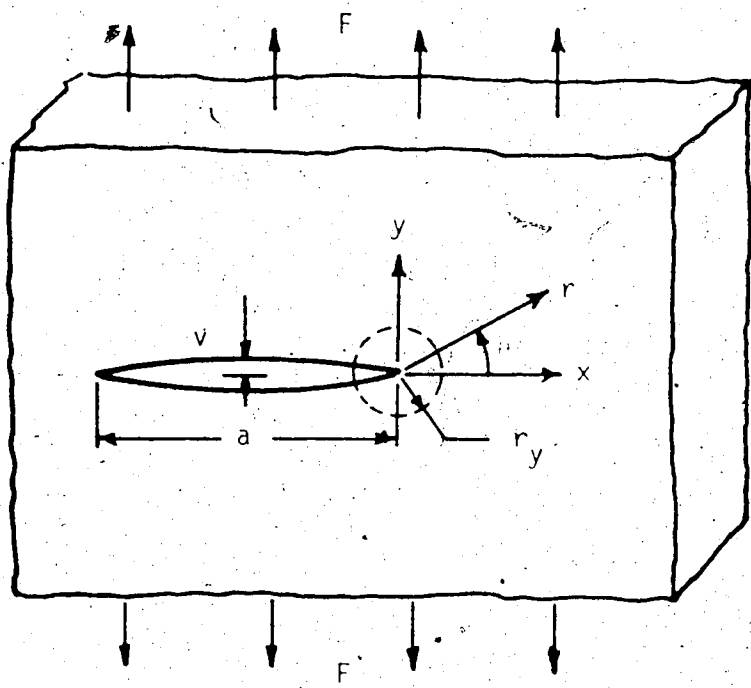


Figure 1. Irwin Crack Model

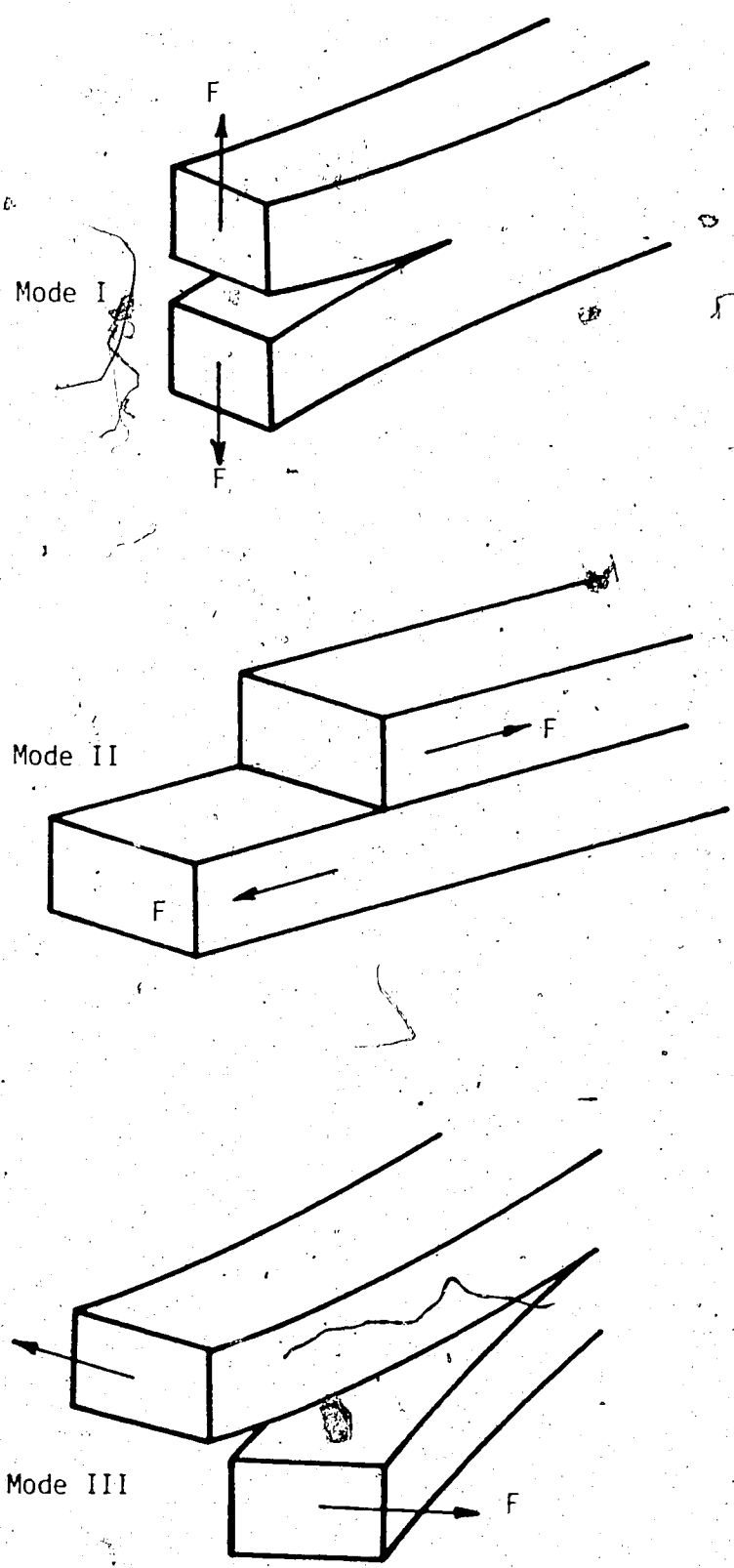


Figure 2 Modes of Fracture

portion of Figure 1). Because the plastic zone may be regarded as a line disturbance zone, the locus for the leading edge is set at a central position.

Based on the Westergaard solutions, the Irwin (7) Mode I crack stress field stress values are:

$$\sigma_x = \frac{K_I}{\sqrt{2\pi r}} \cos \frac{\theta}{2} \left( 1 - \sin \frac{\theta}{2} \sin \frac{3\theta}{2} \right) \quad (7a)$$

$$\sigma_y = \frac{K_I}{\sqrt{2\pi r}} \cos \frac{\theta}{2} \left( 1 + \sin \frac{\theta}{2} \sin \frac{3\theta}{2} \right) \quad (7b)$$

$$\tau_{xy} = \frac{K_I}{\sqrt{2\pi r}} \sin \frac{\theta}{2} \cos \frac{\theta}{2} \cos \frac{3\theta}{2} \quad (7c)$$

$$\tau_{xz} = \tau_{yz} = 0 \quad (7d)$$

additionally, for plane stress  $\sigma_z = 0$  (8)

for plane strain,  $\epsilon_z = \nu (\epsilon_x + \epsilon_y)$  (8b)

and  $K = \sigma \sqrt{\pi a}$  [ $\theta=0, r=a$ ] (9)

The crack opening displacement is given by the relationship:

$$v = \frac{2K}{\pi E} (1-\nu^2) \sqrt{2\pi r} \quad (10)$$

The stress intensity factor K may be related to the Griffith theory

strain energy release rate  $G$  by the equations;

$$K^2 = EG \text{ for plane stress} \quad (11a)$$

$$K^2 = \frac{EG}{1-\nu^2} \text{ for plane strain} \quad (11b)$$

In papers published prior to 1960 (11), the stress intensity is sometimes given by  $K$  (script  $K$ ) which may be related to  $K$  (for Kies) by the relation;

$$K = \pi^2 K \quad (12)$$

Values of fracture toughness, stress intensity factors and strain energy release rates are usually given a subscript "c" to indicate critical values at the onset of rapid crack propagation.

### 2.3 Plastic Zone Influence

To satisfy free surface conditions at the crack surfaces, the stress system adjacent to the advancing edge must be one of plane strain. However, for a through thickness crack (12), the zone of yielding at the advancing edge tends to relax the stress in the thickness direction, and thus the conditions for plane strain are not satisfied. Evidence of this may be seen at the crack plate intersection with the surfaces where the fracturing mode changes from flat tensile to shear. Irwin (12) proposed a representation of this plastic zone stress relaxing influence, in terms of specimen thickness and

fracture toughness. The relation may be arrived at by setting  $\theta = 0$  in equation 7b, from which;

$$\sigma_y = K/\sqrt{2\pi r} \quad \text{at } \theta = 0$$

If the plastic zone radius is denoted by  $r = r_y$ , an estimate of this radius is expressed as (12)

$$r_y = \frac{1}{2\pi} (K/\sigma_y)^2 \quad (13)$$

In general for minimum specimen thickness, the plastic zone size must not intersect the plate thickness, so that plane strain conditions are maintained. Accordingly, for a plate specimen of thickness "B", a non dimensional parameter  $\epsilon_c$  may be defined (13) and is given by:

$$\epsilon_c = \frac{1}{B} (K/\sigma_y)^2 \quad (14)$$

The critical value  $\epsilon_c$  occurs at  $\epsilon_c = 2\pi$  and this degree of toughness is considered as defining a critical crack size at  $r = r_y$  with an effective through crack length approximately equal to  $2B$  (13).

Since  $\epsilon_c$  gives the ratio of the plastic zone size to the material thickness, a decrease in the value of  $\epsilon_c$  indicates that the constraint at the crack tip exhibits a greater degree of plane strain.

Because the plastic zone shape is significant in determining the mode of fracture, other attempts have been made by McClintok and

Irwin (14) and by Wells and Post (15) to define the plastic zone. Presently, Irwin's original approximation is used extensively as the basis for linear stress field analysis.

#### 2.4 Onset and Arrest of Fast Fracture

The stress intensity factor  $K$ , or the crack extension force  $G$  provide a simple one parameter characterization of the stresses tending to promote crack extension. For practical purposes, crack behavior is based on the determination of the critical value of fracture toughness for Mode I behavior. Most research programs utilize plane strain stress systems.

It has been observed during testing, that as  $K_I$  is increased, a crack may be seen to change abruptly from a slowly extending or stationary crack, to a rapidly running (propagating) crack. This point of instability during onset of fast fracture is designated as the critical toughness value  $K_{Ic}$  (13). Similarly, the value of the fracture toughness at the abrupt change from a running crack to an arrested crack is designated by  $K_{Ia}$ , the crack arrest toughness.

#### 2.5 Experimental Test Methods

Practical application of the theory of Linear Elastic Fracture Mechanics requires that the plate thickness meet the requirements of the test stress system in order to control and eliminate plastic zone effects (16). Further it requires that the laboratory test system duplicate expected in-service conditions as nearly as possible.

A number of static and dynamic fracture toughness test methods

have been developed and some have been utilized universally. Generally, for a standard test method, universal acceptance can be attributed to such factors as overall simplicity, low capital equipment costs, ease of specimen preparation, duration of test cycle and consistently predictable results.

Generally all of the tests involve the introduction of one or more notches and the observation of brittle ductile behavior as the test temperature is varied. Additionally, impact tests try to reproduce the dynamic aspects of a propagating crack in an attempt to correlate with service failures. Because each of the tests may emphasize different features of the brittle fracture process, it is found that they tend to rate the toughness of a material differently (6).

The Charpy V-Notch and the Three Point Notch Bend tests employed for this research program, are recognized universally as standards to evaluate toughness of many engineering materials. The third test method, -- Double-Cantilever Beam (DCB) test, was developed only recently to permit laboratory studies and analysis of fracture behavior of running cracks. Hoagland (17) has had moderate success with this test method, as has Schwab (18) using a contoured DCB specimen.

#### 2.5.1 Charpy Impact Test

The Charpy impact test is the best known and most popular method of determining fracture behavior. The Charpy test is used to evaluate the fracture characteristics of a material in the presence of a defect; as well as to correlate between other tests (6). Details of the standard Charpy impact testing procedure are specified in ASTM

specification E23-56T and ASTM STP 381 (19). Generally the V-notch configuration is more widely used, since it is believed to provide a better correlation with service behavior. For all Charpy tests the fracture appearance is the criteria, as the energy absorbed is a variable for different steels. For tests on pipeline materials the 2/3<sup>f</sup> subsize Charpy is used. The standard testpiece configuration is shown in Figure 14. For most Charpy tests, values of energy absorbed versus temperature are recorded, as well as lateral contraction or expansion. Estimates of percentage shear or cleavage area are also made. Some scattering of results is evident in the Charpy test, but considerable reduction of scatter can be achieved by carefully controlling the notch root geometry.

The transition temperature obtained with subsize Charpy specimens is shifted to a lower value due to a decrease in the tri-axiality of the stresses near the root of the notch.

#### 2.5.2 Three Point Notch Bend Test

The notched rectangular section bend specimens were one of the earliest static fracture toughness test methods used. Notch bend tests are suitable for  $K_{IC}$  testing by "pop-in" measurements using a notch terminating in an actual crack. Notch bends are only applicable to  $K_{IC}$  testing when the fracture is predominantly square (19). The load necessary to measure  $K_{IC}$  is less for a bend specimen than any other type, but the accuracy of  $K_{IC}$  is lower due to the greater sensitivity of the calculated value of  $K$  to a small error in the crack depth.



The Standard Three Point Notch Bend specimen configuration is shown in Figure 10 in Chapter III. During testing, values of load versus displacement at various temperatures are recorded. Test data are then analysed and values of  $K_{IC}$  determined using the relationship of Scrawley and Brown (19) later modified by Gross and Scrawley (24) for plane strain conditions:

$$E G_{IC} = (P/B)^2 L^2/W^3 (33.5a/W - 61.7(a/W)^2 + 203(a/W)^3) \quad \text{for } 2 < W/B < 8 \quad (15a)$$

Results may be found in terms of the stress intensity  $K_{IC}$  by substituting for  $G_{IC}$  using equation (11b). Alternatively, test data may be analysed using an Area/Energy method. This technique requires that the surface area of the fracture section be known, and assumes that sections fail cleanly and square. The method cannot be applied accurately in cases where fractures are oblique and not broken through the full specimen depth. With reference to Figure 3, the method of solution is as follows;

The area of the failed section  $A_S$  and the area under the curve  $A_C$  are calculated:

$$A_S = 2(W - a_a) B$$

$$A_C = P\delta/2$$

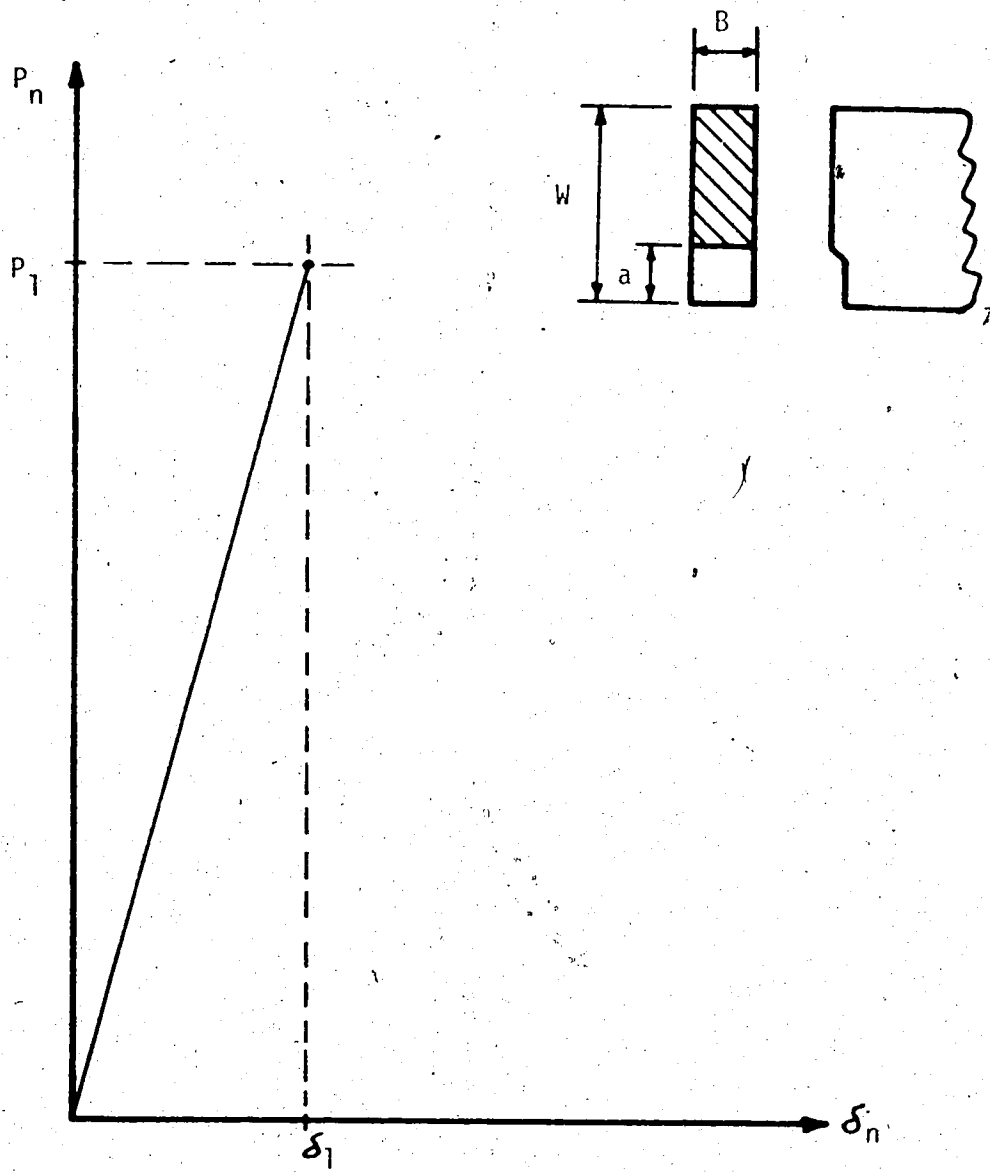


Figure 3 Notch Bend Loading Schematic

Then;

$$\gamma = A_c/A_s = P\delta/2(W-a)B(2)$$

$$G = 2\gamma = 2P\delta/4(W-a)B$$

$$G = P\delta/2B(W-a) \quad (15b)$$

Fracture toughness may be calculated by substituting equation (15b) into equation (11b).

### 2.5.3 Double-Cantilever Beam Test

Recent emphasis on fracture mechanics rate analysis and the desire to obtain a number of plane-strain toughness data from a single specimen of moderate size, has prompted the development of the Double-Cantilever Beam (DCB) specimen by Hoagland (17), and others. Figure 4 shows the standard DCB test specimen and method of loading. The test-piece is of rectangular cross section with two longitudinal opposing milled V-notch sidegrooves; which serve to direct the running crack, maintain a plane-strain stress configuration and form the two specimen arms. Two dowel holes are drilled in one end for tension machine mounting. The crack is started at the pinned end in either a plain sawcut or a sawcut with previously induced fatigue crack. Test data is obtained from a graphical plot of load versus displacement and, in conjunction with specimen compliance, a value of plane-strain fracture toughness  $K_{Ic}$  may be determined.

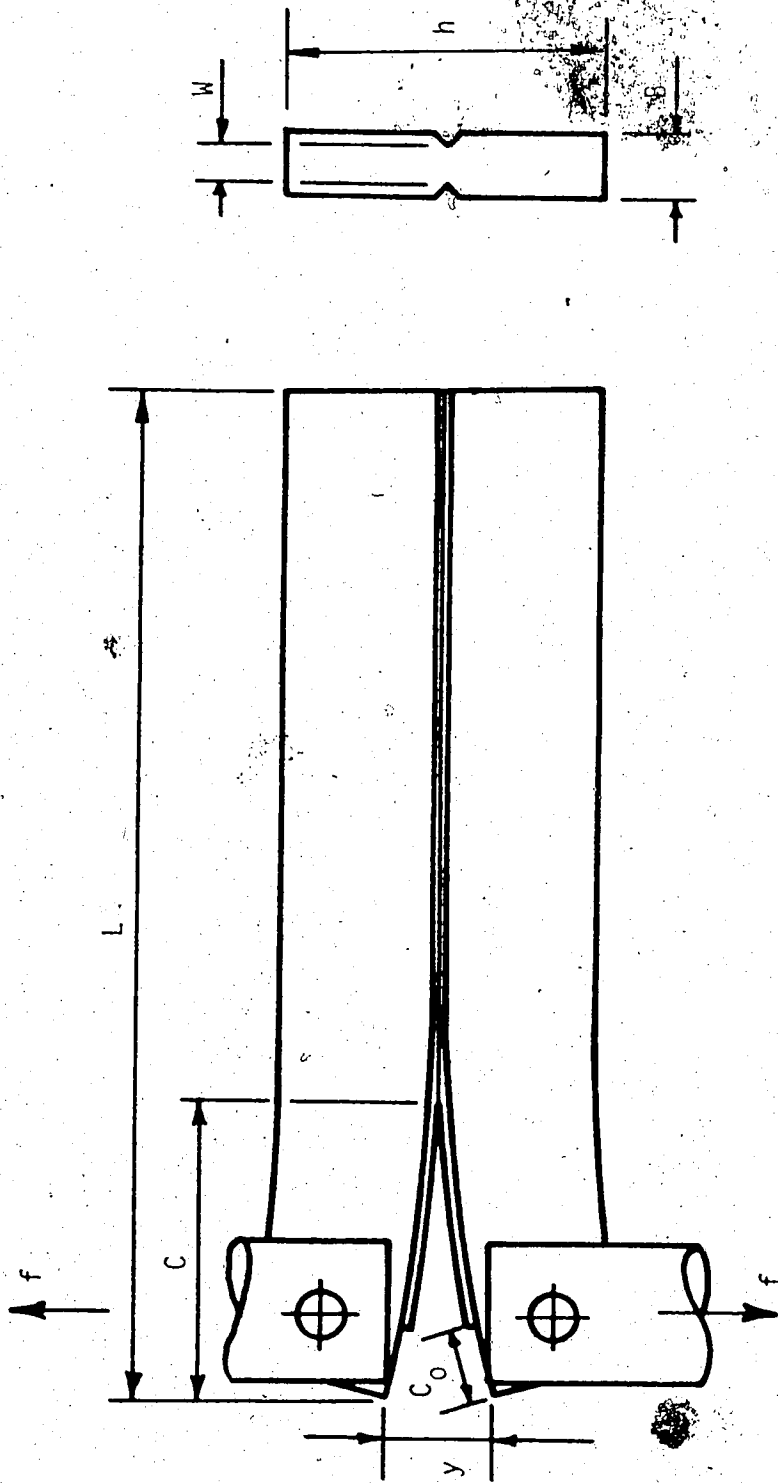


Figure 4 DCB Test Configuration

Advantages cited for the DCB technique include:

1. Both initiation and arrest toughness values may be determined.
2. A number of crack runs may be obtained from a single specimen.
3. Ease of specimen preparation and maximum test material economy.

The inherent advantage is that the technique is based on a running crack, and duplicates in-service crack behavior more accurately.

Extensive analysis of the mechanics of the DCB specimen has been conducted by Berry (20) and Gilman (21), and summarized from the researcher's point of view by Hoagland (17). Hoagland acknowledges that in theory, if a specimen is composed of a material possessing a strain energy release rate which is independent of crack velocity, then stable crack propagation will continue without regard to crack length. However, most materials exhibit some rate sensitive flow and accordingly in DCB specimens, crack instabilities can occur due to the increase in crack resistance force with increasing crack velocity. Thus if the increase in crack length were small relative to the specimen length, a number of fracture data may be obtained from a fracture record of the type shown in Figure 5.

On this basis, Hoagland, using an approach based on an empirical model and certain geometry dependent parameters determined experimentally, has arrived at the following relationship between the applied force and the resultant total deflection of both arms;

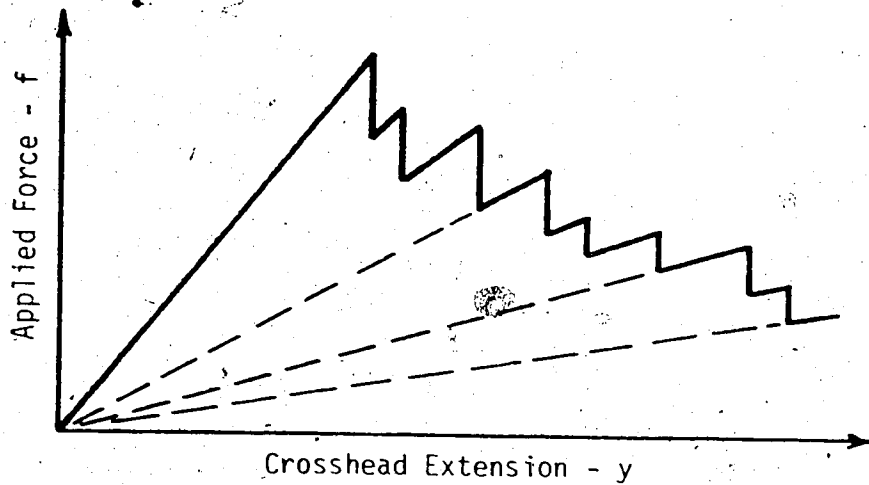


Figure 5 Typical DCB Fracture Behavior

$$y = (\phi/E) f \quad (16)$$

where  $\phi$  = some function of crack length "c" and the moment of inertia "I",

E = modulus of elasticity for the material.

A relationship between  $\phi$  and c may then be determined from the slope of the load extension line when a graphical plot of  $\phi$  versus crack length is made. Analysis of this compliance curve suggests a standard relationship of the form;

$$\phi = Ac^n \quad (17)$$

where A and n are constants. For practical purposes, equation (17)

is found to afford a good approximation to specimen data, except when

the crack is very long or very short relative to the length of the specimen. Hoagland has shown that the variation in  $A$  with moment of inertia for a given beam depth is given by the relationship;

$$A = C_1/I \quad (18)$$

where  $C_1$  is a constant.

Substituting in equation (16) for the appropriate variables yields:

$$y = \frac{f C_1 c^n}{E I} \quad (19)$$

which is of the same form as the simple cantilever beam formula

$$y = \frac{2 f c^3}{3EI} \quad (20)$$

Irwin and Kies (9) have shown that the value of the strain energy release rate  $G$  may be determined experimentally and together with equation (16) will yield the following relationship:

$$G = \frac{f^2 d (\phi)}{2wE dc} \quad (21)$$

Substituting equations (17) and (19) into (21) yields,

$$G = \left( \frac{ny^2 E}{2wA} \right) \left( \frac{Af}{E'v} \right)^{\frac{n-1}{n}} \quad (22)$$

Equation (22) can then be rewritten in terms of  $K_{IC}$  by employing equation (11b). Compliance constants  $A$  and  $n$  are determined experimentally from results of actual physical tests.

## 2.6 Material Damage

An important observation was published by Mylonas et al (23) in 1958 after conducting static laboratory tests on the effects of material damage on steel. It was noticed that by first applying pre-compression/prestrain beyond gross yield and then testing the same specimen in static central tension through failure, that fractures would initiate at average net stresses well below yield. Physical tests were conducted on 3/4 inch by 10 inch square pedigree rimmed project steel type "E" of high brittle-transition range, at temperatures below the lower end of the transition range. The plates fractured at average net stresses below yield level; the lowest was observed to fail at 36% of virgin yield. Mylonas concluded that static initiation of brittle fracture can be achieved by an additional exhaustion of ductility.



## CHAPTER III

### EXPERIMENTAL TEST SPECIFICATIONS

#### 3.1 Introduction

In this chapter the extent of the experimental research program is detailed. Properties of test materials, relevant specimen preparation techniques and details of the three fracture toughness test methods adopted - Three Point Notch Bend, Double-Cantilever Beam and Pre-Cracked 2/3 Charpy V-Notch, are presented. Possible sources of error are also discussed.

#### 3.2 Test Material

Thirty-six inch (outside diameter) API-5LX-65 submerged arc longitudinally welded pipe and parent plate material was used for the majority of the experimental tests conducted. The X65 pipe steel received from Canadian Phoenix Pipe and Steel, consisted of a finished 3 foot long pipe cylinder (Figure 6) and matching adjacent 3 foot by 9 foot plate sheet, (Figure 7) both pieces being from the same heat. The manufacturer's chemical composition and mechanical properties are presented in Tables 3.1 and 3.2 respectively. Fracture toughness evaluation of a line pipe "sinusoidal sawtooth" fracture segment, obtained from an early service failure in a 6 inch diameter pipeline, (Figure 8, 9), was also undertaken. Manufacturer's chemical and mechanical specifications for this latter pipe steel were not available.



Figure 6 Finished X65 Pipe Cylinder



Figure 7 Unformed X65 Skelp Plate



Figure 8 Sawtooth Fracture Segment



Figure 9 Profile Sawtooth Fracture Segment

Table 3.1  
Nominal Chemical Composition - X65 Pipe Steel

	C	Mn	P	S	Si	Co
Ladle specification	0.23	1.33	0.006	0.019	0.03	0.05
Phoenix Check Analysis	0.21	1.28	--	--	--	--

Table 3.2  
Mechanical Properties - X65 Steel\*

Identification: Serial No. CM4302TX  
Top Cut 387  
Heat 353761

Nominal Mechanical Properties

Transverse tensile; 69,700 psi @ 0.05% elongation

Elongation in 2 inch gauge: 34%

Ultimate Tensile

Transverse weld (12:00): 98,100 psi

6:00 Position: 92,300 psi

\*Properties as determined from standard mill tests of Canadian Phoenix Pipe and Steel Ltd., Calgary

### 3.3 Test Material Allocation

The Phoenix X65 pipe and plate sections are shown in Figures 6 and 7. Testpiece locations were chosen to facilitate data correlation between the finished pipe cylinder and plate, the matching unrolled materials and between the various fracture toughness test methods. It was anticipated that this would increase chances for successful development of one or more reliable fracture test methods for pipeline materials.

In order to permit individual specimens to be removed using a band saw, the unrolled X65 plate and the pipe cylinder were torch cut into three (I, II, III) and four (I, II, III, IV) sections respectively. In keeping with current industry reference practice, the submerged arc weld was chosen as the 12 o'clock datum, and individual test pieces were then removed at the 3, 6, and 9 o'clock positions. In all cases a minimum setback of two inches was maintained at the torch cut edges in order to minimize possible adverse effects due to localized heating. Before cutting with the upright bandsaw, testpieces were identified by punch marking. Detailed plate and pipe section subdivision is shown schematically in Figures A1 through A6 in the appendix.

The tight radius of the 6 inch pipe "sawtooth fracture" segment dictated that either Three Point Notch Bend or 2/3 Charpy V-Notch specimens be used. The former were chosen and test piece locations are shown schematically in Figure A7 of the appendix.

### 3.4 Specimen Precracking

In order to simulate field service failure crack notch root conditions as closely as possible, the test specimens used in all three types of physical toughness tests were deliberately artificially precracked.

In accordance with specifications outlined in ASTM STP 381 (19) Notch Bend and Charpy V-Notch specimens were precracked using an Unholtz Dickie Vibration System with Model 100 Electrodynamic shaker table. Specimens were mounted two at one time with notch up on the shaker table, as fixed end cantilever beams. The nominal fiber stress level at the reduced notch section was set at 40 percent of yield stress. During precracking this level was maintained by controlling the amount of free end deflection. Difficulties commonly associated in attempting visual observation of notch root crack progress were obviated by surface grinding and polishing both sides of the specimen full width at the notch.

To precrack the 2/3 Charpy specimens on the shaker table it was necessary to attach an extra weight to their free end. Depth of Charpy notch root precrack was approximately one millimeter and a nominal precrack notch root stress level of 40 percent of yield stress was maintained.

Owing to configuration and size, DCB specimens could not be precracked on the shaker table. Precracking of Double Cantilever Beam specimens was accomplished by cycling in a Sontag Universal Fatigue Testing Machine model SF-1-U, for approximately 150,000 cycles, at a

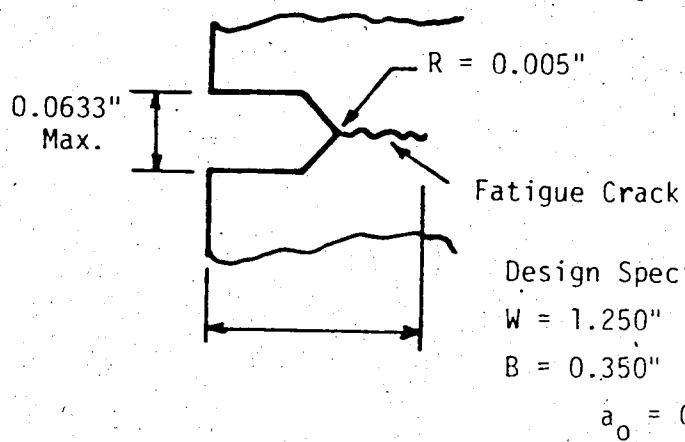
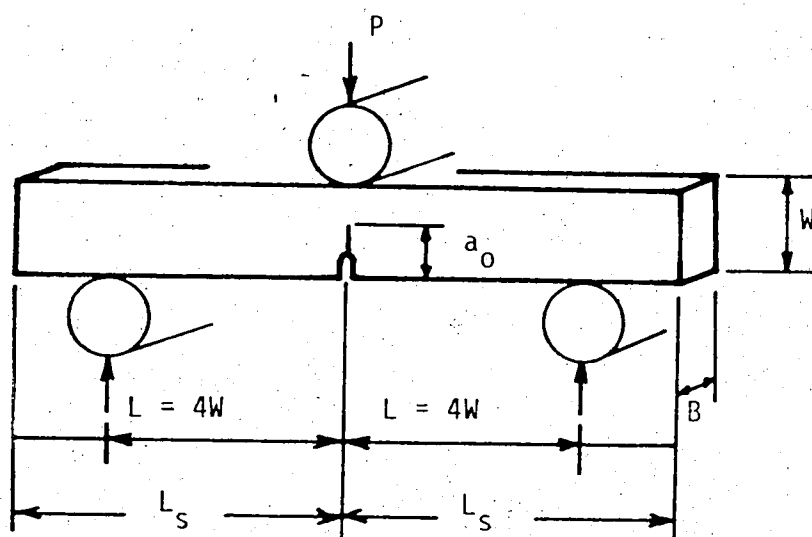
nominal notch root stress level of 40 percent of yield stress. Crack progress on all DCB specimens was difficult to observe; a factor which accounted for the wide variation in DCB fatigue crack lengths. To assist visual observation of crack progress, a combination magnifier lens and light source, dye and ink in the notch root as well as other techniques were tried with limited improvement. Usually specimens cycled the order of 150,000 cycles exhibited reasonable crack progression although specimen cycle histories varied from 80,000 to 400,000 cycles.

### 3.5 Experimental Methods - Three Point Notch Bend

#### 3.5.1 Bend Specimen Design

Notch Bend Specimens are an acceptable fracture toughness indicator for high strength materials and had been used previously with varying degrees of success on medium strength steels. Accordingly, it was decided to use these specimens in this research program.

The bend specimen used in all tests was of the conventional notched rectangular section, three point loaded, single-edge-notch type. Test piece dimensions and notch specifications were chosen in accordance with currently accepted standards of the American Society for Testing Materials cited by Scrawley and Brown (19). Figure 10 details the Notch Bend specimen configuration used for all X65 pipe steel tests. A U-shaped notch of 0.005 inch root radius with natural fatigue precrack was chosen. Notches were prepared using a fly cutter ground to the prescribed root radius. Fly cutter notch root radius was checked periodically for wear using a shadowgraph comparator.



Design Specifications:  $2 < W/B < 8$

$W = 1.250''$        $L_s = 6.0''$

$B = 0.350''$        $L = 5.0''$

$a_0 = 0.25''$

Figure 10 Three Point Notch Bend  
Specimen Configuration



### 3.5.2 Specimen Removal

Notch Bend specimens were removed from the X65 plate material in both the transverse and longitudinal directions to determine the influence of material anisotropy. Pipe cylinder Notch Bends were taken only in the longitudinal direction, as it was considered that cold working of the material in the region of the notch midsection occasioned during coupon straightening, would adversely influence test results. Presently, industry prepares transverse test coupons from material which has been flattened in a hydraulic press\*.

Because of the large pipe cylinder diameter (36 inch), it was not considered necessary to mill the inner and outer surfaces of the longitudinal Notch Bend specimens to offset the effects of eccentric loading. Instead, machined specimens were carefully checked to ensure that the top and bottom faces of each specimen were parallel, so that loading would be as nearly axial as possible. A total of 95 Notch Bend specimens were prepared from the X65 pipe and plate material.

Six longitudinal Three Point Notch Bend specimens designated as  $S_1$  through  $S_6$ , were cut from the 6 inch diameter "sawtooth fracture" segment. Sawtooth notch bends were prepared analogous to the X65 specimens, except that the inner and outer surfaces were machined flat. Nominal sawtooth specimen dimensions are presented in Table 3.3 where length designations are as previously defined in Figure 10.

---

\*Observations IPSCO mill 1970-71

Table 3.3  
Sawtooth Fracture Segment Three Point Notch  
Bend Nominal Specimen Dimensions

$$W = 0.80 \text{ in.}$$

$$a_0 = 0.16 \text{ in.}$$

$$L = 3.20 \text{ in.}$$

$$L_s = 3.50 \text{ in.}$$

### 3.5.3 Notch Bend Test Facilities

All Three Point Notch Bend Tests were conducted using a Gilmore Universal Testing System and a Hewlett Packard-Moseley Autograf X-Y Plotter Model 2D-2A. The Gilmore testing machine and cold temperature bath are shown in Figure 11. A one-half inch thick gusseted base structure was fabricated to support the bath. The cold temperature bath consisted of an inner flat bottom steel tank with drain valve, insulated from an outer plywood jacket with 1 inch styrofoam insulation on four sides. Two one inch by two inch steel bars were positioned to minimize deflection of the bath bottom plate, and to allow placement of one inch thick styrofoam sheet insulation between the bath and the support structure.

Specimen tests at temperatures from ambient to minus 120 degrees Centigrade were conducted using commercial grade 97 percent ethanol as the coolant medium. Temperatures through minus 70 degrees centigrade were obtained by adding dry ice (solid  $\text{CO}_2$ ) to the ethanol.

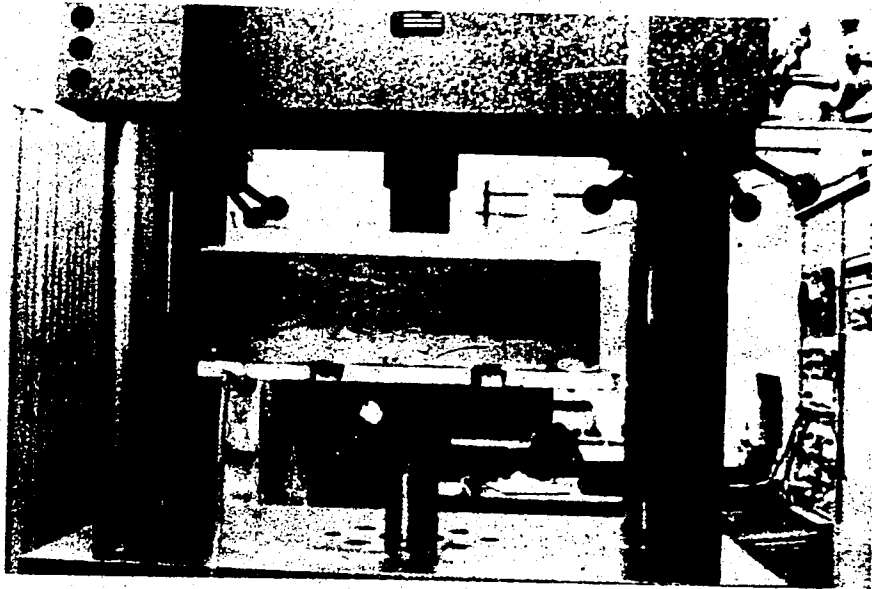


Figure 11 Gilmore with Low Temperature Bath

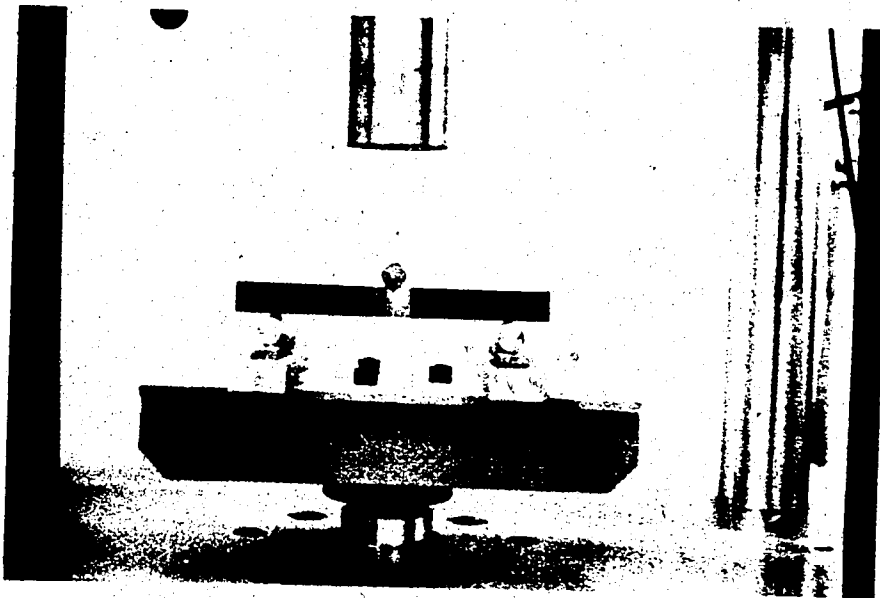


Figure 12 Specimen Positioned for Notch Precompression

Lower test temperatures to minus 115 degrees centigrade were achieved by first cooling rapidly to minus 70 degrees centigrade using dry ice, then cooling with liquid nitrogen to the desired temperature level.

Midrange - minus 160 degree centigrade specimen tests, were attempted using normal pentane as the coolant medium. These were discontinued after an explosion occurred. Specimen tests at minus 193 degrees were conducted by filling the bath with liquid nitrogen.

During all tests, a ten minute holding time at temperature was maintained prior to testing. Two thermometers located on either side of the notch midsection were used to verify specimen temperature and minimize errors. Experimental test records were obtained graphically by plotting a load-displacement record for each specimen using the X-Y plotter. X-Y recorder input was connected directly through the Gilmore console, eliminating the use of shielded coaxial leads. Notch bend tests were conducted in the powerhouse mechanical testing laboratory during 1970 building renovations and accordingly, wide fluctuations in room temperatures from 60 to 100°F were experienced.

#### 3.5.4 Notch Bend Specimen Testing Procedures

Pipeline materials are low to medium strength steels and are generally strain rate sensitive. To overcome this a uniform strain rate is used throughout. Accordingly a constant maximum Notch Bend loading rate of 4,000 pounds per minute was used. The programmed rate control capability of the Gilmore testing system was found to be particularly well suited for this application. Controlled loading was accomplished by programming a sawtooth ramp input control

function and monitoring automatically in the load mode sequence. Calibration of the X-Y recorder was done by manually loading each testpiece in successive 100 pound increments to 500 pounds maximum. Crosshead displacement was recorded using the Gilmore visual digital readout. The latter was verified by comparing the center notch deflection obtained from two dial gauges with the Gilmore Wavetek readings. To reduce electronic equipment errors, the Gilmore console was allowed to warmup for a period of one-half hour before being used. As a further precaution, digital readout calibrations (load versus displacement) were taken for all tests. This latter procedure was mandatory in the very low temperature ranges (below minus 60 degrees centigrade) due to noticeable cooling of the bath lower support structure and upper loading cylinder.

During a typical testing sequence, Notch Bend testpieces were first positioned notch down, on two one inch diameter support rollers located as shown in Figure 10. A third roller was centered immediately opposite the notch root. Once placed in position, a static load of approximately ten pounds was held on each specimen. This was done to prevent movement due to vigorous coolant boiling as the specimen was cooled to the desired test temperature. The X-Y plotter was calibrated by plotting load versus displacement in one hundred pound increments through 500 pounds and back to zero load. The specimen was then loaded automatically in the constant load mode sequence through to failure. At temperatures resulting in ductile failures, specimens were loaded to a maximum center deflection of one inch, as limited by specimen

contact with the bottom of the cold temperature bath. After testing, approximately one half of the ethanol was drained to permit accurate positioning of the next test specimen. During all tests, temperature readings using two thermometers positioned on either side of the notch root, were taken at the start and finish of each test run. Average temperature values were recorded.

#### 3.5.5 Material Damage - Precompression

The effects of material precompression, occasioned by material damage resulting from machinery impact of the type observed during pipeline laying or backfilling operations, are recognized to be significant factors. Investigators have linked material damage as direct causes of in-service pipeline failures.

In order to experimentally assess the influence and effects of material damage on X65 line materials, Notch Bend specimens at the 9 o'clock position were precompressed at the notch root region. All specimens were precompressed at room temperature using a loading rate of 1,500 pounds per minute. Specimens were first positioned as shown in Figure 12 and then loaded until yielding of the material at the notch root occurred. The yield point was verified by observing the deviation from linearity of the load versus crosshead displacement record. At yield, loading records indicate that notch root stress levels were typically of the order of 1.1 to 1.4 times nominal yield stress.

Precompression damage resulted in bulging of material at the notch root area, some closing of the U-notch and a prominent com-

pression zone, as evidenced by a series of fine concentric distortion lines symmetrically positioned about the notch root. Precompressed specimens were then tested in accordance with the standard Notch Bend procedure.

### 3.6 Tensile Tests

Tension tests were conducted in accordance with specimen specifications outlined in API Standard 5LX and ASTM Standard A370. Transverse plate specimens and longitudinal plate and pipe cylinder specimens of the configuration shown in Figure 13 were used.

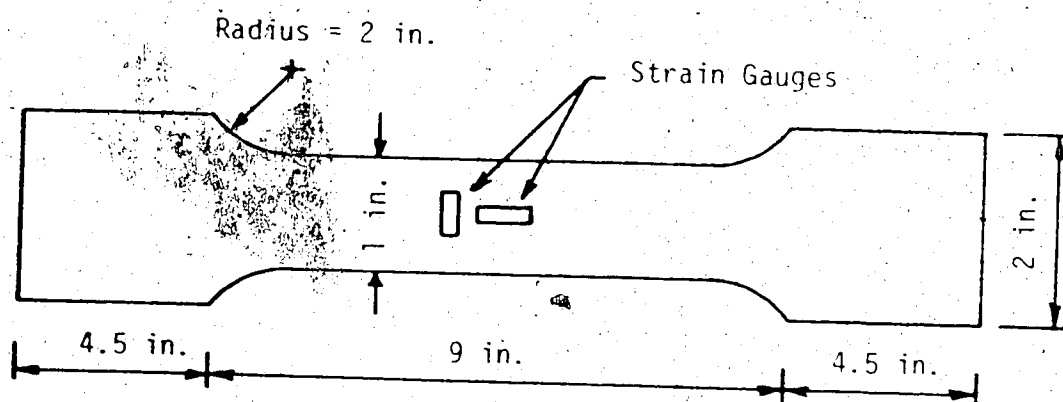


Figure 13 Schematic - 1e Specimen Design

A Tinius Olsen Deluxe Super L - 400,000 pound Universal Testing machine was used for the tensile tests. All tests were conducted at room temperature. Specimens were loaded to failure with load and strain values being recorded at 1,000 pound intervals. A four arm strain gauge bridge circuit was used throughout and final results were based on the average of two strain gauge values. During

each test, a secondary check of material performance was made using an Olsen S-400-2AB extensometer of two inch gauge length. A plot of load versus strain was obtained on the Tinius Olsen Chart Recorder.

Strain gauges were placed symmetrically about the specimen centerline. Standard and high elongation (15%) strain gauges were used for tests on both plate and pipe materials.

### 3.7 Two-Thirds Charpy V-Notch Tests

#### 3.7.1 Charpy Specimen Design

As Charpy impact energy values are a recognized fracture toughness indicator in the design of pressure vessels and pipelines, it was decided to obtain Charpy V-Notch impact values for the X65 pipe materials.

The limited plate thickness of 0.350 inches dictated that a Two-Thirds Charpy specimen configuration be used. Testpiece dimensions were chosen in accordance with the standards of the American Gas Association (6) and the ASMT (19) per Figure 14. A pre-cracked V-notch design was adopted to reduce notch effects. Pre-cracking was accomplished using an Unholtz-Dickie Vibration System.

Specimens were removed at the 3 o'clock position from the plate and pipe, in both the transverse and longitudinal directions. Charpy test specimens were prepared from one of the halves of the failed notch bend specimens, with four specimens being obtained from each. These were located alphabetically as either the A, B, C, or D subsection of the respective Notch Bend Location. A total of 118 Charpy specimens were machined and precracked.



$$L = 2.165''$$

$$B = 0.262''$$

$$W = 0.394''$$

$$a_0 = 0.079''$$

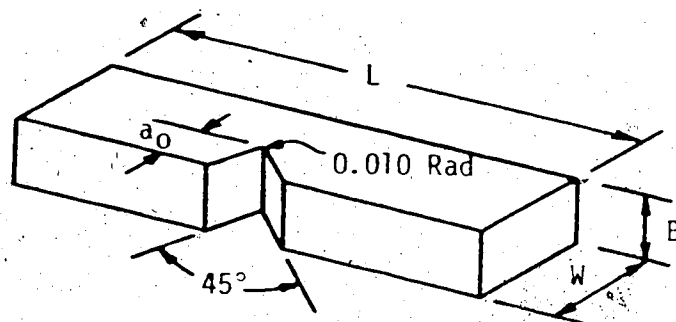


Figure 14 Two-Thirds Charpy Test Specimen

### 3.7.2 Charpy Test Facilities and Loading Procedure

A conventional Tinius Olsen free pendulum impact testing machine was used. Tests were conducted from minus 100 degrees centigrade to plus 100 degrees centigrade. Cold temperature Charpy test pieces were pre-cooled to the required temperature in an ethanol low temperature bath and held for ten minutes before testing. The cold temperature bath was positioned adjacent to the impact tester. This permitted rapid transfer and positioning of the test specimens, thus minimizing heat gain from the surroundings. To reduce errors, three Charpy specimens were tested at each temperature. Temperature and energy absorption values were recorded for each test. Fracture surfaces were analyzed using a magnifier with square grid lines to determine the

percentage shear values. "Hot" Charpy tests were conducted using specimens warmed to the required temperature by immersing in heated water. All Charpy specimens had identification marks on both ends to allow rapid test sequences at the given temperature.

### 3.8 Double-Cantilever Beam Test

#### 3.8.1 Specimen Design

Double-Cantilever Beam fracture toughness test procedures were developed by Hoagland (17) and others (18) to obtain an average toughness value from multiple crack runs and arrests using a single testpiece. DCB toughness results from tests on Nuclear Reactor and other high strength steels have proven successful. Tests on medium strength materials such as line pipe steels have met with limited success. Accordingly, it was decided to attempt to obtain DCB toughness data on the X65 pipe steel, and to correlate such data with results from the Charpy and Notch Bend tests.

Preliminary Double Cantilever Beam specimen design was determined in accordance with size specifications and recommendations of Hoagland (17) and Radon and Turner (4). The 0.350 inch material thickness was a governing factor in specimen sizing. After initial tests using cold-rolled and mild-steel materials of various beam depths and side groove angles were completed, the configuration shown in Figure 15 was chosen for the DCB plate specimens. Testpieces were removed from the X65 plate in both the transverse and longitudinal directions at locations as shown in Figures A1, A2, and A3 of Appendix

A. 8

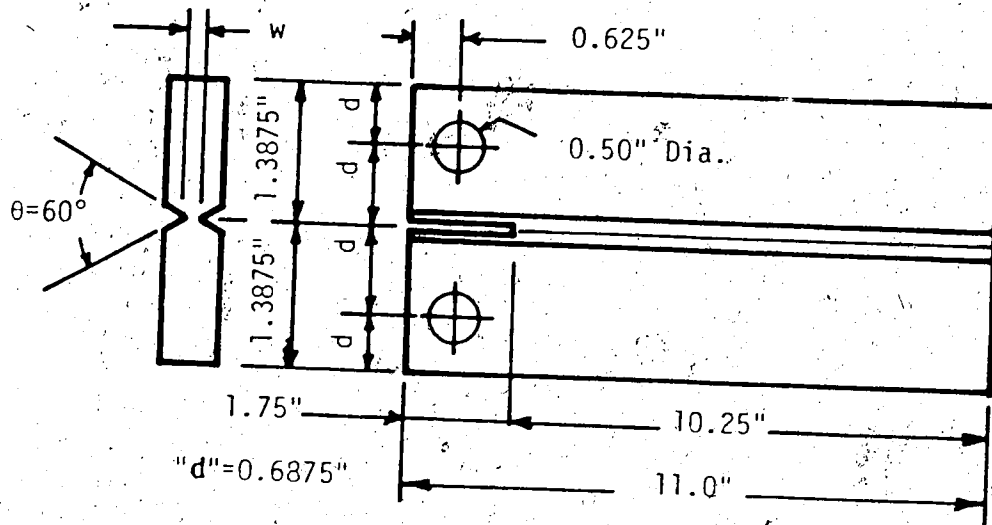


Figure 15 DCB Plate Test Specimen

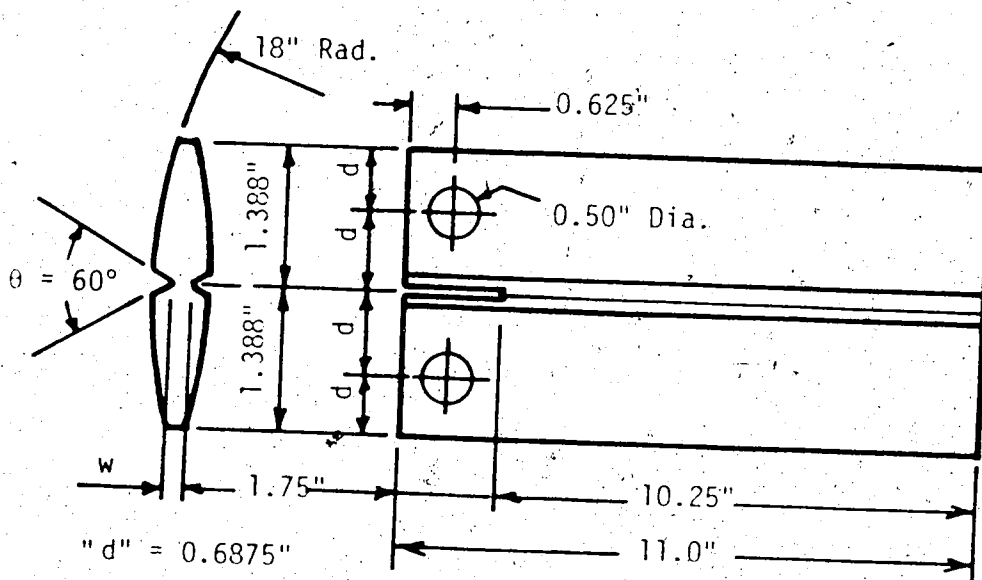


Figure 16 DCB Pipe Test Specimen

DCB specimens were removed from the pipe cylinder in the longitudinal direction only, as the pipe radius in the transverse direction would have necessitated rolling or hydraulically flattening each specimen before machining. The inner (concave) surface of the pipe DCB specimens was milled in four facets to closely approximate the radius of curvature of the outside (convex) pipe surface (see Figure 16), to minimize possible load eccentricity during testing. Pipe DCB specimens were removed at positions indicated in Figures A4, A5, A6 of Appendix A. Final pipe DCB specimen design is shown in Figure 16.

The starting crack notch for all DCB specimens was prepared by hacksawing the V-groove side notch cantilever to a depth of 1-3/4 inch. The notch was then fine cut an additional one-tenth inch deeper with a 0.005 inch notch root radius jewelers saw. DCB specimens were then fatigue cracked on a Sontag Fatigue machine for approximately 150,000 cycles each. After preliminary tests were concluded, it was decided to modify the original specimen design to eliminate arm break off at temperatures above minus 70 degrees centigrade. The sidegroove depth was increased to 0.230 inches from the original 0.170 inches. This was in accordance with the thirty percent net section criteria recommended by Radon and Turner (4). The starter crack notch depth was also increased from the original 1-1/4 inches to 1-3/4 inches; to decrease the load required to initiate a crack run. The decreased load reduced the inherent jump noticeable in the load versus displacement record during the crack initiation to crack arrest phase; and also permitted use of an expanded graphical load scale.

### 3.8.2 DCB Test Facilities

An Instron Universal Testing Instrument System Model TTD Serial 1705 with 20,000 pound load cell and frame capacity, was used for all the tests. DCB test facilities are shown in Figure 17. A schematic diagram of the DCB mounting configuration and O-Ring seal between the bath and lower load head, is shown in Figure 19. Standard 1-1/8 inch diameter O-Rings were used and proved serviceable up to very high rates of crosshead displacement. One-half inch press fit dowel pins were used to vertically position the test specimens. A 3/8 inch diameter pipe drain was installed to drain the coolant from the bath between specimen changes. Commercial grade 97 percent ethanol was used as the coolant medium, and cooling was achieved by adding dry ice and/or liquid nitrogen. Two thermometers were used to verify temperatures. Double Cantilever Beam specimens were tested over a range of temperatures from room temperature to minus 110 degrees centigrade. Additionally, one pipe DCB and one plate DCB specimen were tested at minus 193 degrees centigrade using liquid nitrogen only. Load versus displacement records were obtained for all DCB specimens tested.

During initial DCB testing, some difficulty in zeroing the load record was experienced. This problem was attributed to the overhung mass of the DCB specimen, which tended to cause a slight misalignment of the mounting heads. It was decided to support the free end of the DCB specimen in order to correctly zero the Instron Chart Recorder. This was accomplished by passing a light wire under the free



Figure 17 DCB Test Facilities

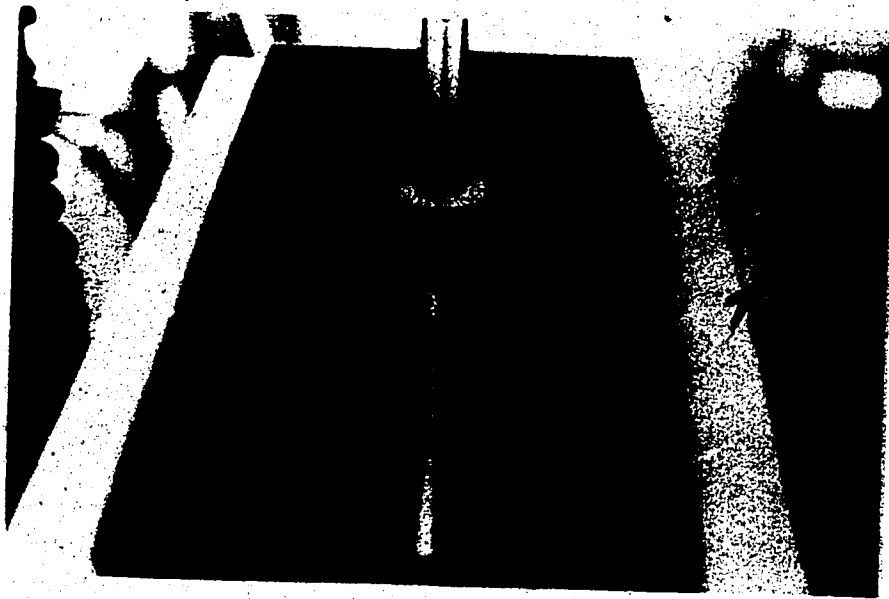


Figure 18 DCB Specimen At Zero Load

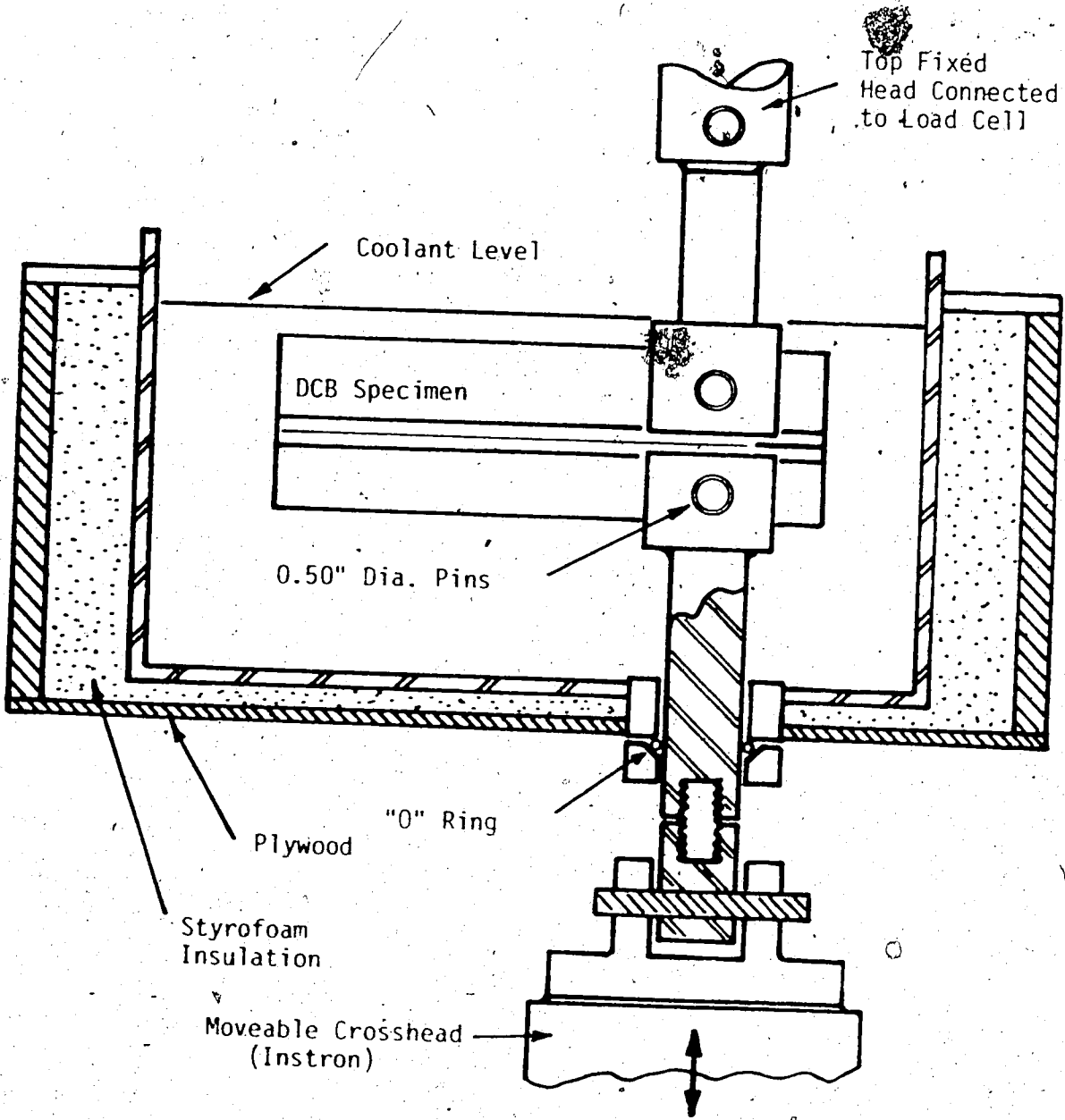


Figure 19 DCB Mounting Schematic

end of the DCB specimen and attaching the ends of the wire to the sides of the bath as shown in Figure 18. Once loaded, the wire support was not required.

### 3.8.3 DCB Loading and Instrumentation

Because it was desired that a correlation between test results be achieved where possible, it was decided to adhere to the 4,000 pounds per minute loading rate used for the Notch Bend tests. It was recognized that a more accurate assessment could be made if the nominal stress level at the base of the notch root of the DCB specimens was the same as that at the notch root of the Notch Bend specimens. Additionally, the DCB notch root stress level would change as each succeeding crack propagated due to an increasing moment arm, while the nominal stress level at the notch root of the Notch Bend specimens would remain approximately constant across the specimen section. Nevertheless, initial crack stress levels for DCB specimens would approximate those for Notch Bend specimens for given test conditions.

Basing all calculations on simple beam theory, the nominal notch root stress levels for Notch Bend and DCB specimens were determined as follows:

Three Point Notch Bend Specimens:

$$a_0 = 0.250 \text{ in.} \quad L = 10.0 \text{ in.}$$

$$\dot{P} = 4000 \text{ lb/min} \quad B = 0.350 \text{ in.}$$

$$W = 1.250 \text{ in.}$$

$$\begin{aligned} \text{at the notch root} \quad Z &= BW^2/6 = 0.350(1.250)^2/6 \\ &= 0.583 \text{ in}^3 \end{aligned}$$



$$\begin{aligned}\dot{S} &= M/Z = PL/4Z = P(10.0)/4(0.0583) \\ &= 42.9P \text{ psi}\end{aligned}$$

$$\text{at } \dot{P} \text{ 4000 lb/min, } \dot{S} = 42.9(4000) = 171,600 \text{ psi/min}$$

#### Double-Cantilever Beam Specimens

$$h = 1.375 \text{ in.} \quad W = 2.75 \text{ in.}$$

$$B = 0.350 \text{ in.} \quad L = 1.125 \text{ in.}$$

$$\text{at the notch root} \quad Z = Bh^2/6 = 0.350(1.375)^2/6 = 0.038 \text{ in}^3$$

$$\begin{aligned}I &= Bh^3/12 = 0.12(1.375)^3/12 \\ &= 0.026 \text{ in}^4\end{aligned}$$

$$\begin{aligned}\dot{S} &= M/Z = PL/2Z = P(1.125)/2(0.038) \\ &= 5.14P \text{ psi}\end{aligned}$$

To maintain the same nominal stress levels;

$$\dot{S}_{NB} = \dot{S}_{DCB} = 171,600 \text{ psi/min}$$

Therefore:

$$\dot{S}_{DCB} = 5.14P_{DCB} = 171,600$$

and

$$P_{DCB} = 33,400 \text{ #/min.}$$

To determine the required crosshead rate:

$$\begin{aligned}\delta &= PL^3/3EI = 33,400(1.125)^3/3(30 \times 10^6)(0.026) \\ &= 0.00715 \text{ in/min}\end{aligned}$$

The total required crosshead displacement is:

$$\delta = 2\delta = 2(0.00715) = 0.015 \text{ in/min}$$

Instron crosshead rates are controlled by varying gear ratios between "low-High" and "Driver" sectors in even multiples. Accordingly a crosshead speed of 0.02 in/per minute was selected. Initial tests on the short starter notch DCB specimens were conducted using a cross head speed of 0.005 in per minute.

All test records of Double-Cantilever Beam tests were obtained by plotting load versus crosshead displacement curves using the X-Y chart recorder integral with the Instron operating console. A machine warmup period of one hour was allowed, during which time initial cooling of the bath was completed. A crosshead displacement transducer was mounted between the travelling crosshead and a fixed micrometer head. Zeroing of the transducer was accomplished by using an oscilloscope to observe the null transition point.

The rapid cracking behavior of the X65 material would not readily permit slow crack growth measurements required to generate an accurate specimen compliance curve. Accordingly an alternative technique was developed. DCB specimens were loaded automatically using the Instron drive programmer and then stopped manually at each crack arrest point. Crack arrest lengths were then observed using a dental mirror and a hand held light source. Prior to testing, DCB specimens were fitted with a piece of masking tape running the full length beside the milled sidegroove. The masking tape was scaled in one tenth of an inch increments. Crack arrest lengths were determined visually by using the dental mirror and recording the corresponding tape measurement.

A number of DCB specimens tested at temperatures above minus 70 degrees centigrade exhibited considerable plastic bending of the specimen arms. To offset these nonlinear effects, specimen unloading curves similar to those suggested by Hoagland (17) were recorded.

The low crosshead velocity of 0.02 in. per minute maximum

made accurate control of bath temperatures below minus 80 degrees quite difficult. Thermal layering caused by adding liquid nitrogen occurred frequently, and a bath temperature variation of  $\pm 2$  degrees centigrade could be considered nominal.

During testing of the two DCB specimens at minus 193 degrees centigrade considerable load creep was observed; due principally to contraction of the loading fixtures during cooling. In each case, testing of the DCB specimens was commenced only after all mechanical creeping had subsided. Instron chart scales were increased ten fold to permit expansion of the load displacement record. This was necessitated by the small total crosshead displacement, decreased load required and the numerous crack initiation and arrest points. The liquid nitrogen was drained immediately following each test to warm up the pin joints and facilitate removal of the testpiece.

To prevent rusting of DCB fracture surfaces, all specimens were warmed after testing; and surfaces dried by air blowing. Fracture surfaces were then sprayed with a water resistant hair spray.

### 3.9 Metallurgical Photomicrographs

Photomicrographs of both X65 plate and pipe were removed at two 6 o'clock locations to determine the effects of steel mill rolling practise and pipe mill cold working. Specimen surfaces were etched using a two percent nitric acid solution. Specimens were set in clear plastic to assist in identification. Glass plate negatives taken through a microscope with camera adapter, were made at magnifications ranging from 100X to 500X. Results of the photomicrographic examination

are presented in Chapter IV.

### 3.10 Sources of Error

In general, physical experimentation encourages "built-in" sources of error, which may undermine even the most careful preparations of the researcher. In this research program, the following possible sources of error existed; and could conceivably have affected the accuracy of the results to be presented in the next chapter.

1. Direct physical measurement.
2. Temperature fluctuations.
3. Test specimen positioning.
4. Electronic breakdown.
5. Inaccuracies in the X-Y plotter.
6. Insufficient number of test data at a given reference point.
7. Data tabulation.

CHAPTER IV  
TEST RESULTS AND DISCUSSION

4.1 Introduction

Results from the experimental tests outlined in Chapter III are presented. Interpretation of test results, and conclusions drawn, are based on macroscopic considerations. Test methods are considered individually after which an attempt is made to correlate the findings. Experimental test data is presented in tabular as well as graphical form. Discussion is directed toward the establishment of a sound fracture toughness testing procedure for currently available line pipe materials.

4.2 Tensile Tests

Results of the tension test program are shown graphically in Figures 20 through 24. Table 4.1 presents the mechanical properties of the X65 plate and pipe materials obtained from the experimental tests. A series of nine tensile specimens were tested to failure. Seven of the specimens failed in the same ~~general~~ region - at a point approximately midway between the gauge points below the tensile neck radius of curvature. All fracture surfaces exhibited considerable ductile tear and none displayed evidence of any sliding in the Olsen wedge grips. The specimens from the plate showed marked surface separation similar to the blistering observed on poorly chrome plated auto parts. This condition

Table 4.1  
Experimental Mechanical Properties of X65 Pipe Steel

Material Form	Specimen Orientation and Location	Specimen No.	E psi	$\sigma_{ys}$ psi	$\sigma_{ult}$ psi	% Elongation (2" gauge)	Poisson's Ratio $\nu$
Plate	Long.-6:00	90	29.6	69,500	87,400	33.5	0.290
	Long.-9:00	111	30.2	69,700	88,500	34.0	0.277
	Transv.-6:00	91	30.2	74,200	89,000	32.0	0.299
	Transv.-6:00	110	30.6	71,600	88,200	32.5	0.282
Pipe	Long.-6:00	92	28.4	56,000	88,200	33.5	--
	Long.-6:00	93	28.8	58,300	88,900	32.5	--
	Long.-6:00	94	28.7	59,200	89,300	36.0	--
	Long.-3:00	95	28.7	59,200	89,800	31.0	--
	Long.-9:00	97	28.7	62,300	90,600	34.0	--

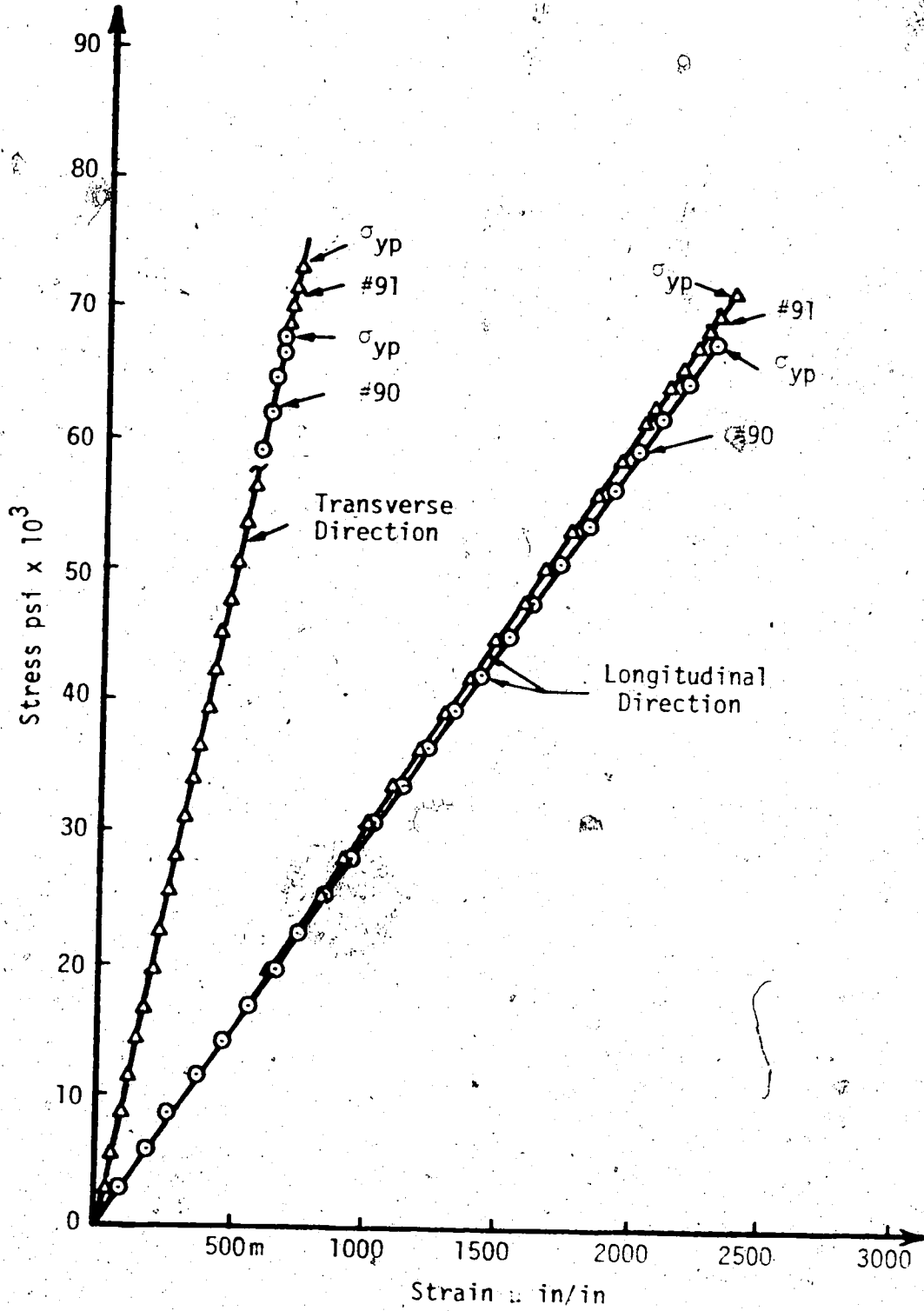


Figure 20 X65 Plate, Tensile Stress versus Strain

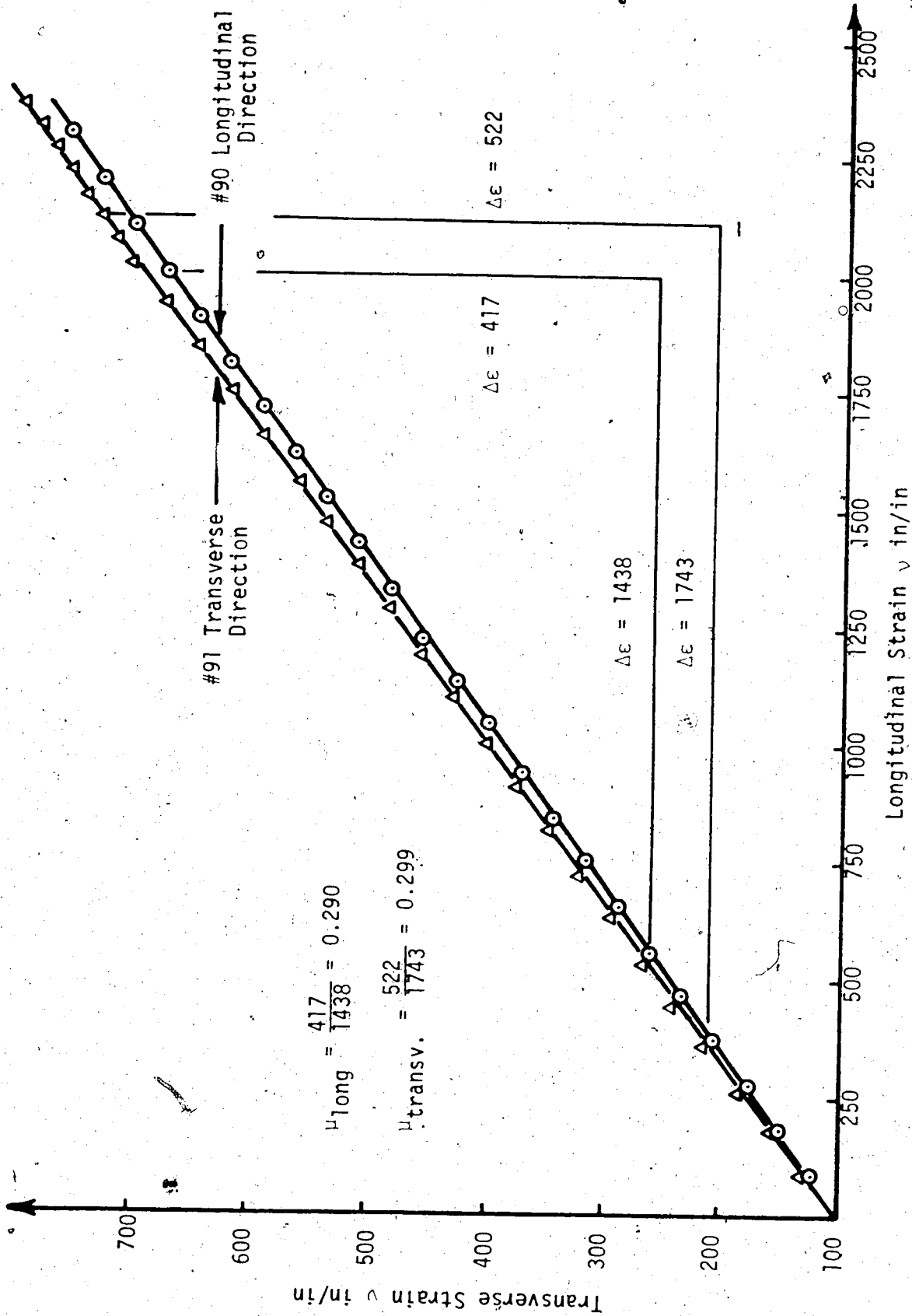


Figure 21 X65 Plate, Poisson's Ratio ( $\nu$ )



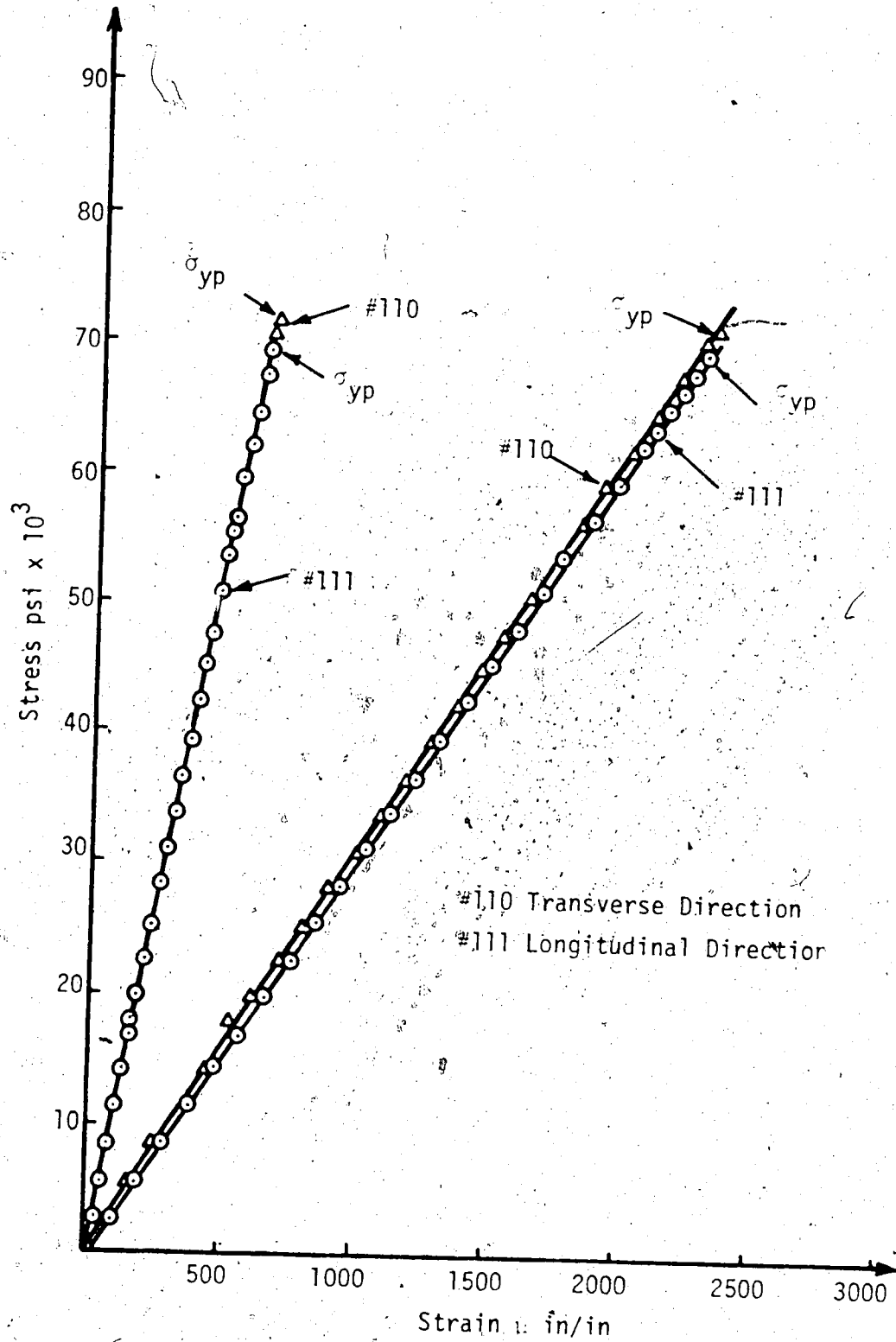


Figure 22 X65 Plate, Tensile Stress versus Strain

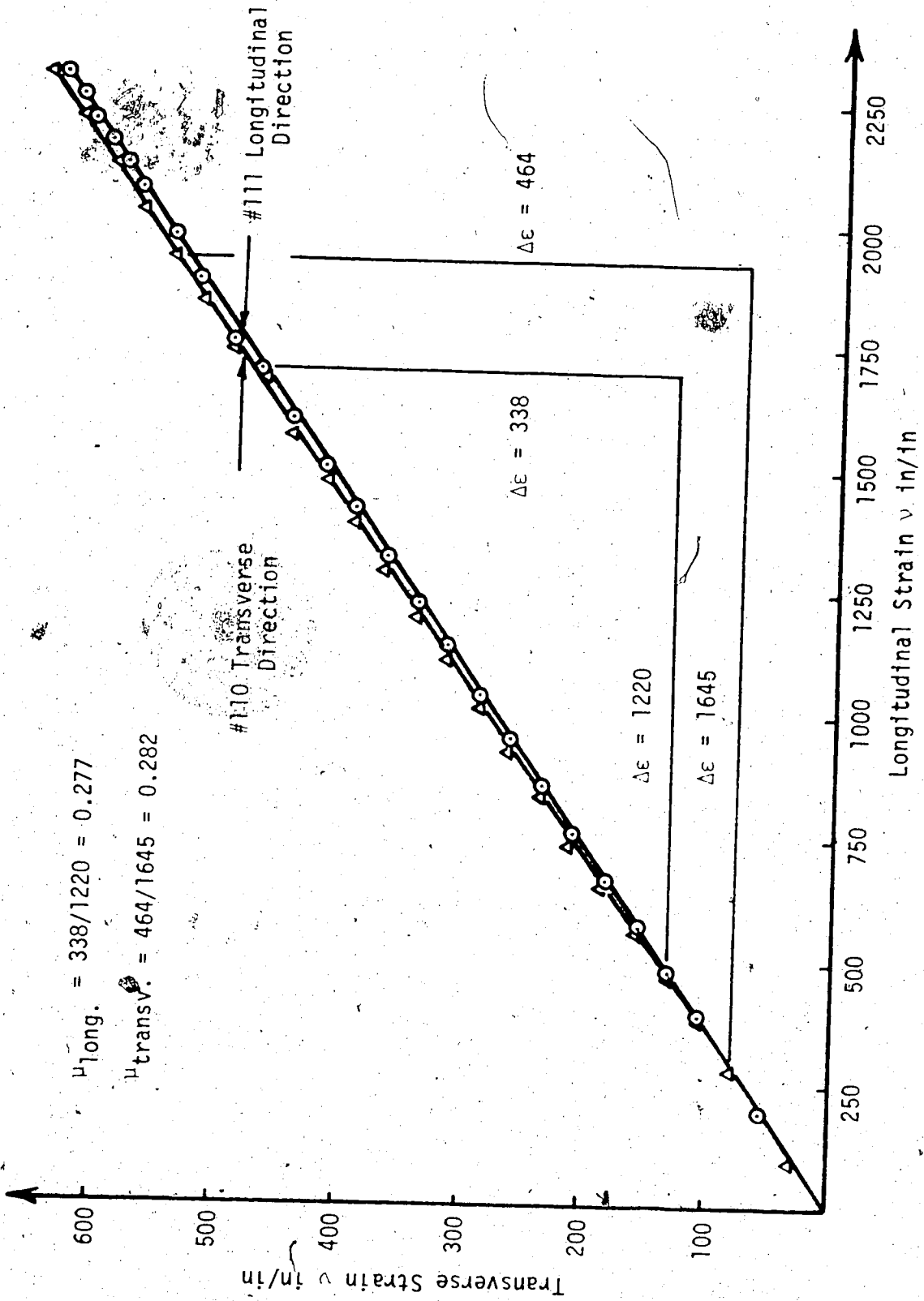


Figure 23 X65 Plate, Poisson's Ratio ( $\nu$ )

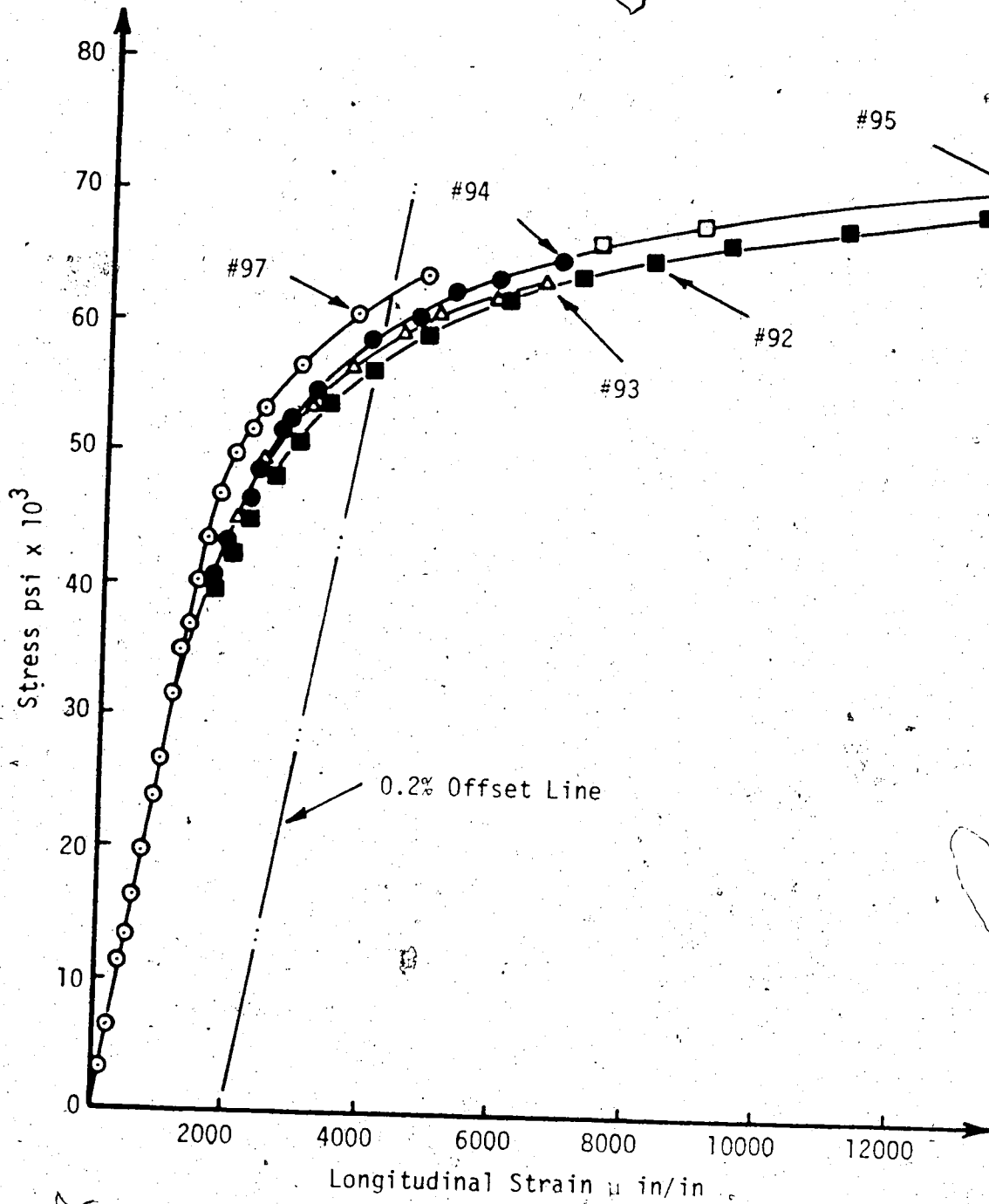


Figure 24 X65 Pipe, Tensile Stress versus Strain

was not seen on any of the pipe tensile specimens. The 15 percent high elongation strain gauges remained intact beyond the specimen yield point, whereas the standard elongation gauges loosened and separated at or near the yield point.

Stress versus strain values for transverse and longitudinal plate tensile specimens are presented graphically in Figures 20 and 22. The stress-strain curves are linear, with nominal yield stress values in the longitudinal direction lower than for corresponding positions in the transverse direction. Ultimate strengths at failure for plate tensile specimens in both directions were approximately the same. Experimental values of Poisson's ratio for the X65 plate material are determined from Figures 21 and 23.

Pipe cylinder test results are summarized in Figure 24 for the five specimens tested. Comparison of longitudinal test results indicates that although ultimate strengths for both pipe and plate materials were approximately equal, the tensile pipe specimens exhibited yield stress levels lower than those for similarly oriented plate specimens. All X65 pipe tensile stress-strain curves were non linear. The X65 pipe tensile test results indicate that based on the 0.2 percent off-set yield criteria, the material tested did not meet the minimum specified yield strength of 65,000 psi. Experimental pipe yield strength values ranged from 56 - 62,000 psi for the five samples tested.

#### 4.3 Metallurgical Photomicrographs

Examination of photographs taken during the microscopic examination of the specimen surfaces, indicated that the X65 test ma-

materials showed a narrow alignment band at specimen mid-thickness for both pipe and plate materials in the transverse and longitudinal directions. Elongation of pearlite and ferrite grains was evident, being most pronounced in the longitudinal direction. Considerably less grain elongation was observed in the central band in either direction. In general the longitudinal direction displayed a more regular ordered grain alignment in both plate and pipe photomicrographs.

Typically, the longitudinal direction was more "ferrite" rich and the transverse more "pearlite" rich. The center band in both pipe and plate was predominantly ferrite. Grain sizes were larger than in non-banded regions. No metallurgical differences were seen between corresponding sections of plate and pipe materials to account for cold working effects.

Two parallel shadow bands in addition to the usual central band, were present in one pipe photomicrograph. This "ghosting" phenomena sometimes occurs when the original ingot desegregates during the rolling operation. This particular instance was found to be a localized case; as photomicrographs of other pipe areas exhibited only the single central band.

The foregoing observations suggested that some difference in fracture toughness as well as mechanical properties should be expected between tests performed in the longitudinal and transverse directions; and that little or no difference should be noted between similarly oriented plate and pipe fracture tests. It should be recognized that these conclusions are drawn on the basis of a superficial metallurgical examination.

#### 4.4 Two-Thirds Charpy V-Notch Test

Experimental results of Charpy impact tests and Charpy surface crystallinity measurements, are summarized and presented graphically in Figures 25 through 28. Typical fracture surfaces are shown in photographs presented in Figures 29 through 32, for both plate and pipe materials in the transverse and longitudinal directions.

Room temperature precracked notch energy values for the transverse specimens were determined to be approximately twice the corresponding energy values for longitudinal samples. Room temperature (20°C) values were 36 ft. lb. and 17 ft. lb. for plate specimens and 35 ft. lb. and 17 ft. lb. for pipe specimens, respectively. At minus 28°C, directional energy preferences coalesced for both plate and pipe materials and were 7 ft. lb. Figures 25 and 26 indicate a well defined transition temperature range of from 0 to 10°C (32 to 50°F) for transverse specimens. The transition temperature for longitudinal specimens is not well differentiated, but may be assumed to be about 10°C. Accordingly, the average transition temperature for X65 pipe steels in either test direction is approximately 10°C. Comparison of energy values for respective materials in corresponding directions, indicates a decrease in transverse impact energy after rolling for temperatures above -10°C. Test data also indicate an increase in impact energy between -20°C to +20°C for longitudinal pipe specimens and a decreasing impact energy for longitudinal pipe specimens at temperatures above +20°C. A more exacting investigation would be required to confirm this observation, as variations in notch precrack depth could be a contributing factor

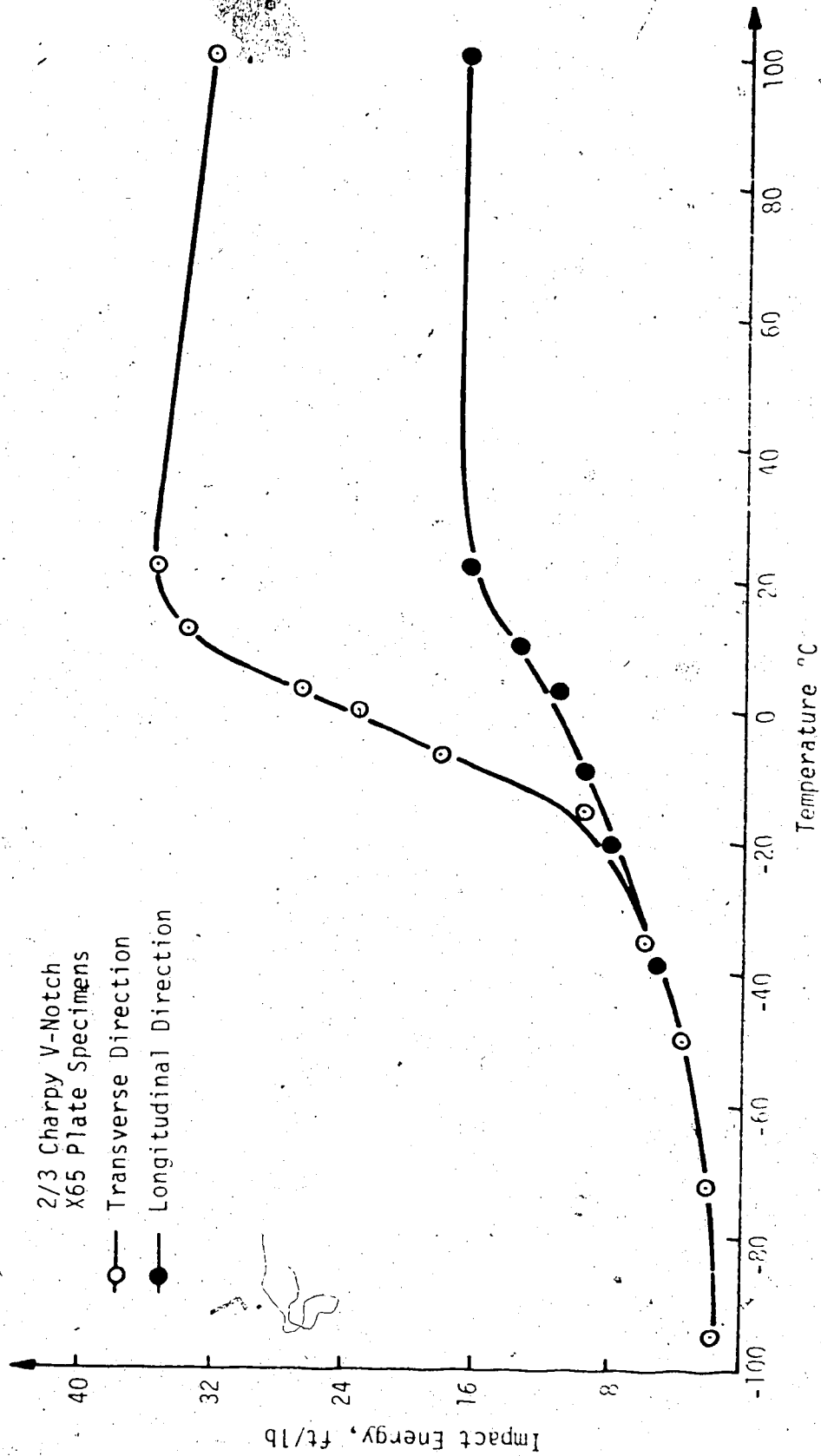


Figure 25 X65 Plate, Impact Energy versus Temperature

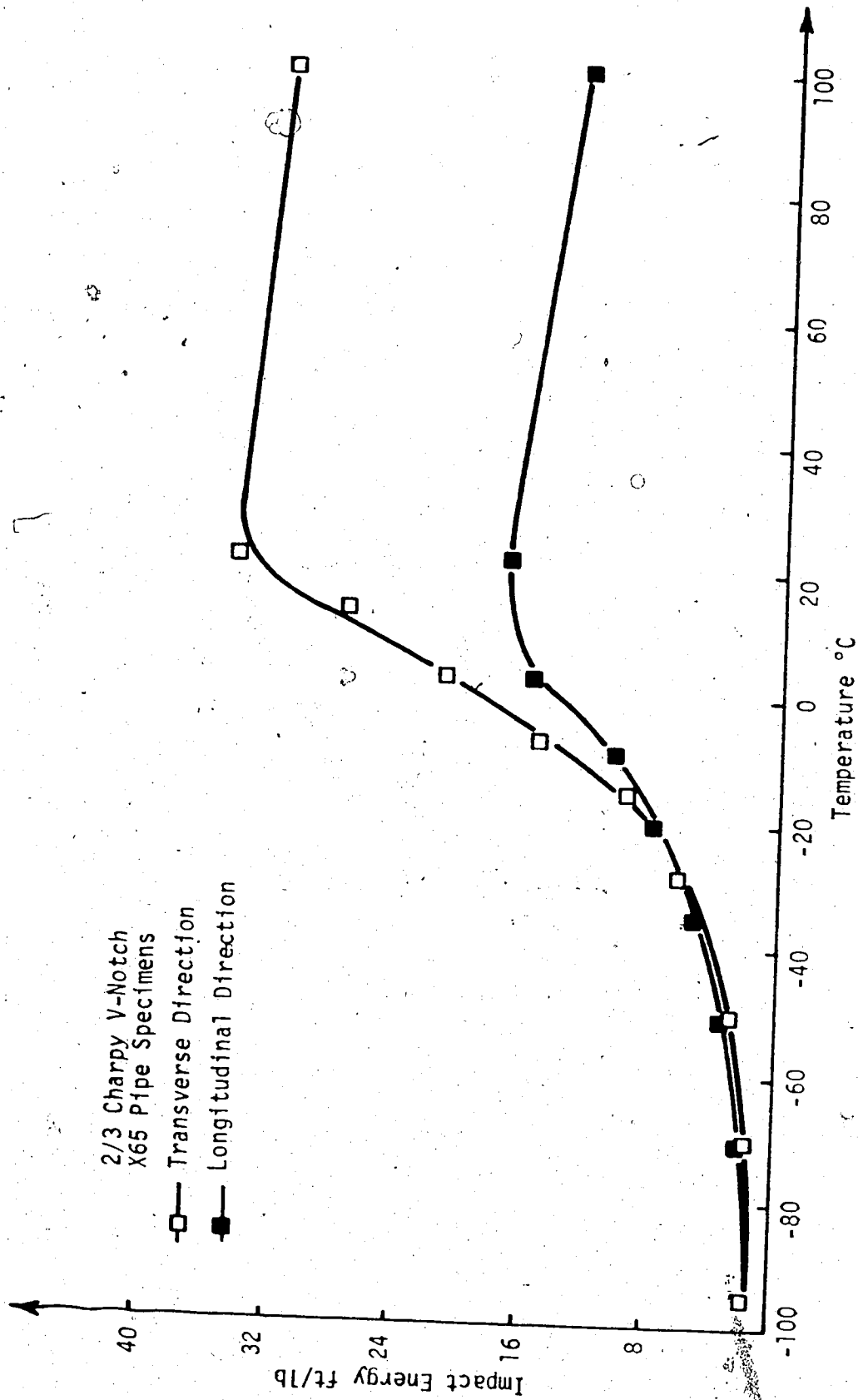


Figure 26 X65 Pipe, Impact Energy versus Temperature



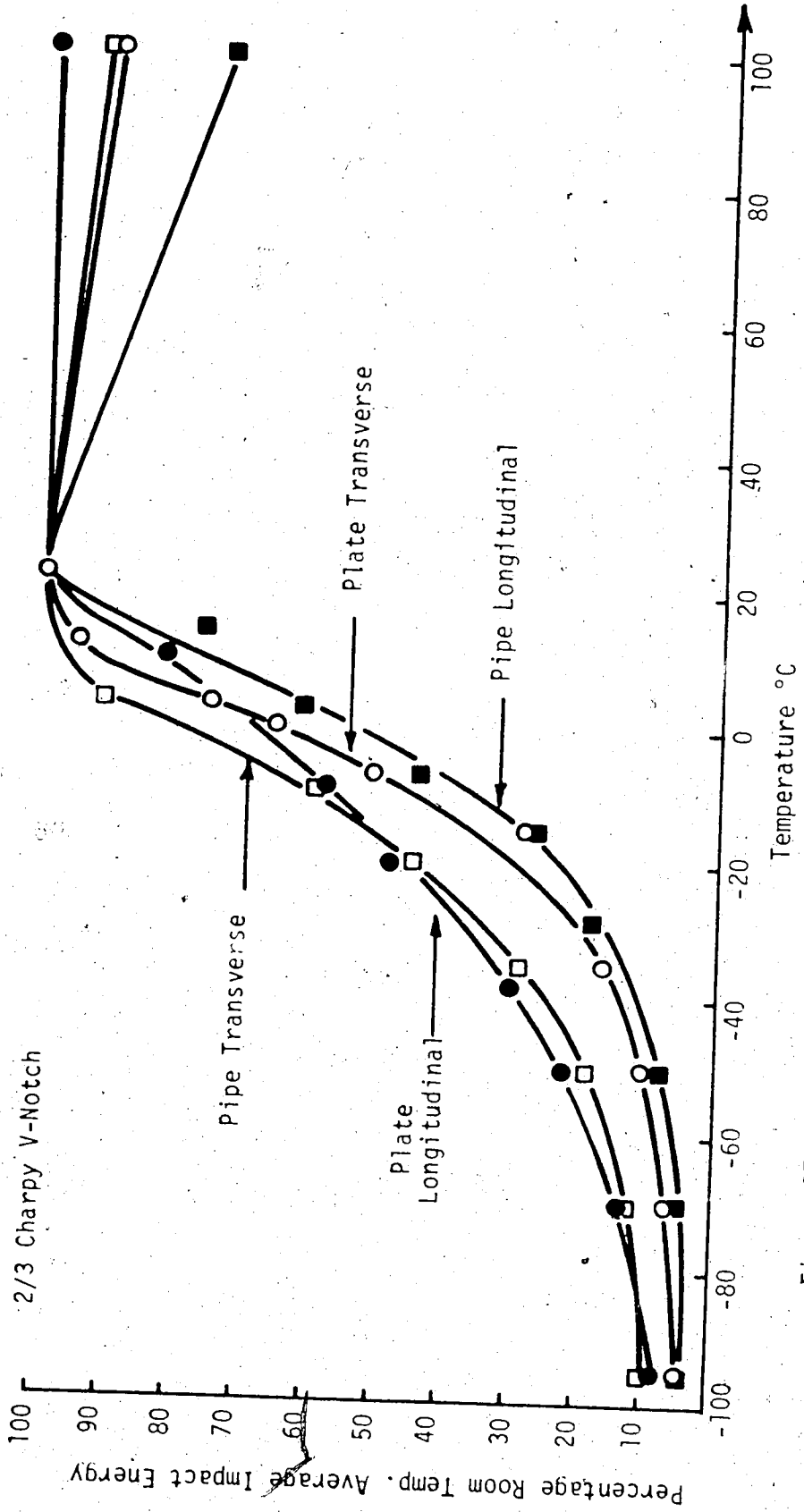


Figure 27 Percentage of Room Temperature Impact Energy versus Temperature

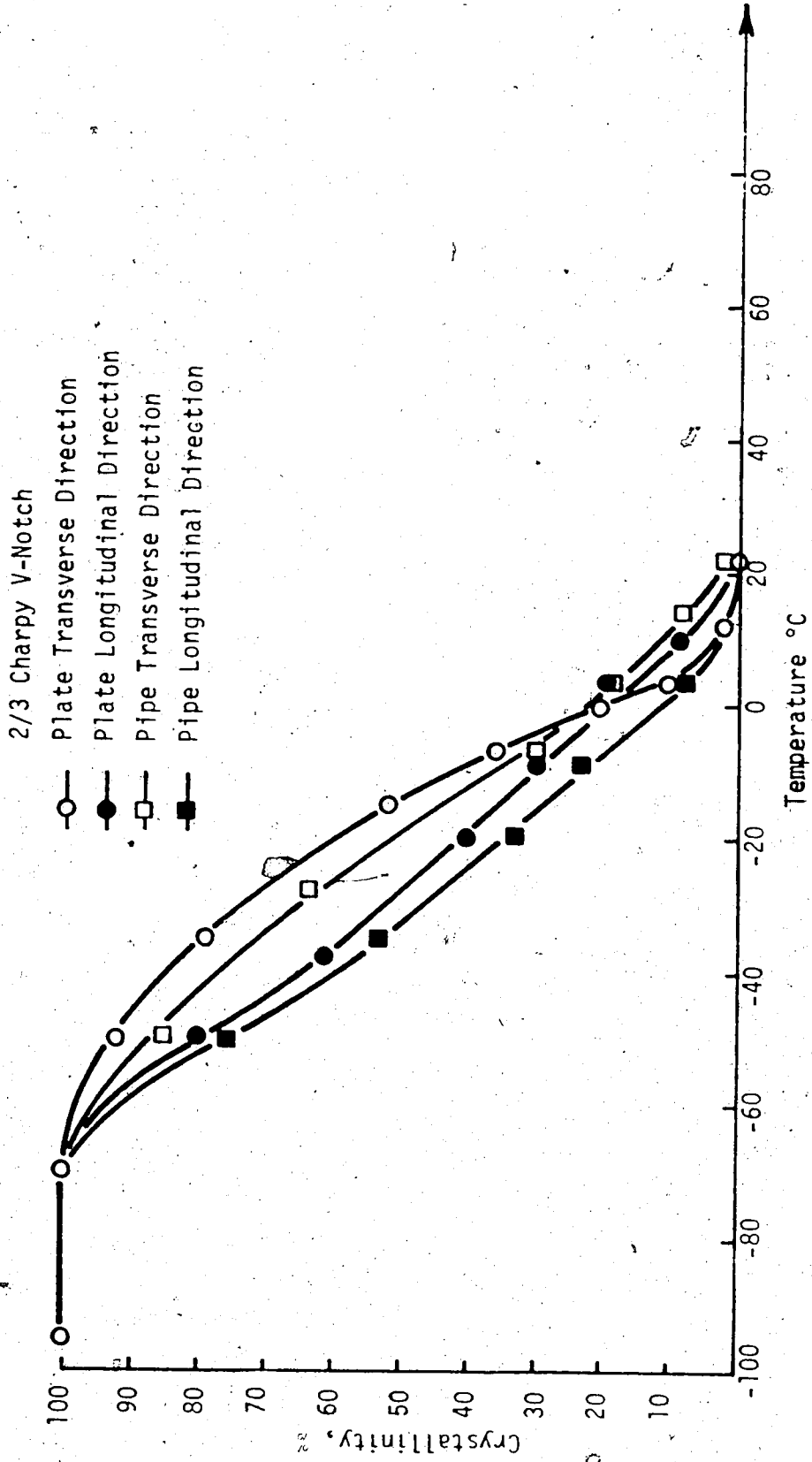


Figure 28 Percentage Crystallinity versus Temperature

to these changes.

Impact energies expressed as a percentage of the Charpy room temperature energy value versus temperature are shown in Figure 27. Results indicate that X65 materials attain the 50 percent drop off energy level in the  $-20^{\circ}\text{C}$  to  $0^{\circ}\text{C}$  range. From Figure 28, percentage crystallinity versus temperature curves, fractures are 100 percent crystalline (brittle) below  $-80^{\circ}\text{C}$ . The fracture appearance transition temperature at 50 percent crystallinity for plate and pipe materials are determined to be about  $-20^{\circ}\text{C}$  and  $-26^{\circ}\text{C}$  respectively. Accordingly, to guarantee shear (ductile) type failures, line pipe temperatures above  $-26^{\circ}\text{C}$  would have to be maintained. In summary, Two-Thirds Charpy impact energy values for X65 plate and pipe materials at the respective fracture transition temperatures are:

plate:  $-20^{\circ}\text{C}$  - transverse and longitudinal 7 ft. lb.

pipe:  $-26^{\circ}\text{C}$  - transverse and longitudinal 7 ft. lb.

A comparison of transverse pipe and plate fracture surfaces in Figures 29 and 30 does not indicate any marked surface dissimilarities. Pipe specimens appear to fracture with a characteristic center separation over a much greater range than do corresponding plate samples. Percentage crystallinity values are approximately the same at any given temperature. Longitudinal fracture surfaces shown in Figures 31 and 32, display similar fracture appearances and crystallinity values for both plate and pipe materials.

Marked fracture surface differences between the longitudinal and transverse fracture directions are evident. Longitudinal surfaces



Figure 29 X65 Pipe, Charpy Transverse  
Crack Fracture Surfaces



Figure 30 X65 Plate, Charpy Transverse  
Crack Fracture Surfaces

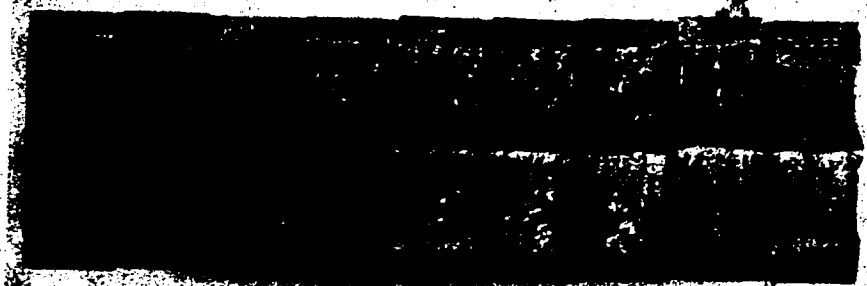


Figure 31 X65 Pipe, Charpy Longitudinal  
Crack Fracture Surfaces



Figure 32 X65 Plate, Charpy Longitudinal  
Crack Fracture Surfaces

do not display the center separation split characteristic of the warmer transverse specimens. Room temperature longitudinal surfaces exhibit less side deformation and appear more regular than corresponding transverse specimens. At low temperatures (below  $-50^{\circ}\text{C}$ ) the Charpy tests on longitudinal specimens displayed a coarser brittle fracture surface. Corresponding tests on transverse specimens were typically granular or faceted in appearance.

#### 4.5 Three Point Notch Bend Tests

##### 4.5.1 X65 Pipe Steel

Fracture toughness ( $K_{IC}$ ) values were determined by substituting research test data into equation (15a), (24). Equation (15a) was rewritten in program form using Fortran IV language and a computer used to analyse test data and output values of  $G_{IC}$ ,  $K_{IC}$ , and  $a_0$ . From computer results, graphs of fracture toughness versus temperature were plotted and are presented in Figures 33 through 37. A typical fracture surface test sequence is shown photographically in Figure 38.

The X65 test material appeared well suited to the Three Point Notch Bend test method. At temperatures below  $-30^{\circ}\text{C}$ , fractures were usually square and failed through the full section depth. Specimens tested at higher temperatures exhibited some plastic deformation and did not tend to break through the full section depth. Room temperature tests produced oblique fracture surfaces and fractures were not full depth. Generally Notch Bend specimens were easy to position for testing and could be tested rapidly to failure. Necessarily, load at failure and fracture time decreased with decreasing test temperature.

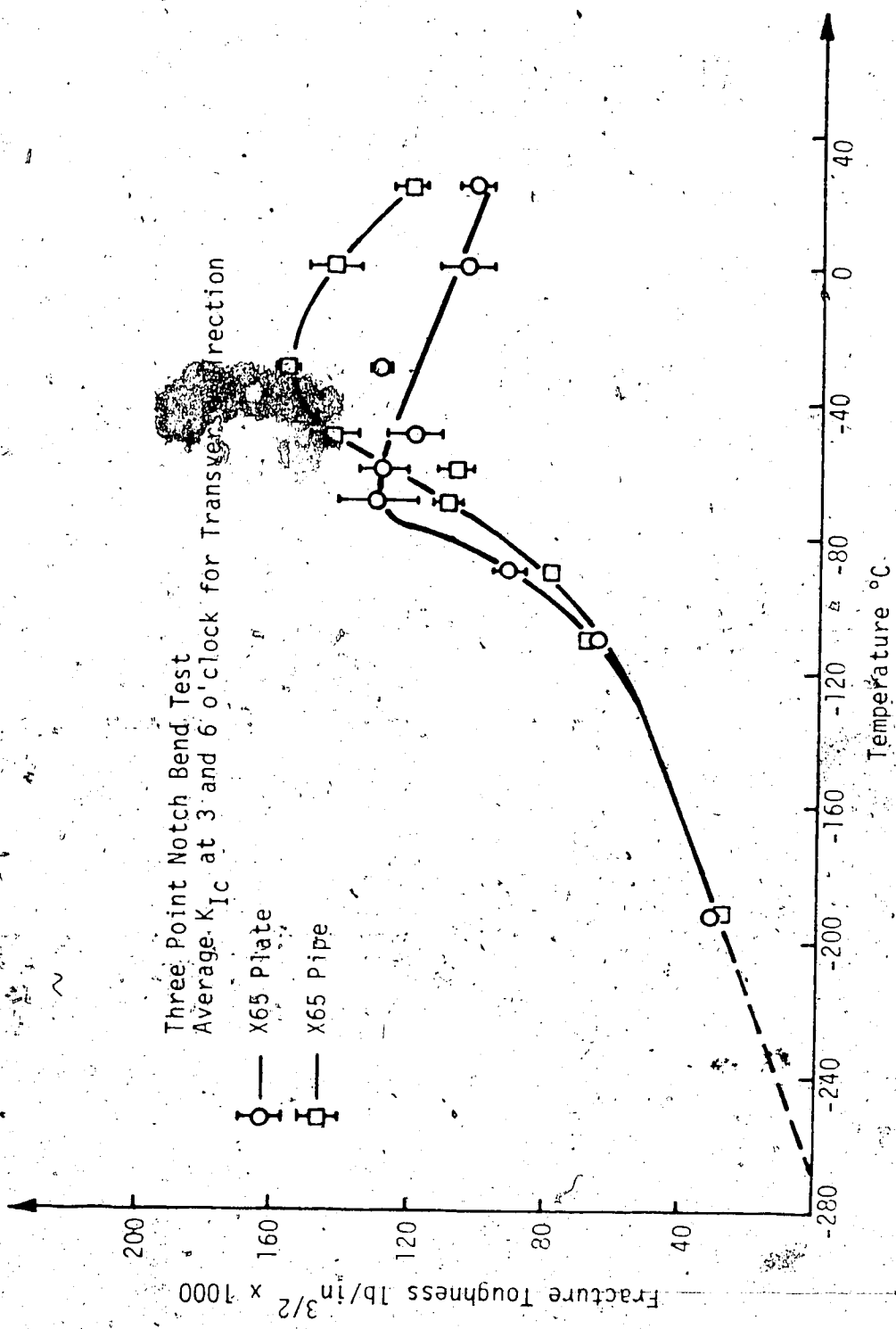


Figure 33 Average  $K_{Ic}$  versus Temperature for Static Notch Bend Tests

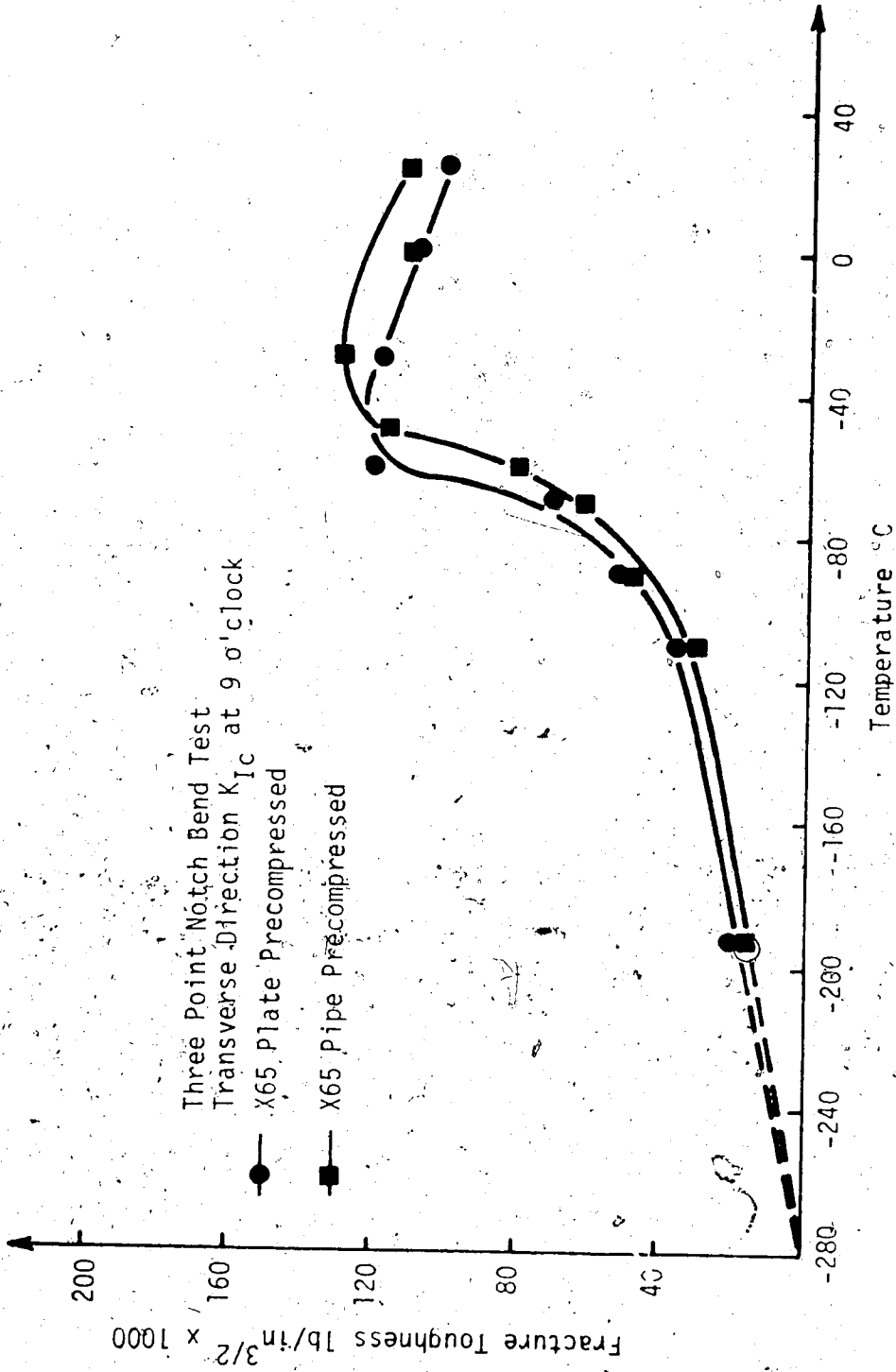


Figure 34  $K_{Ic}$  versus Temperature for Precompressed Static Notch Bend Specimens



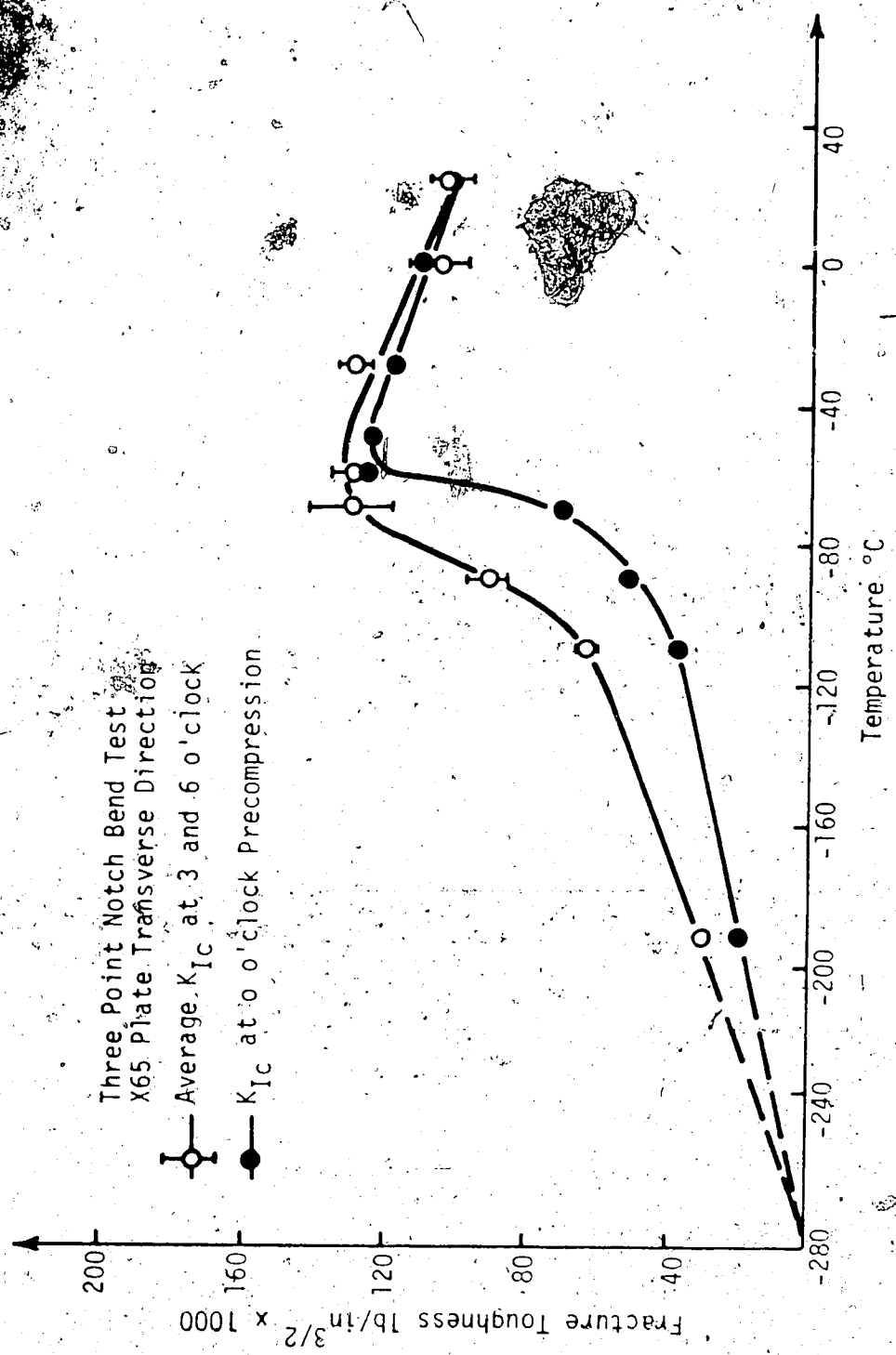


Figure 15 X65 Plate, Transverse  $K_{Ic}$  versus Temperature

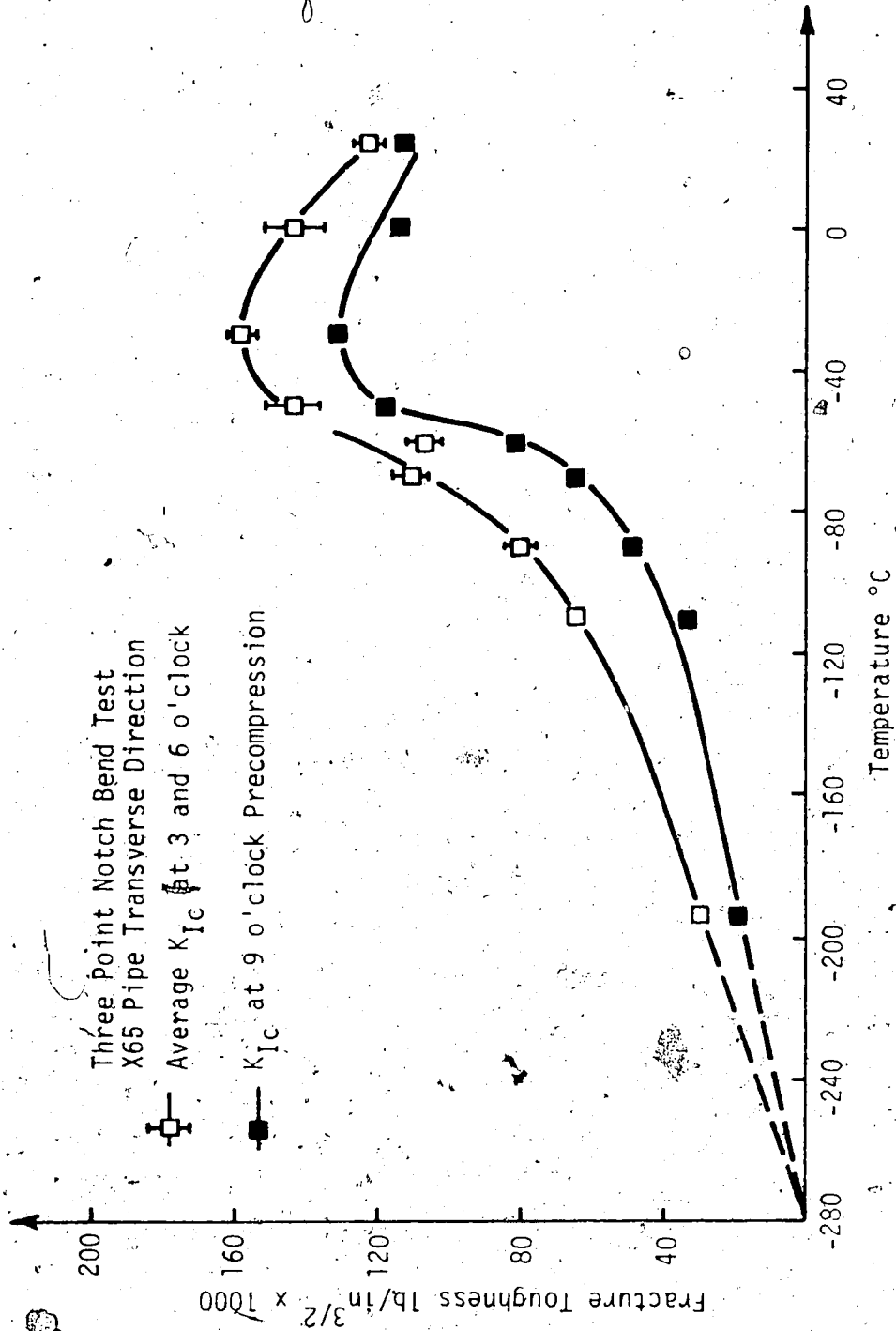


Figure 36 X65 Pipe, Transverse  $K_{IC}$  versus Temperature

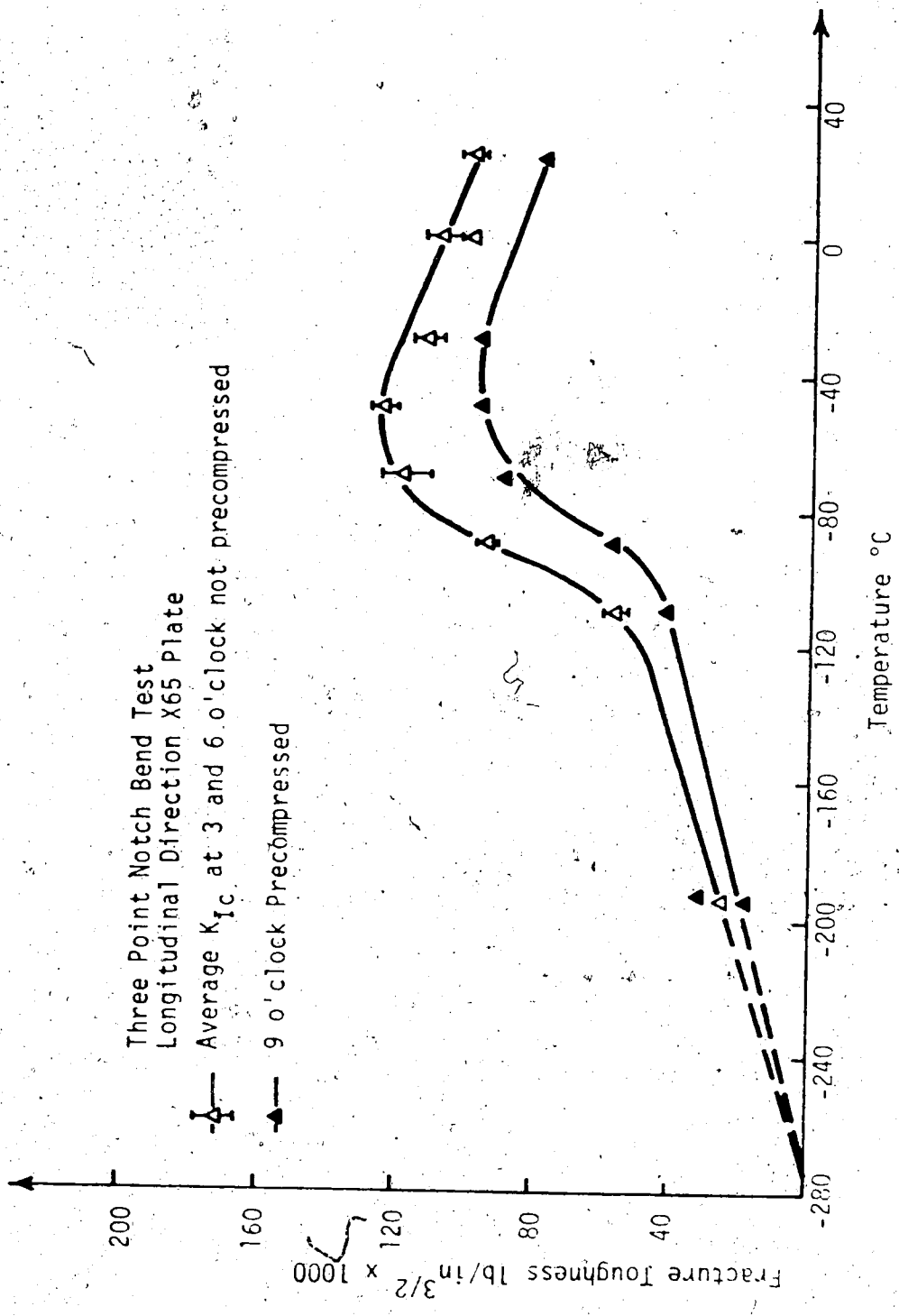


Figure 37. X65 Plate, Longitudinal  $K_{Ic}$  versus Temperature

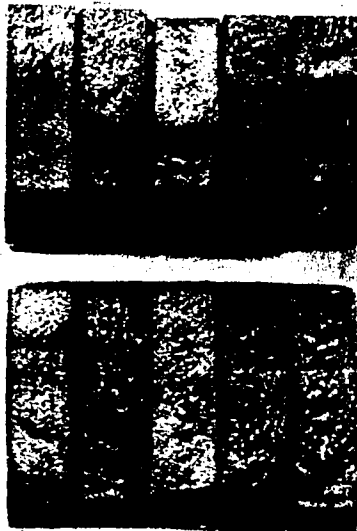


Figure 38. Typical Three Point Notch Bend Fracture Surfaces

From test results presented in Figure 33 based on equation (15), the average maximum toughness values for the transverse direction were determined to be:

$$\text{Plate } -70^{\circ}\text{C} \quad K_{Ic} = 130,000 \text{ lb/in}^{3/2}$$

$$\text{Pipe } -30^{\circ}\text{C} \quad K_{Ic} = 158,000 \text{ lb/in}^{3/2}$$

Test results indicate that for temperatures above  $-100^{\circ}\text{C}$  plate rolling and/or cold expansion final pipe sizing, increases the fracture toughness while unfavorably shifting the transition temperature. This trend also appears to be valid for precompressed materials to a lesser degree as indicated in Figure 34. Figures 35 and 36 indicate that the effects of notch root precompression are more severe on finished pipe materials. A reduction in maximum transverse fracture toughness for plate materials of  $9,000 \text{ lb/in}^{3/2}$  with a shift in transition temperature of  $10^{\circ}\text{C}$  was found; as against a corresponding decrease in pipe fracture toughness of  $28,000 \text{ lb/in}^{3/2}$ , with no appreciable change in transition temperature. From test results presented in Figures 35 and 36 the average maximum fracture toughness values for precompressed notch root X65 materials was determined to be:

$$\text{Plate } -60^{\circ}\text{C} \quad K_{Ic} = 121,000 \text{ lb/in}^{3/2}$$

$$\text{Pipe } -30^{\circ}\text{C} \quad K_{Ic} = 130,000 \text{ lb/in}^{3/2}$$

As stated in Chapter III, longitudinal fracture toughness tests on X65 pipe materials were not conducted. Average longitudinal plate fracture toughness values were obtained and are presented in Figure 37. Comparison of results shown in Figures 35 and 37 indicate

a decrease of 4000 lb/in<sup>3/2</sup> in fracture toughness in the longitudinal direction and an upward shift (decrease) of approximately 20°C (to -50°C) in the maximum toughness transition temperature. From Figure 37 the average maximum longitudinal fracture toughness values were determined to be:

Plate -50°C	$K_{Ic} - 126,000 \text{ lb/in}^{3/2}$
Precompressed Plate -40°C	$K_{Ic} - 96,000 \text{ lb/in}^{3/2}$

From these test results it is observed that a greater reduction in longitudinal fracture toughness due to precompression of the specimen notch root has occurred, than was determined previously for transverse plate specimens.

For purposes of comparison, fracture toughness values were calculated using the "Area Under the Load-Displacement Curve" method by substituting in equation (15b). Results are tabulated in Table 4.2. Area method calculations were not computed for specimens tested at temperatures greater than -40°C as these test specimens did not fail through the full section depth. From comparison of fracture toughness values determined by the two alternate methods it can be seen that values obtained using the Area method tend to range from equal to approximately 10 percent greater than those calculated using the Scrawley-Gross equation.

#### 4.5.2 Sawtooth Fracture Segment

Three Point Notch Bend test results for the sawtooth fracture segment were analyzed using the same procedures outlined for the X65 pipe steels, and are presented graphically in Figure 39. Toughness values ranged from 52,000 to 62,000 lb/in<sup>3/2</sup> and all specimen fractures

Table 4.2  
Notch Bend Fracture Toughness

Crack Direction	Test Temperature	Scrawley $K_{Ic}$ (lb/in <sup>3/2</sup> )	Area $K_{Ic}$ (lb/in <sup>3/2</sup> )	Material Type
Longitudinal	R.T.	99,500	--	Plate
	0°C	108,000	--	Plate
	-30°C	112,500	--	Plate
	-50°C	127,000	125,500	Plate
	-70°C	119,500	120,000	Plate
	-90°C	94,750	88,500	Plate
	-110°C	56,750	61,000	Plate
	-193°C	24,750	28,000	Plate
Transverse	R.T.	102,000	--	Plate
		121,500	---	Pipe
	0°C	104,500	--	Plate
		143,000	--	Pipe
	-30°C	156,000	--	Plate
		158,500	--	Pipe
	-60°C	128,000	140,000	Plate
		106,500	106,000	Pipe
	-70°C	130,500	115,000	Plate
		124,500	128,000	Pipe
	-90°C	90,000	90,000	Plate
		79,000	89,000	Pipe
-110°C	64,000	62,000	Plate	
	65,000	73,000	Pipe	

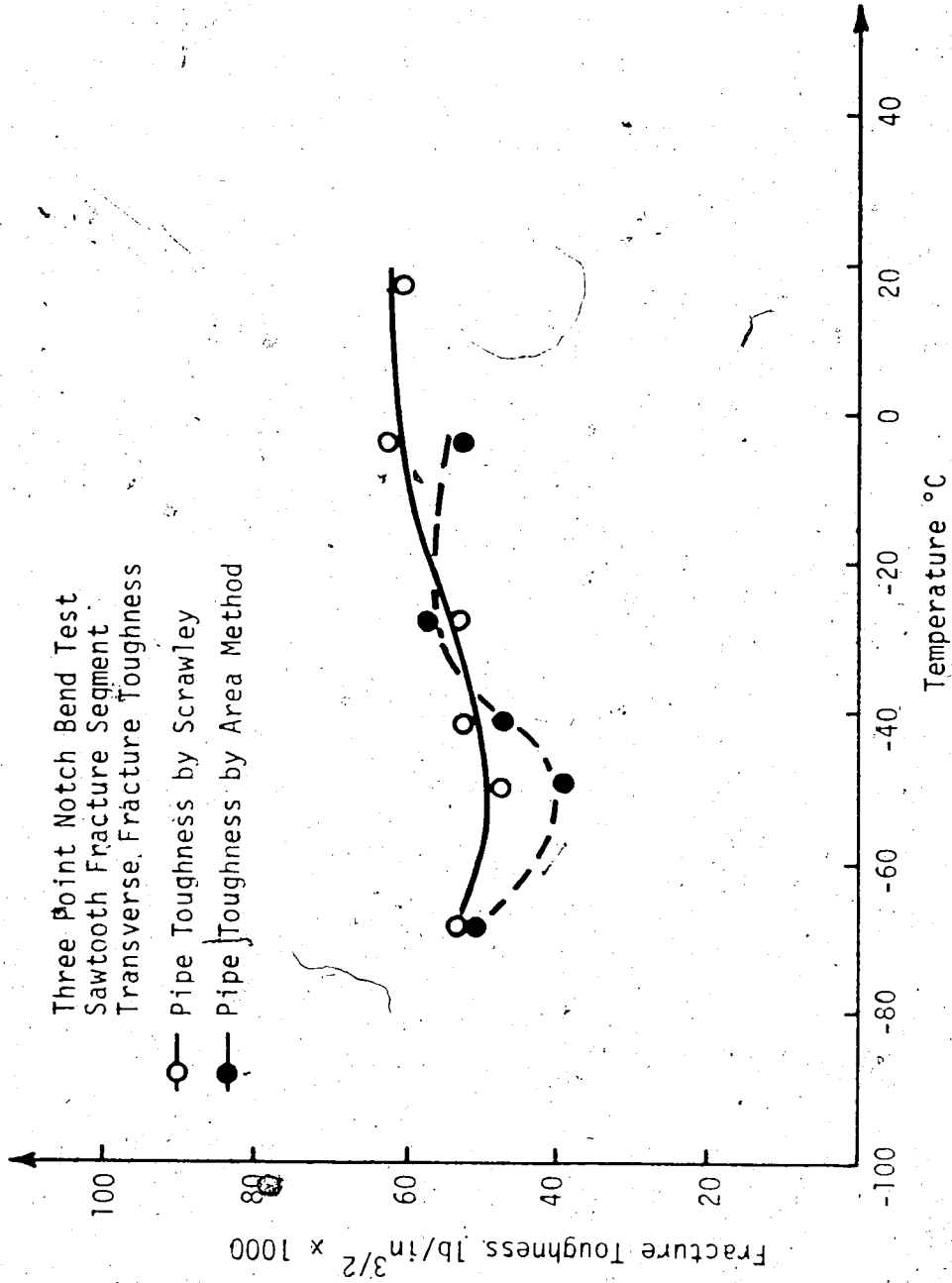


Figure 39 Sawtooth Fracture Segment, Transverse  $K_{Ic}$  versus Temperature



0°C and lower were square and brittle. The room temperature specimen did not fail through the full specimen section depth, and the fracture surface was oblique and ductile. On the basis of the few specimens tested the material was likely well below specification. Fracture toughness values obtained indicate that line pipe should not be made from a steel such as that tested due to the susceptibility to brittle fracture and consequent high probability of failure.

#### 6. Double-Cantilever Beam Tests

The Double-Cantilever Beam (DCB) test method developed by England (17) and others (20,21) had not been previously applied to laboratory fracture analysis studies of X65 pipeline steels. Accord- based on information obtained from preliminary DCB tests using aluminum and mild steel test pieces of varied dimensions, the final testing procedures detailed in Chapter III were developed and applied to the X65 steel.

All X65 DCB tests were performed on pre-cracked test specimens. Generally, accurate gauging of the precrack notch depth was very difficult to achieve. In most cases it was assumed that a given number of cycles would produce a given crack depth. However, a few DCB specimens were lost during cycling when cracks propagated during fatigue cycling at room temperature. These few specimens failed in a brittle manner after but a few cycles, and since preparation of test-pieces was similar, it is concluded that these brittle type failures likely occurred at a metallurgical defect.

Fracture toughness values for the DCB test specimens were

obtained by substituting experimental compliance constants and required test data into equation (22). To simplify calculation of  $K_{IC}$  values, a Fortran IV computer program was written to provide values of  $G_{IC}$  and  $K_{IC}$  and the DCB compliance constants. Results of the DCB research program are presented graphically in Figures 40 through 43 inclusive.

Average maximum longitudinal DCB fracture toughness values for the X65 pipe steel were determined to be:

X65 Plate	(-70°C)	$K_{IC}$ initiation:	132,000 lb/in <sup>3/2</sup>
		$K_{IC}$ arrest:	58,000 lb/in <sup>3/2</sup>
X65 Pipe	(-50°C)	$K_{IC}$ initiation:	124,000 lb/in <sup>3/2</sup>
		$K_{IC}$ arrest:	108,000 lb/in <sup>3/2</sup>

These results indicate that plate rolling and cold sizing increases the X65 pipe transition temperature by about 20°C, while simultaneously decreasing the fracture toughness at crack initiation by approximately 8,000 lb/in<sup>3/2</sup>. Additionally, the maximum crack arrest fracture toughness value for the finished pipe is about twice the corresponding value for the unrolled plate skelp. Accordingly, DCB test results indicate that the longitudinal crack arrest properties of X65 pipe steels are considerably enhanced by the rolling and/or cold sizing process.

Average transverse plate initiation and arrest toughness values are presented in Figure 43. A limited number of specimens were tested in the lower temperature region and a comparison with Figure 41, indicates that initiation toughness values are slightly higher in the transverse direction. Conversely, transverse arrest toughness values are approximately 10,000 lb/in<sup>3/2</sup> lower at corresponding

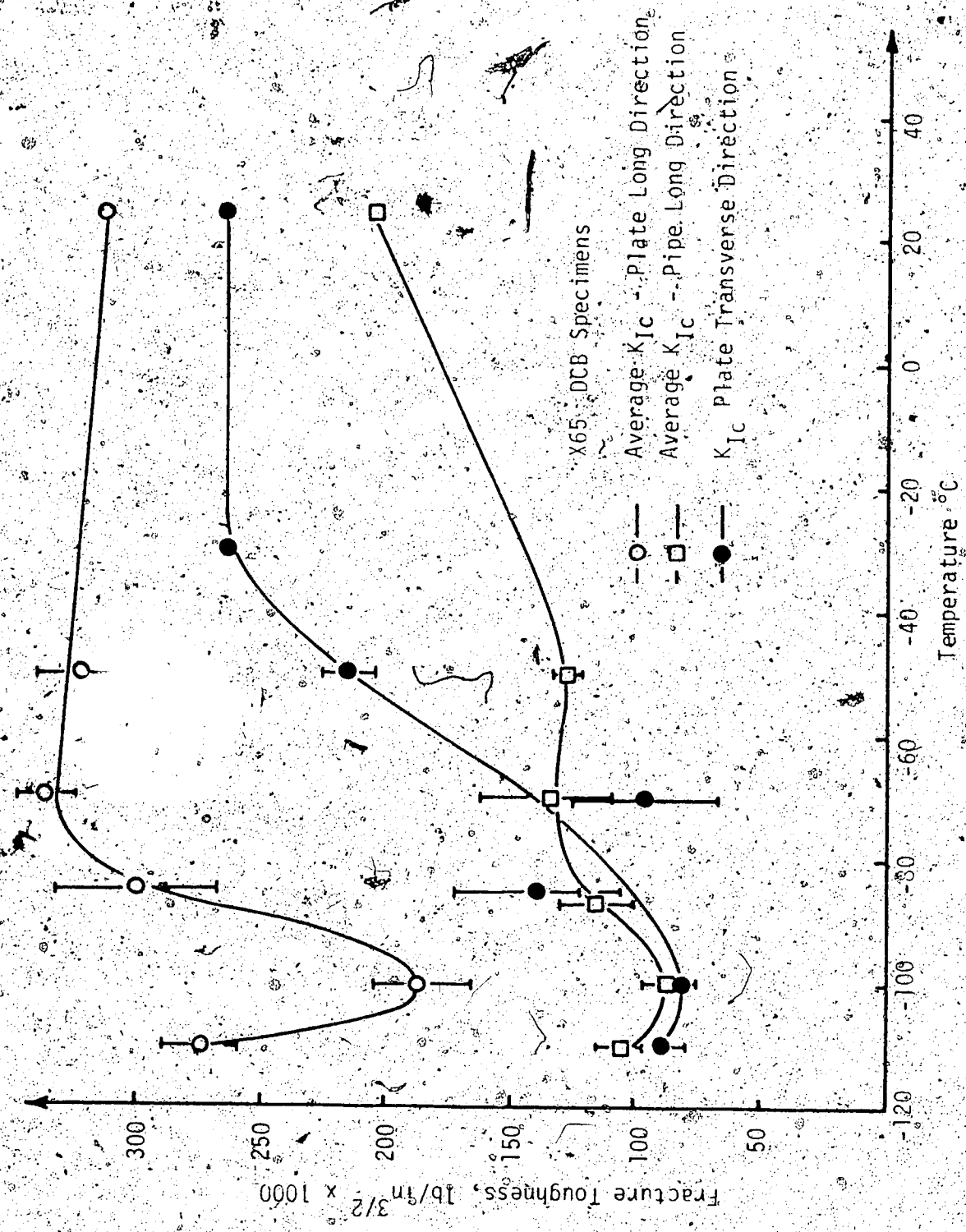


Figure 40  $K_{Ic}$  versus Temperature for X65 DCB Specimens at First Initiation Point

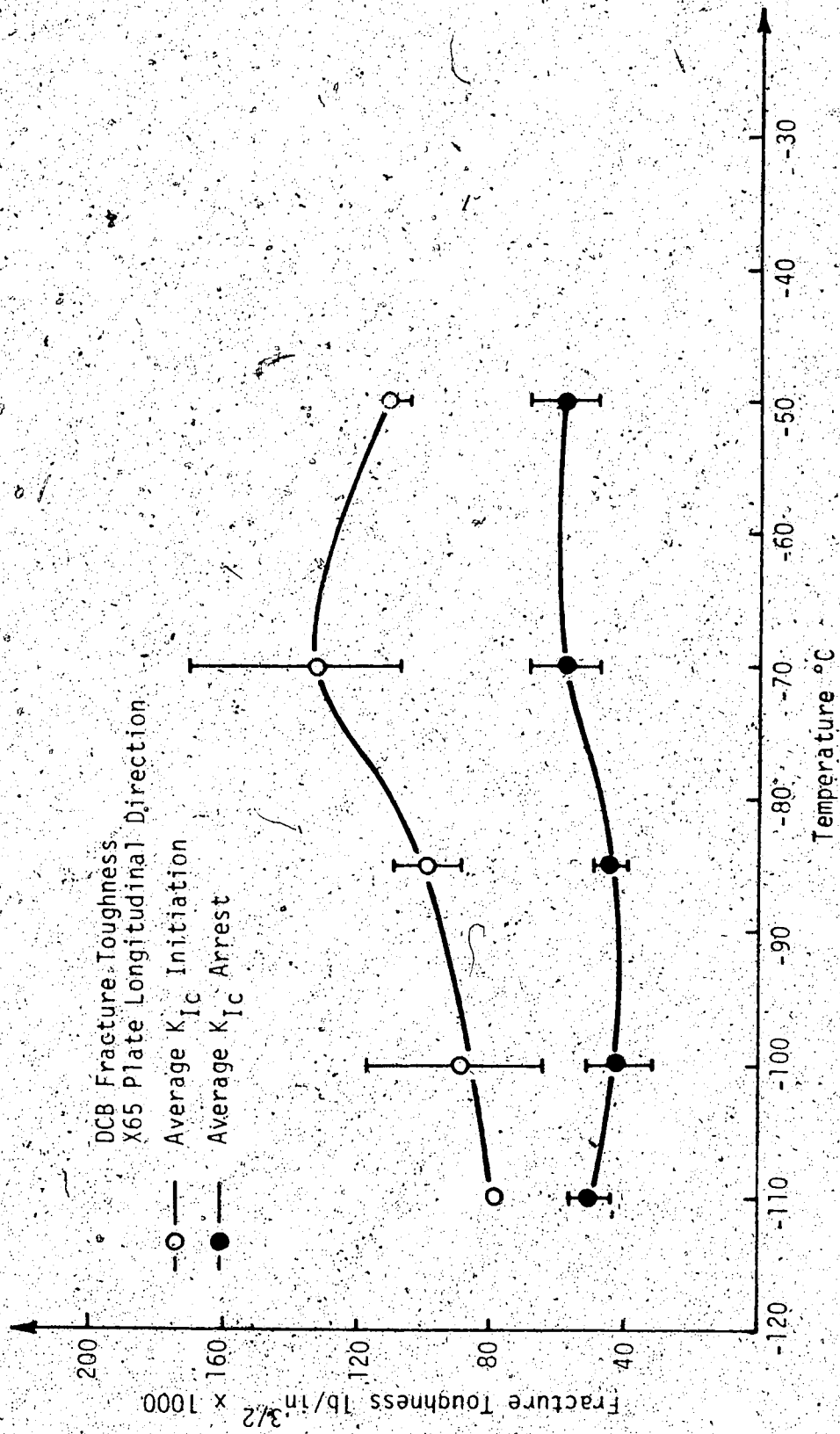


Figure 41 X65 Plate, Average Longitudinal  $K_{Ic}$  versus Temperature

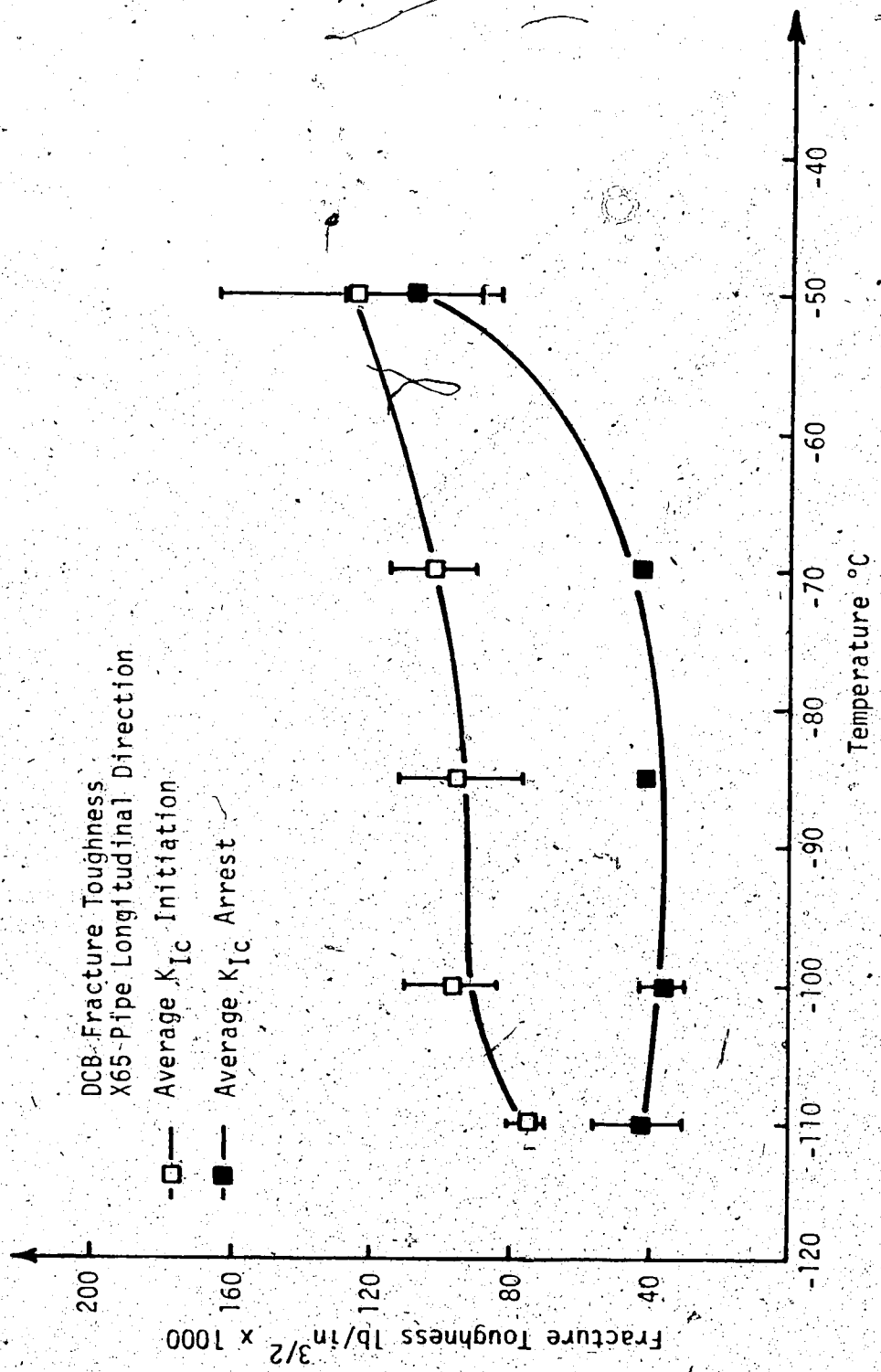


Figure 42 X65 Pipe, Average Longitudinal  $K_{Ic}$  versus Temperature

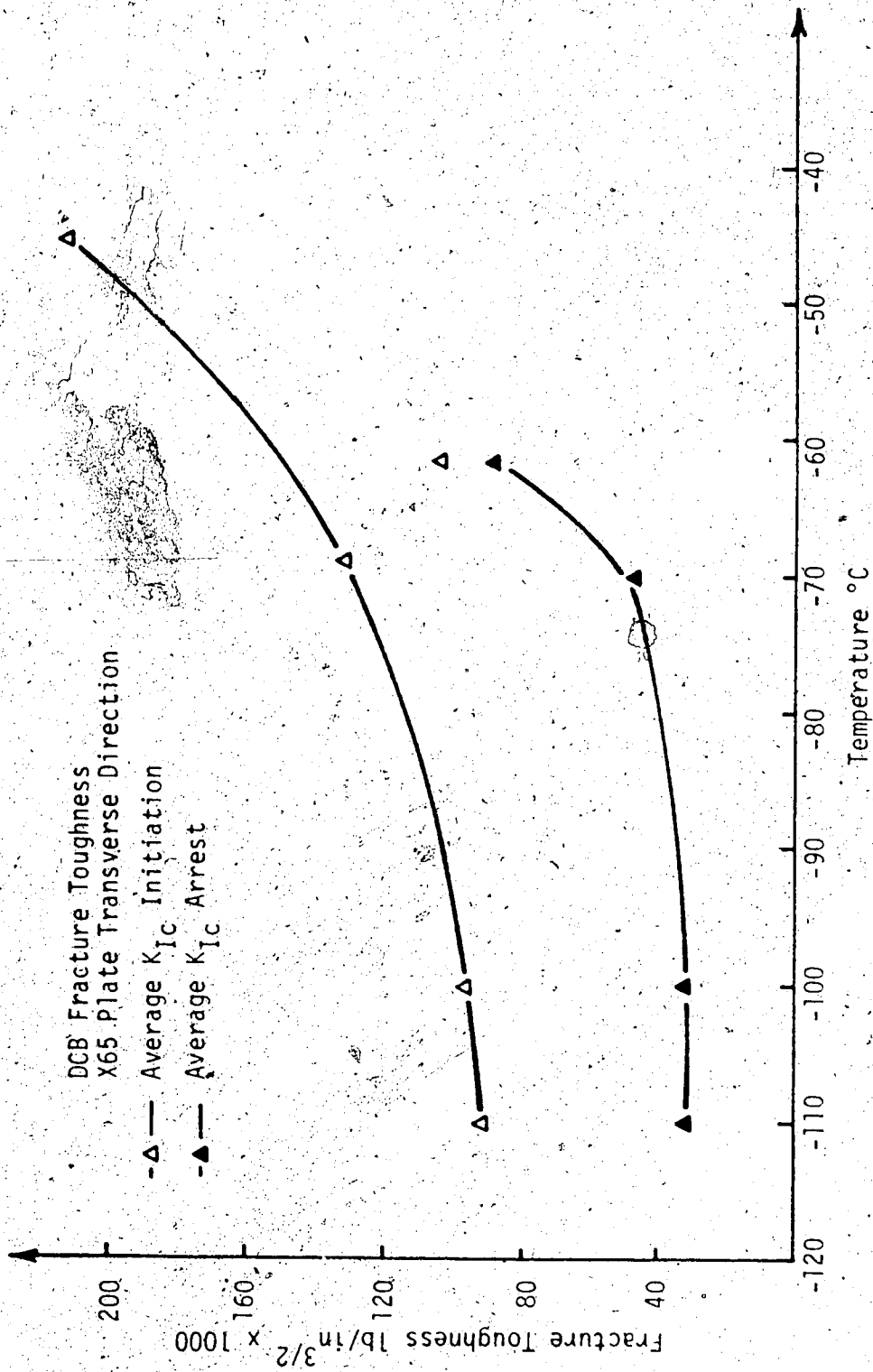


Figure 43 X65 Plate, Average Transverse  $K_{Ic}$  versus Temperature

temperatures. Average maximum transverse toughness values were determined to be:

X65 Plate (-70°C)	$K_{Ic}$ initiation:	130,000 lb/in <sup>3/2</sup>
	$K_{Ic}$ arrest:	48,000 lb/in <sup>3/2</sup>

Figures 41 and 43 indicate that for plate and pipe materials initiation and arrest curves for either plate or pipe material categories will be similarly shaped. Additionally, DCB toughness versus temperature curves for plate and pipe materials are distinctly shaped; and initiation toughness tests are subject to considerably more scatter at a given test temperature than are comparable arrest toughness test results.

Few DCB tests were conducted at temperatures above -50°C as specimen side arms displayed considerable plastic deformation with increasing temperatures; and crack runs were primarily of the ductile tear type. The limited tests at room temperature yielded initiation fracture toughness values ranging from 200,000 lb/in<sup>3/2</sup> for X65 pipe, 315,000 lb/in<sup>3/2</sup> for plate material.

DCB specimens tested at -50°C and lower temperatures, performed very satisfactorily. Little or no sidearm bending was observed, and usually one could expect from one to two crack runs at -50°C, increasing to 3 to 5 crack runs at -110°C. The DCB load versus displacement curve for pipe specimen #044 tested at -100°C is reproduced in Figure 44. This loading curve is typical of the experimental test data recorded for the X65 pipe steel. Some "crosshead jump" is evident and is most noticeable at the first initiation point. Crosshead deflection is related to the physical construction of the testing machine, and can

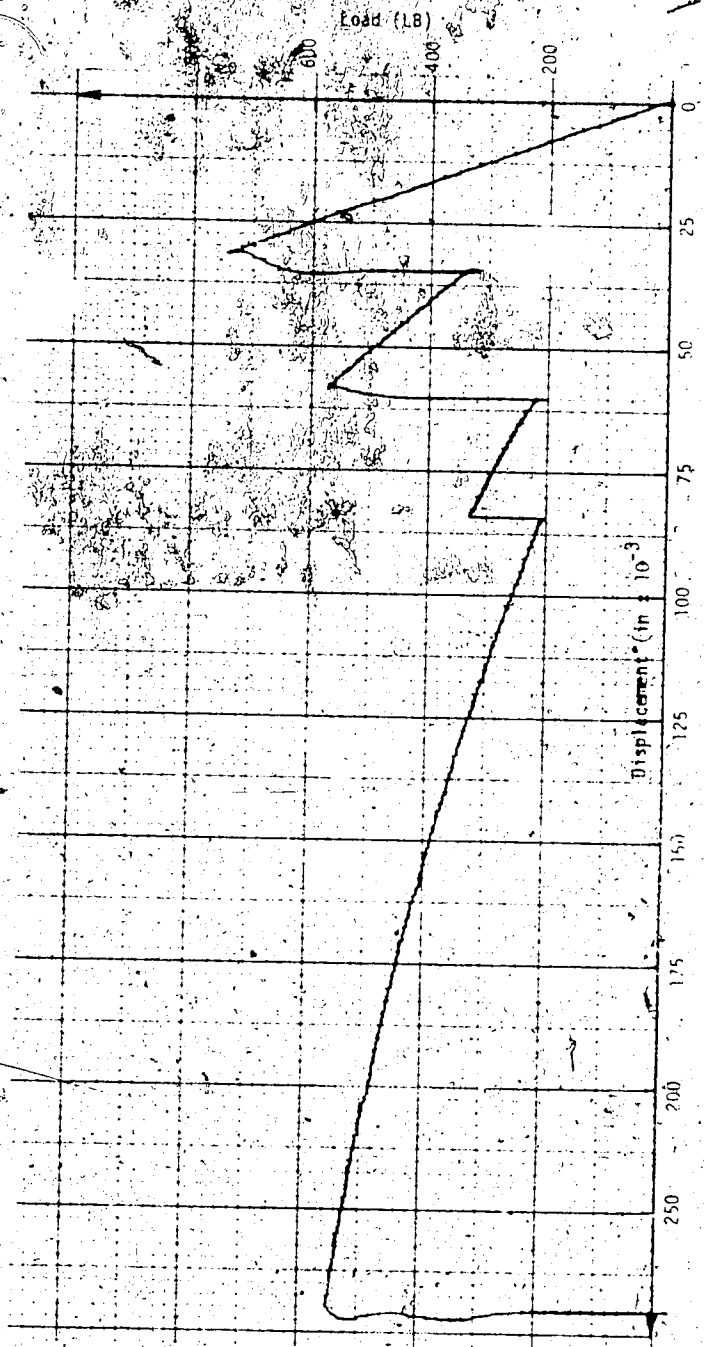


Figure 44 X65 Pipe, Load versus Displacement  
at -100 Degrees Centigrade



be minimized or eliminated through proper selection of the testing machine. Excellent DCB brittle crack runs were obtained during tests conducted at  $-193^{\circ}\text{C}$  on a plate and a pipe specimen. Specimen fracture surfaces were flat and very fine grained as shown in Figures 45 and 46. It was not possible to define actual crack stops and starts on the fracture surfaces. This is understandable, as in excess of 30 individual crack runs were observed during the testing of the plate specimen. Fracture toughness values for both specimens were approximately  $30,000 \text{ lb/in}^{3/2}$  at  $-193^{\circ}\text{C}$ . The DCB load versus displacement chart printout for plate specimen number 26 tested at  $-193^{\circ}\text{C}$  is reproduced in Figure 47. An enlargement of the plate fracture surface is shown in Figure 48.

As shown in Figures 45 and 46, pipe DCB fracture surfaces tended to be more fine grained, flat and regular at a given temperature, than were corresponding plate fracture surfaces. Some side groove tearout of specimen material is evident at temperatures the order of  $-50^{\circ}\text{C}$ . As previously mentioned, the specimen design was selected on the basis of preliminary tests on mild steel and on dimensional recommendations of Hoagland (17) and Turner et al (4). Test results indicate that the DCB specimen design chosen was within the allowable tolerance permitted for the practical application of the DCB testing technique.

#### 4.7 Correlation Between Test Methods

The Charpy V-Notch 50 percent fracture transition temperatures were determined to be  $-20^{\circ}\text{C}$  (plate) and  $-26^{\circ}\text{C}$  (pipe). Charpy results indicate that DCB and Notch Bend maximum toughness occurred at percentage fracture crystallinity levels ranging from 75 percent to 100 percent.



Figure 45 X65 Pipe, DCB Fracture  
Surface Sequence

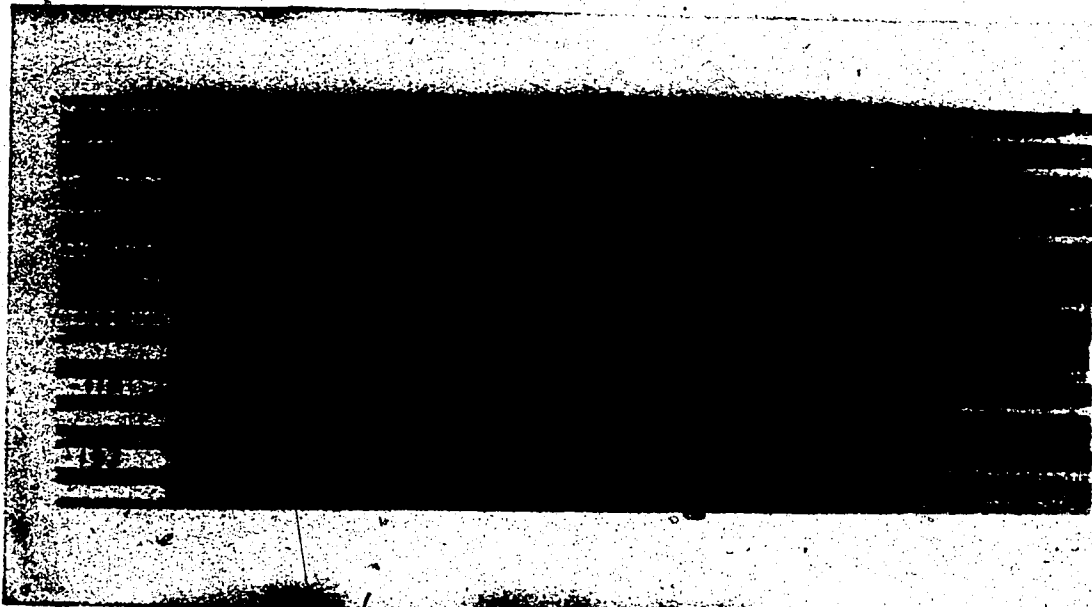


Figure 46 X65 Plate, DCB Fracture  
Surface Frequency

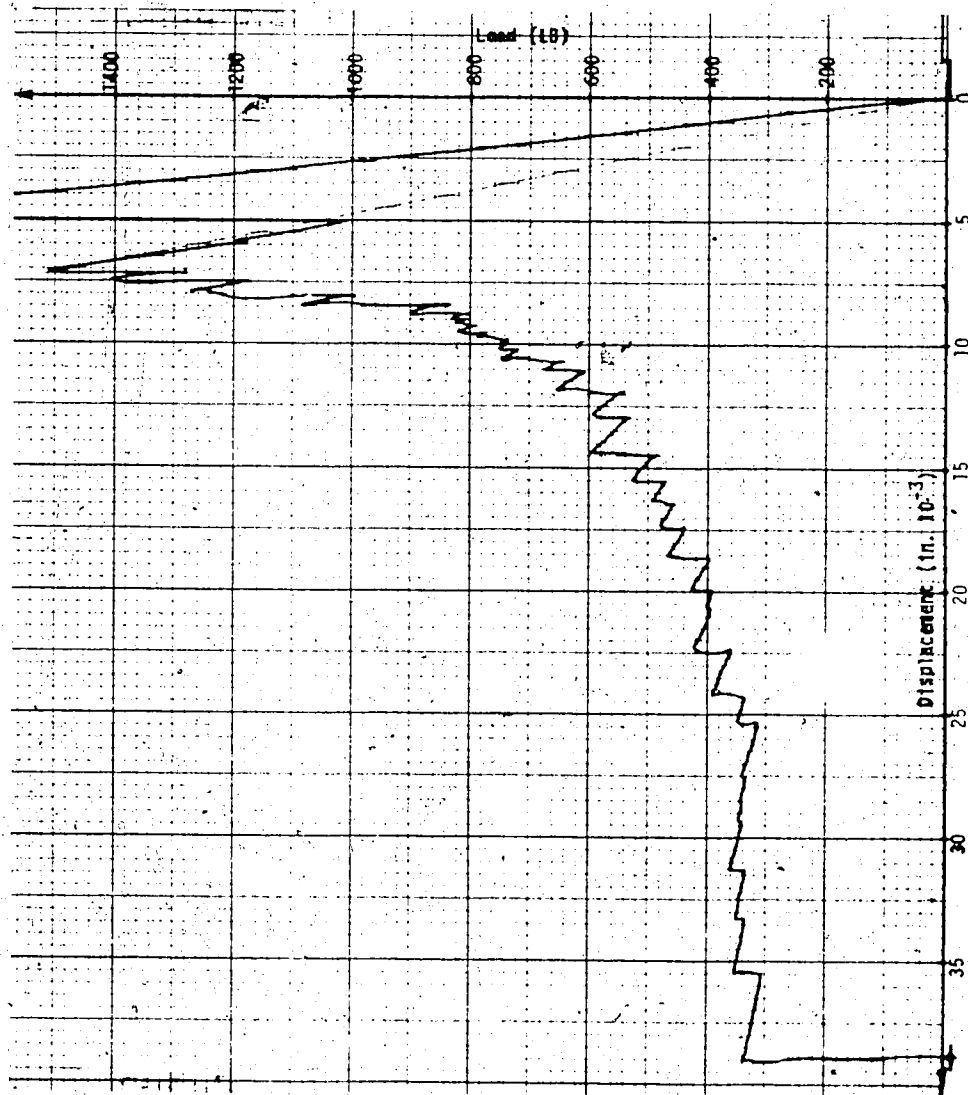


Figure 47 X65 Plate, DCB Load versus Displacement at -193 Degrees Centigrade



Figure 48 Enlargement X65 DCB Fracture  
Surface at -193 Degrees Centigrade

Precracked Charpy impact energies in this range were typically the order of 2-4 ft. lb. or approximately 5 - 10 percent of the average room temperature impact energy.

Inspection of DCB and Three Point Notch Bend temperature and toughness test results, indicates that a close correlation between these two test methods was achieved. In summary comparative test results are presented in Table 4.3.

Table 4.3

Summary - Comparative Test  
Results for X65 Steel

		Three Point Notch Bend	Double Cantilever Beam Test
Maximum Transverse $K_{Ic}$ (lb/in <sup>3/2</sup> )	Plate	(-70°C) 130,000	(-70°C) 130,000
	Pipe	(-30°C) 158,000	-- --
Maximum Longitudinal $K_{Ic}$ (lb/in <sup>3/2</sup> )	Plate	(-50°C) 126,000	(-70°C) 132,000
	Pipe	-- --	(-50°C) 124,000

A check of temperature-toughness values in Figure 37 for the longitudinal Three Point Notch Bend plate specimen indicates that the 20°C temperature differential is well within the tolerance of the statistical scatter at these temperatures. Accordingly, experimental results indicate that both test methods were equally good for the evaluation of the fracture performance behavior of X65 API pipeline steel. A point by point comparison of temperature-toughness values for both test methods, shows that Notch Bend plate toughness values tend to drop off more sharply

at temperatures increasingly higher or lower than the maximum toughness temperature than do DCB plate toughness values.

Based on the experimental results of this research program, it is observed that test results from application of both the Three Point Notch Bend and the Double-Cantilever Beam test methods are in good agreement. Additionally, both methods can be applied successfully in the laboratory to API X65 pipeline steel and are effective in evaluating plain strain fracture toughness for this steel.

#### 4.8 Specimen Orientation

Data obtained from the test methods utilized during this program, verified that the X65 pipe steel is anisotropic - the mechanical properties vary with direction. Charpy impact tests demonstrated that impact energy absorption capacity in the transverse direction was twice that in the longitudinal direction. Maximum Notch Bend toughness values were found to be slightly higher in the transverse direction. DCB tests further substantiated that for temperatures above  $-100^{\circ}\text{C}$ , fracture toughness values were higher in the transverse direction. These test results are in good agreement with the conclusions drawn from the earlier metallurgical photomicrographic examination and the directional relationship of the X65 plate tensile yield strengths.

#### 4.9 Specimen Precracking

Almost all of the tests conducted on the X65 pipe steel in this research program were conducted using precracked specimens. A few DCB, Charpy V-Notch, and Three Point Notch Bend specimens were

tested in the regular notched state. Generally, results of these latter few test samples indicated that impact energies and fracture toughness values are considerably reduced when precracked notches are used. Regular Charpy test specimens yielded energy impact values approximately 25 percent higher than those for precracked specimens at corresponding temperatures. DCB and Notch Bend testpieces required greatly increased initial load levels to initiate fracture. Subsequent crack initiation loads (in the case of DCB specimens) remained at approximately the same level as for other corresponding crack tests. Regular specimens produced considerably more crosshead jump on first initiation crack runs. Undoubtedly, more comprehensive test programs would have to be undertaken to verify the foregoing observations.

#### 4.10 Effects of Material Damage

Detailed analysis of precompression Notch Bend test results (Figures 34 and 37) indicates that room temperature precompression of the specimen notch root on X65 steels, produces a detrimental effect on specimen fracture response. Marked reductions in  $K_{Ic}$  values in both specimen test directions were recorded; and these were of the order of 10 percent in the transverse direction and 25 percent in the longitudinal direction. The latter characteristic is particularly significant in that most major line pipe line failures in recent years have been attributed to longitudinally running fractures. Although this technique of laboratory simulation of material damage may not be totally representative of the actual field condition, the test results obtained are significant. Research indicates that any field damage which produces an

area in an X65 pipeline steel in which there is a sharp notch root condition as well as material precompression, is potentially dangerous, and should be rectified. The latter can be accomplished in the field by either removing the affected section, or by repairing and locally stress relieving the repaired area.

Although precompressed Notch Bend specimens failed at test loads correspondingly lower than undamaged X65 pipe steels tested, load levels were generally in excess of those required to produce normal yielding. All specimen fractures initiated at average net stress levels above yield. These test results are unlike those observed by Mylonas et al (23) during a similar research program using mild steel.

#### 4.11 X65 Material Design Concept

On the basis of the limited research program undertaken it is premature to establish an acceptable design concept for pipelines, or similar applications involving X65 pipeline steels. It is equally difficult to extend such an hypothesis, if one were established; and to generalize it for all API 5LX pipeline steels. However, on the basis of the information compiled during this research program it is possible to project a "design generalization" upon which an engineering pipeline material evaluation could be based. Implementation of such a "design generalization" program would permit a more comprehensive evaluation of pipeline metallurgy prior to in-field implacement.

Accordingly, it is proposed that prior to actual line material commitment, the following properties should be thoroughly in-



investigated and information compiled for engineering analysis:

1. A fracture toughness versus temperature relationship over the extreme operating range of the proposed installation for the alternate materials under consideration in the longitudinal crack direction.
2. Establishment of the actual dropoff in energy levels and toughness values resulting from initiation of fractures at precracked notches versus non precracked notches for the longitudinal direction.
3. Evaluation of the effects of material damage at the critical temperature for the longitudinal direction.
4. Establishment of crack initiation and crack arrest fracture toughness energy values for the longitudinal direction at the critical temperature region.

Currently, test procedures based on the Drop Weight Tear Test, Charpy V Notch and Tensile tests, do not adequately establish the fracture behavior of API line pipe materials. Daily industry mill production schedules involving enormous hourly throughput, do not permit the control and accuracy required to thoroughly establish the "fracture history" for each particular grade of line pipe steel. Present industrial test programs are directed to the determination of mechanical metallurgical properties that are most desirable from the pipe manufacturer's point of view. Often times such factors do not relate entirely to field performance/service conditions which are the prime consideration of the purchaser.

## CHAPTER V

### CONCLUSIONS AND RECOMMENDATIONS

#### 5.1 Summary

The fracture toughness behavior of X65 pipeline steel in the unrolled skelp and manufactured submerged arc longitudinally welded pipe condition, was evaluated from room temperature through minus 193 degrees centigrade. This was accomplished using three distinct types of laboratory physical test methods developed previously for high tensile engineering materials. A good correlation between two of the test methods, Three Point Notch Bend and Double Cantilever Beam test, was achieved.

The effects of material damage based on laboratory tests on X65 pipe steel was determined. Precompression test results generally agreed with that found by previous researchers using mild steel test-pieces (23).

Notch Bend Fracture toughness values on an old field service failure "sawtooth fracture segment" were obtained. Results indicated that the failure was to be expected when the fracture toughness of the pipe material is considered.

The Double Cantilever Beam test method was successfully applied to an X65 pipeline steel. Test results indicated that this method correlates quite closely with standard Three Point Notch Bend test data. The DCB two parameter laboratory performance, where initiation

and arrest data are obtained from a single specimen, indicates that properly applied, the method could economically resolve the increasing backup data requirements for higher strength API pipeline materials.

In general, the research program verified that currently available manufacturer's API line pipe specifications do not adequately describe the average fracture performance of X65 line pipe steel. Results also indicate that finished line pipe mechanical properties are directionally dependent. Additionally, finished pipe properties do not relate directly to original manufacturer's properties for the unmanufactured plate skelp steel.

## 5.2 Areas of Further Study

Necessarily the scope of this research program dictated that areas studied could not be investigated in great detail. A number of factors were fixed so that evaluation of test results would be simplified; and accordingly, variations in specimen size, sidegrooving, notch root radius and loading rate were not considered.

It has been assumed throughout that a fatigue crack reliably reproduces an actual crack end. Thorough investigation of this area would benefit present and future fracture programs.

It would be of value to conduct a series of tests based on using the DCB and Three Point Notch Bend test methods; comparing test results of precracked and non precracked testpieces. Likely the results of such research would allow establishment of a toughness range for particular pipeline steels. This would be of material value to engineers and designers.

Undoubtedly one of the most interesting research programs would involve a thorough investigation of the fracture behaviors of identical grades of submerged longitudinally welded line pipe and spirally welded line pipe. Preliminary results of full scale field burst tests on spiral welded line pipe conducted by Trans Canada Pipelines are proprietary in nature. However, test results indicate that spiral pipe is more effective at arresting a running crack than conventional pipe.

## BIBLIOGRAPHY

- (1) Griffith, A.A., "The Phenomenon of Rupture and Flow in Solids", Philosophical Proceedings of the Royal Society (London), Series A, Vol. 221, 1920, p. 163-198.
- (2) Irwin, G.R., "Fracture Dynamics", Fracturing of Metals, American Society of Metals, Symposium (Chicago), 1947 p. 147-165.
- (3) Orowan, E., "Energy Criteria of Fracture", Welding Research Supplement, Vol. 34, 1955, p. 157s-160s.
- (4) Turner, C.E., Radon, J.C., "Fracture Toughness Measurements on Low Strength Structural Steels", Proceedings of the Second International Conference on Fracture, Brighton, April 1969, Paper No. 14.
- (5) Ford, G., Radon, J.C., Turner, C.E., "Fracture Toughness of a Medium Strength Steel", Journal of the Iron and Steel Institute, Vol. 205, August 1967, p. 854-860.
- (6) McClure, G.M., et al., "Research on the Properties of Line Pipe", American Gas Association Catalog 40/PR, 1967.
- (7) Irwin, G.R., "Analysis of Stresses and Strains Near the End of a Crack Traversing a Plate", Journal of Applied Mechanics, Vol. 24, 1957, p. 361-364.
- (8) Irwin, G.R., Kies, J.A., "Fracturing and Fracture Dynamics", Welding Journal Research Supplement, Vol. 31, 1952, p. 95s-100s.

- (9) Irwin, G.R., Kies, J.A., "Critical Energy Rate Analysis of Fracture Strength", Welding Research Journal Supplement, Vol. 33, 1954, p. 193s-198s.
- (10) Westergaard, H.M., "Bearing Pressures and Cracks", Journal of Applied Mechanics, June 1939, p. A49-A53.
- (11) Irwin, G.R., "Structural Aspects of Brittle Fracture", Applied Materials Research, Vol. 3, 1965, p. 13-14.
- (12) Irwin, G.R., "Fracture Mode Transition for a Crack Traversing a Plate", Journal of Basic Engineering, Vol. 82, 1960, p. 417-425.
- (13) Irwin, G.R., "Relation of Crack Toughness Measurements to Practical Applications", Welding Research Journal Supplement, Vol. 41, 1962, p. 519s-528s.
- (14) McClintock, F.A., Irwin, G.R., "Plasticity Aspects of Fracture Mechanics", ASTM STP 381, p. 84.
- (15) Wells, A.A., Post, D., "The Dynamic Stress Distribution About a Running Crack", Proceedings of the Society of Experimental Stress Analysis, Vol. XVI, No. 1, 1958, p. 69.
- (16) Irwin, G.R., "Fracture Mechanics", Pergamon Press, London, 1960, p. 557-592.
- (17) Hoagland, R.G., "On the Use of the Double-Cantilever Beam Specimens for Determining the Plane Strain Fracture Toughness of Metals", Journal of Basic Engineering, ASME Transaction, Paper 67-MET-A, 1967, p. 1-8.
- (18) Schwab, R.C., "Use of Tapered Double-Cantilever-Beam Specimens for Fatigue Crack Growth Studies", Transactions ASME, Paper 69-MET-16, 1969, p. 1-7.

- (19) "Fracture Toughness Testing and its Applications", ASTM, STP 381, American Society for Testing and Materials, 1964.
- (20) Berry, J.P., "Some Kinetic Considerations of the Griffith Criterion for Fracture - I Equations of Motion at Constant Force", J. Mech. Phys. Solids, Vol. 8, 1960, p. 194-206.
- (21) Gillis, P.P., Gilman, J.J., "Double-Cantilever Cleavage Mode of Crack Propagation", Journal of Applied Physics, Vol. 35, 1964, p. 647-658.
- (22) Irwin, G.R., and Wells, A.A.; "Continuum Mechanics View of Crack Propagation", Metallurgical Reviews, Vol. 10, No. 38, 1965, p. 223-235.
- (23) Mylonas, C., Drucker, D.C., and Brunton, J.D., "Static Brittle-Fracture Initiation at Net Stress 40% of Yield", Welding Journal Research Supplement, October 1958, p. 473s-479s.

APPENDIX A

Test Material Specimen Sectioning



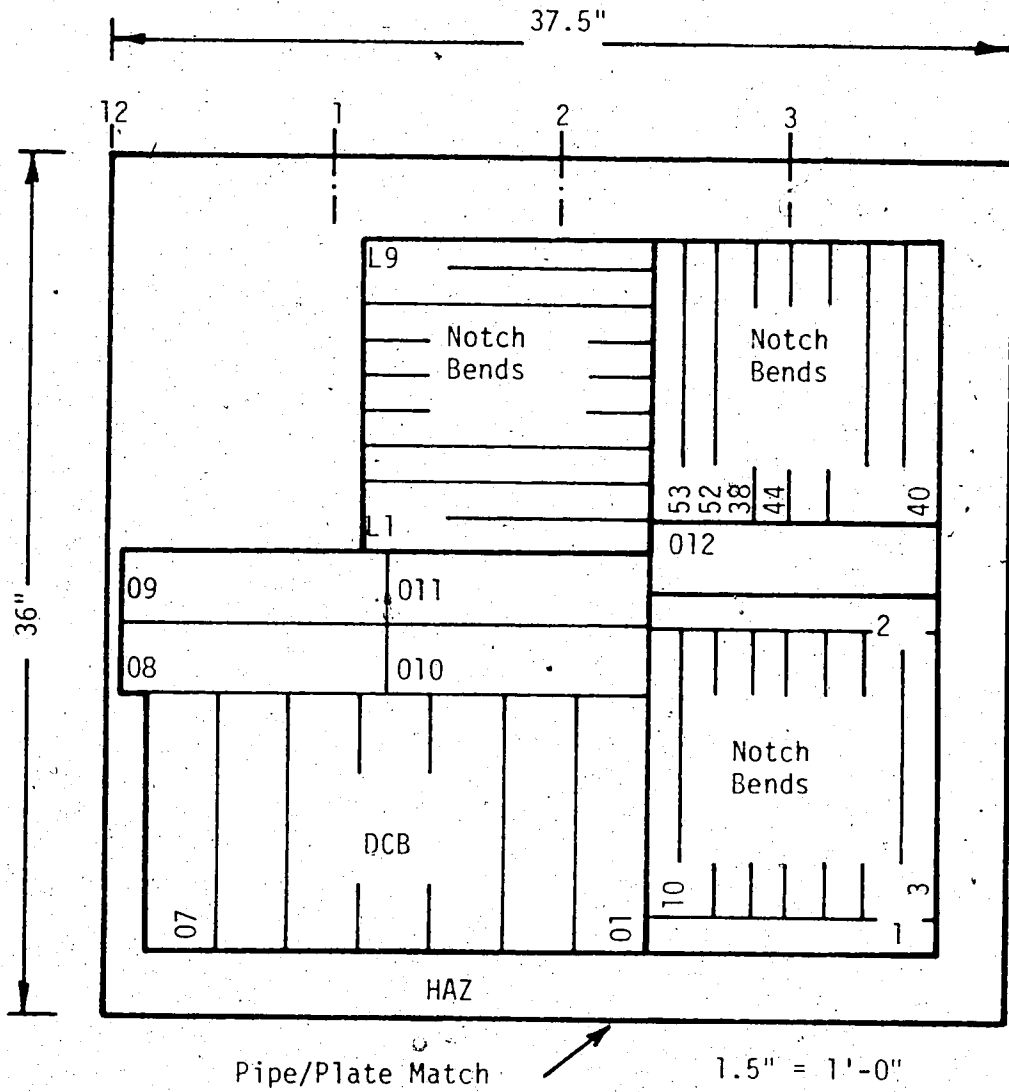


Figure A1 X65 Plate Section I

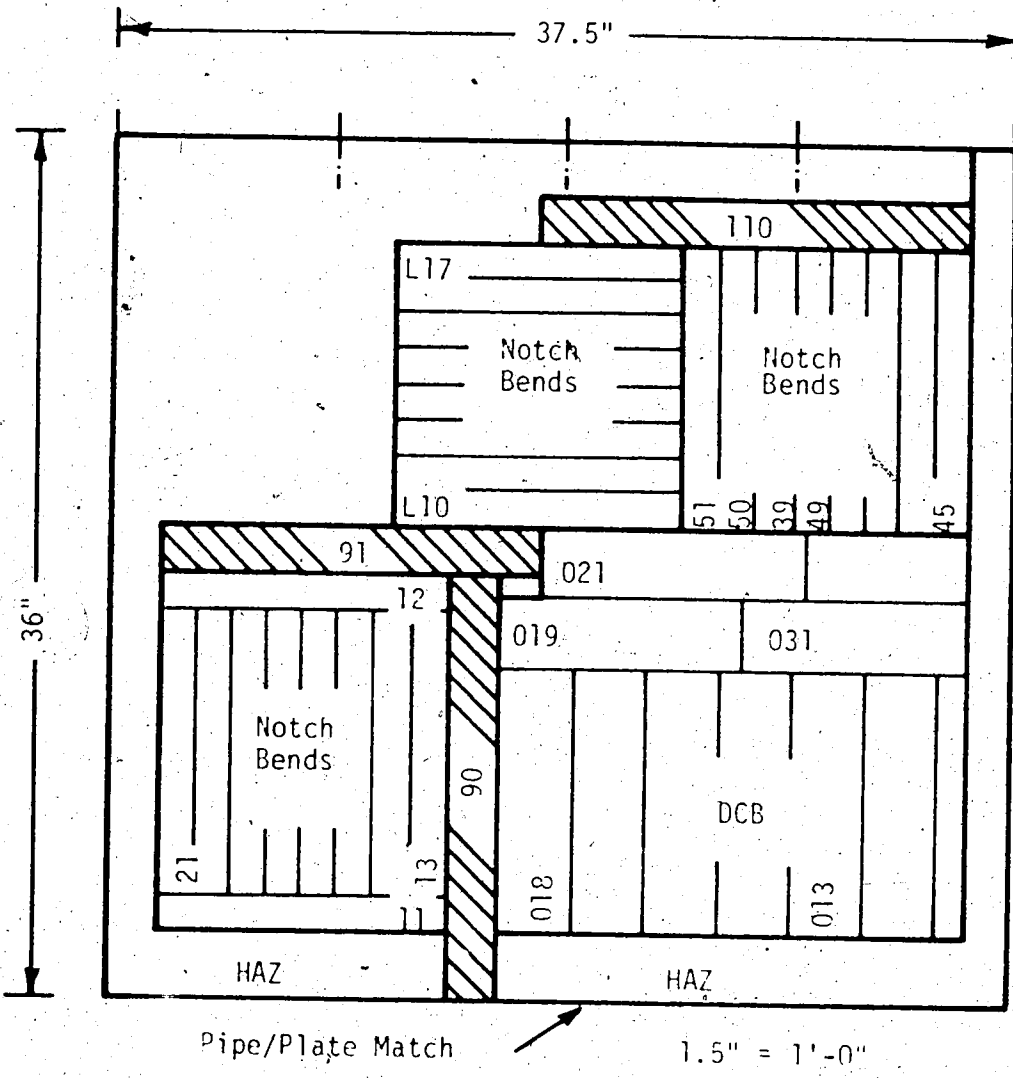
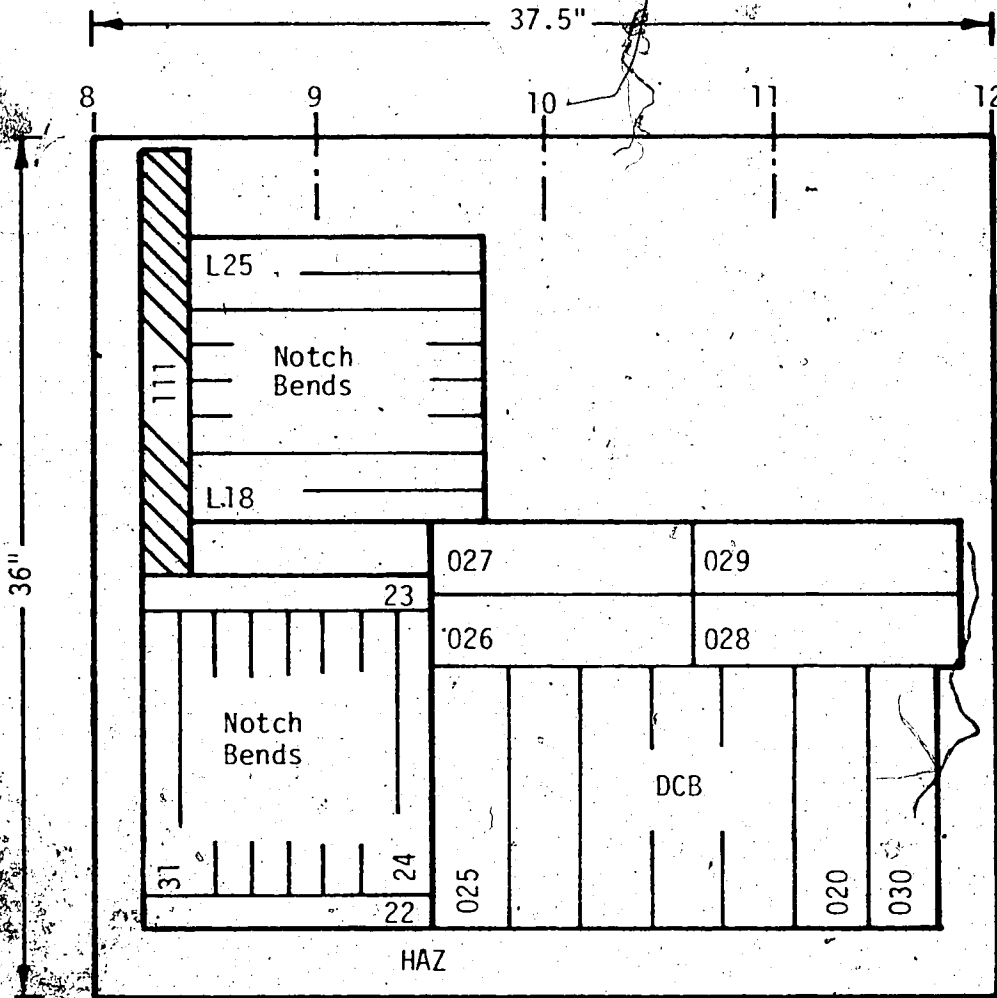


Figure A2 X65 Plate Section II



Pipe/Plate Match

1.5" = 1'-0"

Figure A3 X65 Plate Section III

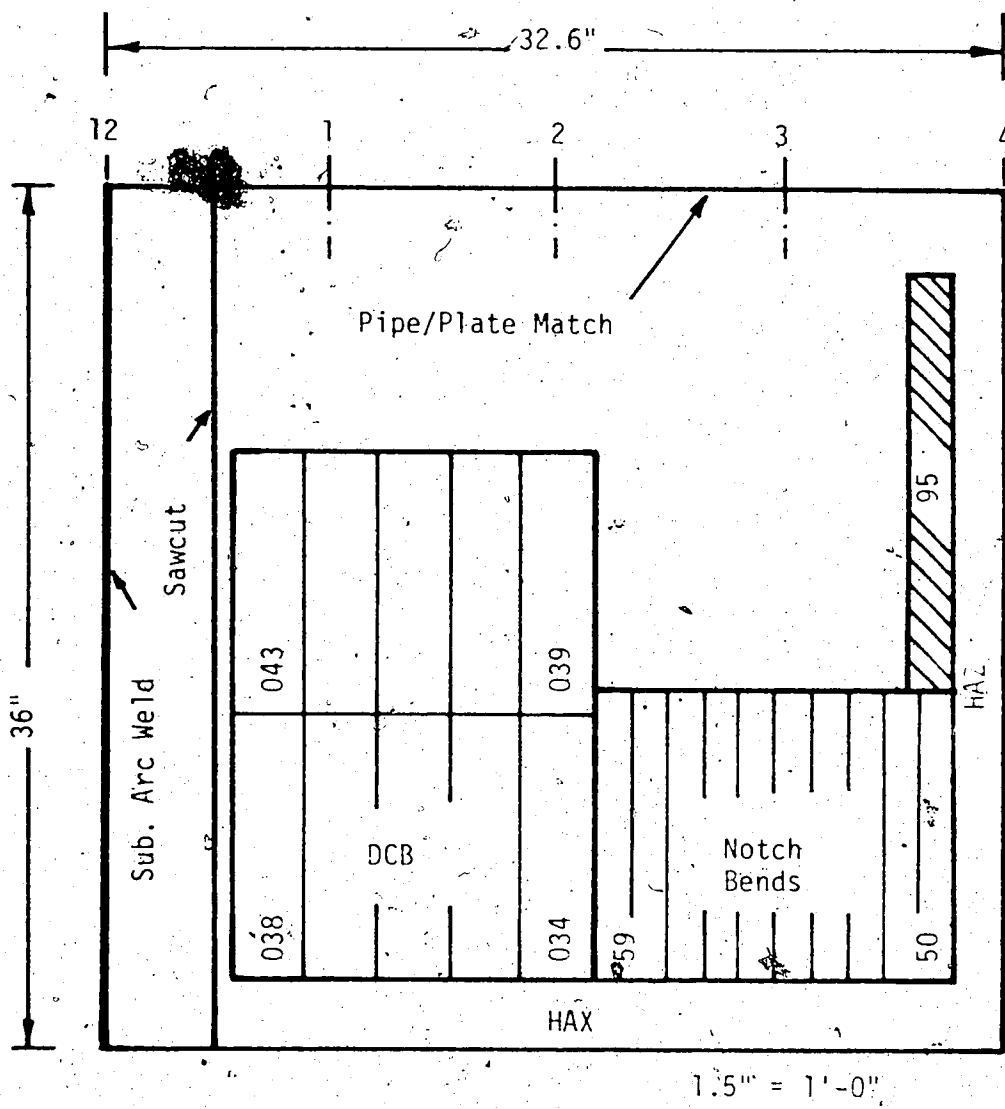


Figure A4 X65 Pipe Section I

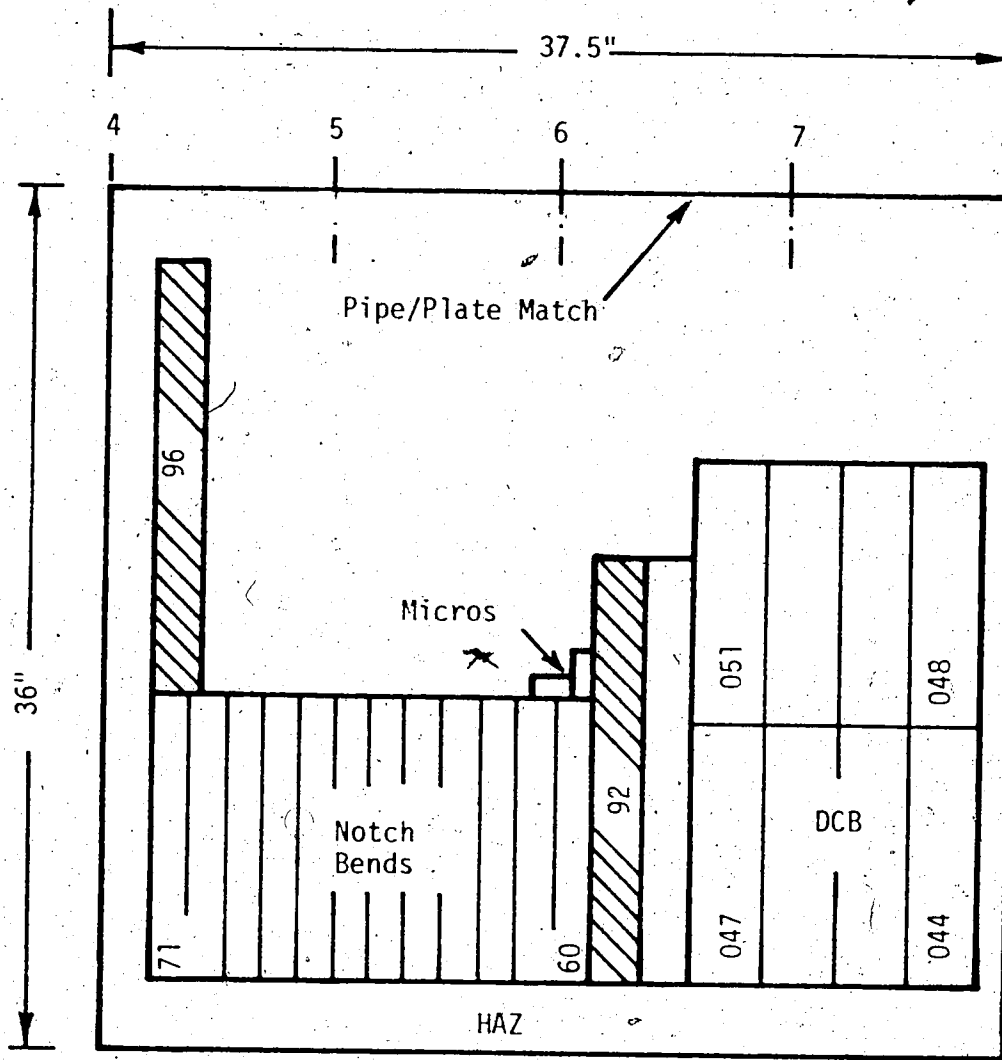


Figure A5 X65 Pipe Section II

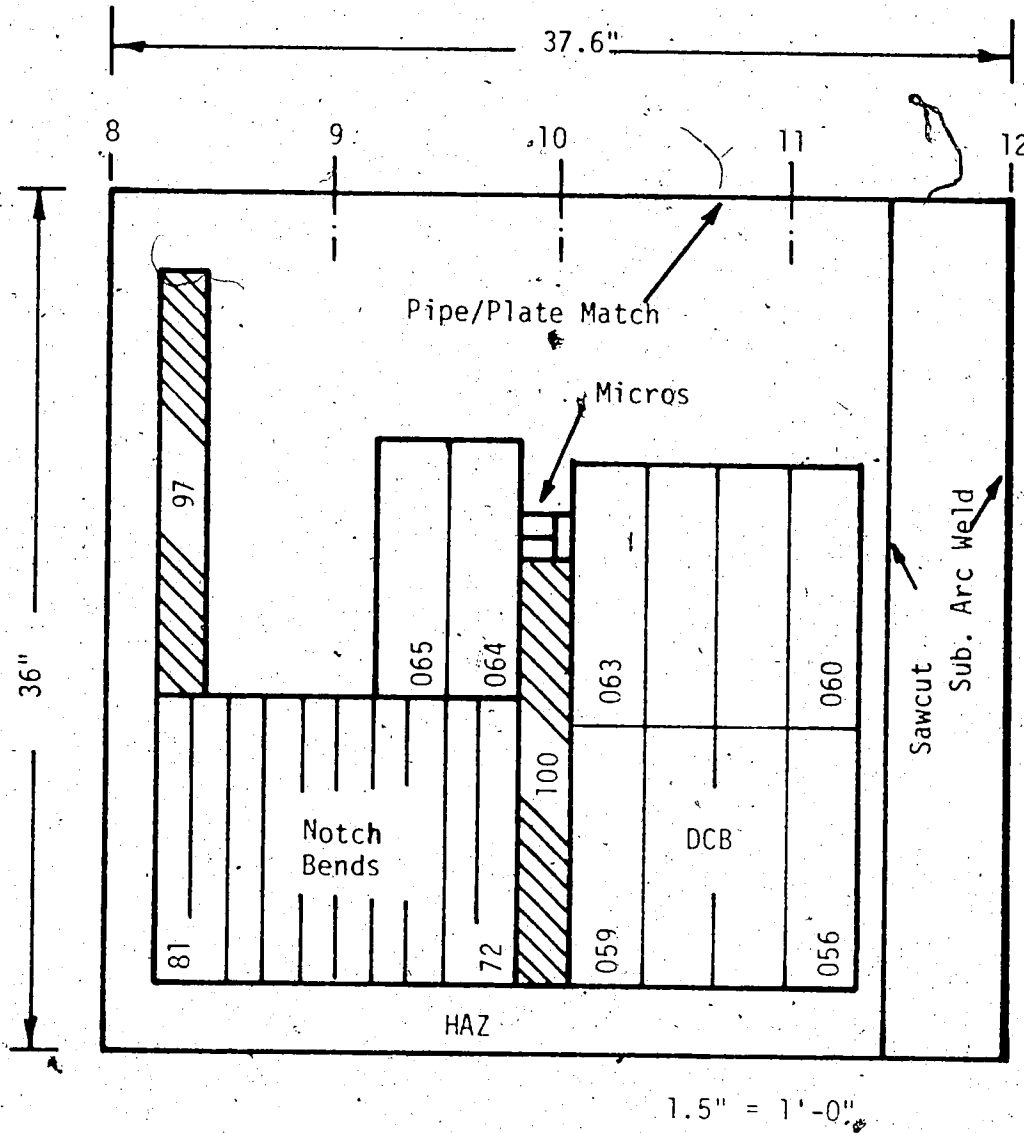


Figure A6 X65 Pipe Section III

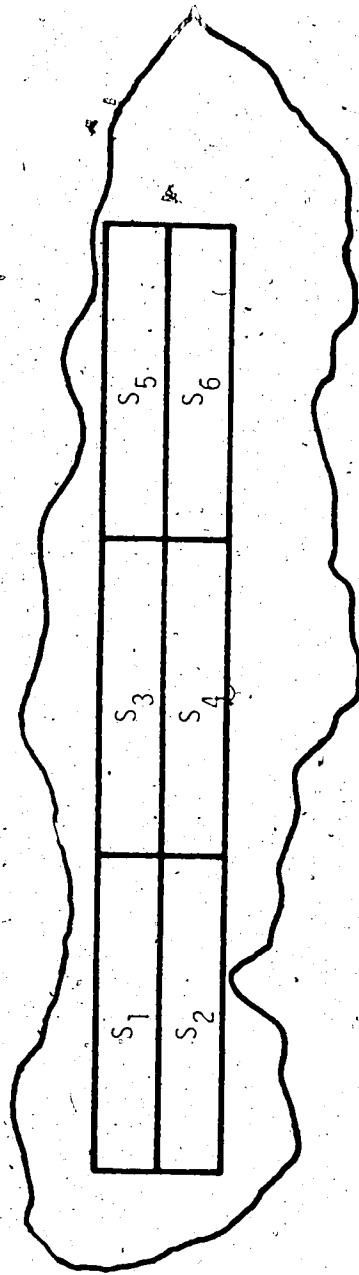


Figure A7 Sawtooth Fracture Segment, Notch Bend Specimen Locations